The Thesis Committee for Ahmet Serkan Kabakci
Certifies that this is the approved version of the following thesis:

Multicomponent-Seismic Characterization of the Utica Shale

APPROVED BY
SUPERVISING COMMITTEE:

Supervisor:

William Fisher

Bob A. Hardage

David Mohrig

Multicomponent-Seismic Characterization of the Utica Shale

by

Ahmet Serkan Kabakci, B.S.

Thesis

Presented to the Faculty of the Graduate School of

The University of Texas at Austin

in Partial Fulfillment

of the Requirements

for the Degree of

Master of Science in Geological Sciences

The University of Texas at Austin

May 2015

Dedication

I dedicate this thesis to my family Nuran, Necmi and Hakan KABAKCI and Ozge Aktuna for their support, encouragement and endless love.

Acknowledgements

As an industry partner, Geokinetics and Geophysical Pursuit provided the 3C3D seismic data; Chesapeake Energy provided the digital well data. Landmark Graphics Corporation provided software for the 3C3D seismic interpretation via the Landmark University Grant Program. Some of the illustrations were prepared by the Bureau of Economic Geology graphics department.

I would like to thank Dr. Bob A. Hardage and Dr. William Fisher for their thoughtful guidance. My gratitude is also to my committee member Dr. David Mohrig.

I would like to offer my special thanks to Michael V. De Angelo for his great support in every steps of my research. His guidance was not only for research purposes but also for life experiences. His thoughts would always be remembered for all my career work.

This study was also accomplished by thanks to the Turkish Petroleum Corporation for providing scholarship program and being sponsor for my graduate work in the University of Texas at Austin.

Lastly, I would like to thank my friends for all their support and love during my research.

Abstract

Multicomponent-Seismic Characterization of the Utica Shale

Ahmet Serkan Kabakci, MSGeoSci

The University of Texas at Austin, 2015

Supervisors: William Fisher, Bob A. Hardage

Recent development of gas shales in North America yield worldwide interest in gas production from shale formations. The methodology used in this thesis was to demonstrate multicomponent seismic technology for the characterization of shale-gas systems. The study area covers the Utica Shale across the Appalachian Basin in Bradford County, Pennsylvania. Concepts documented in this thesis can be used for other shale-gas systems. Unlike most shale-gas system studies, S-wave modes were used in addition to P-wave data in this study to better characterize the Utica Shale. Fast S-converted shear (P-SV_1) and slow S-converted-shear (P-SV_2) volumes provide new seismic imaging options for shale-gas studies and enable expanded seismic attributes that can be used to characterize shale-gas systems.

Table of Contents

List of Tables

List of Figures

CHAPTER 1 GEOLOGIC OVERVIEW OF THE UTICA SHALE

Introduction

This chapter presents a geologic overview of the Utica Shale in the northeastern part of the Appalachian Basin where my study area is located in Bradford County, Pennsylvania. The focus of my thesis research is to use multi-component seismic data (3C3D) to analyze the Utica Shale and its associated stratigraphy. Because there has been recent focus on the Utica Shale by the gas industry, there is considerable regional geologic information about the Utica Shale system. My objective is to determine if 3C3D seismic data can improve reservoir characterization of the Utica Shale Formation.

Bradford County, Pennsylvania, is located in the northeastern part of the Appalachian Basin (Fig. 1). The basin itself extends in a southwest-northeast direction. The eastern margin is bounded by the Appalachian Mountains, and the western margin extends into Ohio and Kentucky. In the east-to-west direction, sedimentation is controlled by passive margin environments and sediment starvation.

The Middle-Upper Ordovician Utica Shale covers an area of 170,000 mi^2 of the Appalachian basin. This regional shale extends into central Ontario to the north, New York, Pennsylvania and West Virginia to the east, eastern Tennessee and Kentucky to the south, and Ohio to the West (Fig. 1). Although the Utica Shale covers a large area, it has not been extensively developed in Bradford County because its significant depth involves high cost for horizontal drilling and hydraulic fracturing operations.

The Utica Shale outcrops in New York State and extends into the subsurface in Quebec and Ontario, Canada. The limit of the Utica Shale play is defined mostly by the Utica Shale-Trenton Limestone outcrop belts to the north, south, east and west (Fig. 2). The northern boundary extends along the Utica Shale-Trenton Limestone boundary. The

facies change from the Trenton Limestone to black shales describes the southern boundary. Eastern and western sides of the Utica Shale boundary are described by thrust-faulted regions across the Appalachian Basin.

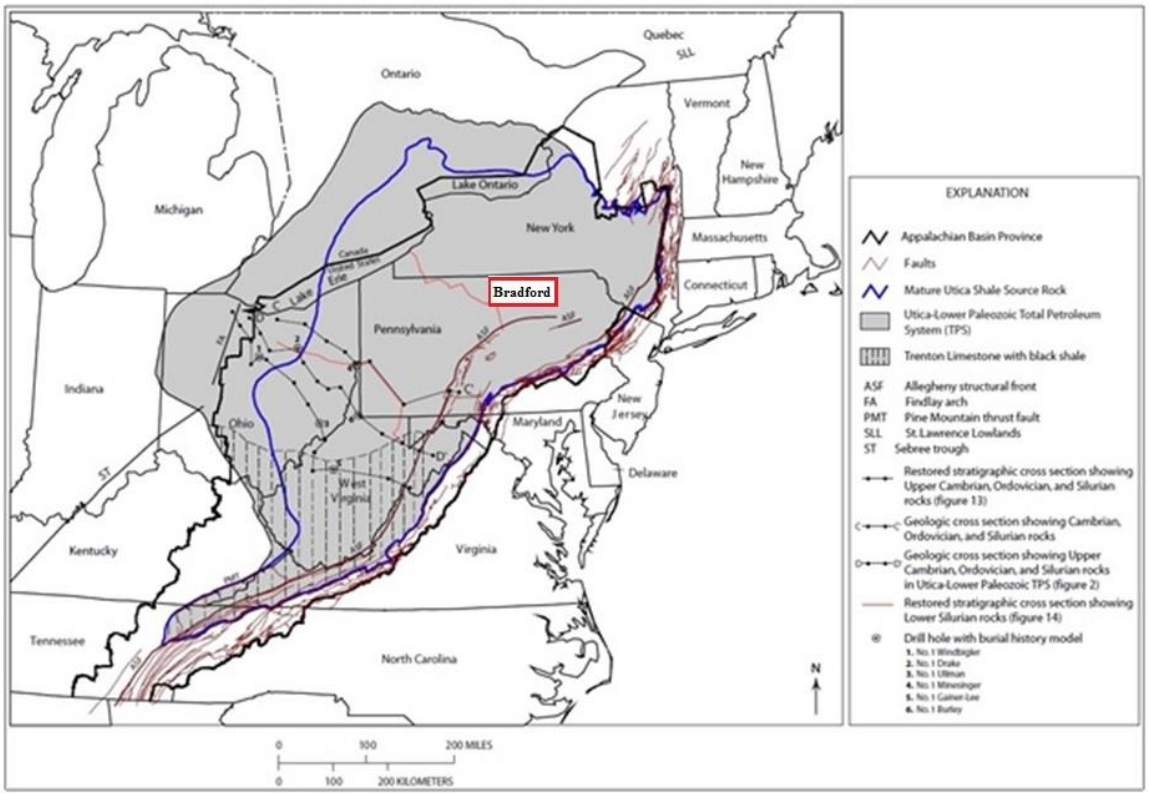

Figure 1: Distribution of Middle-Upper Ordovician Utica Shale in the Appalachian Basin (Ryder, 2008).

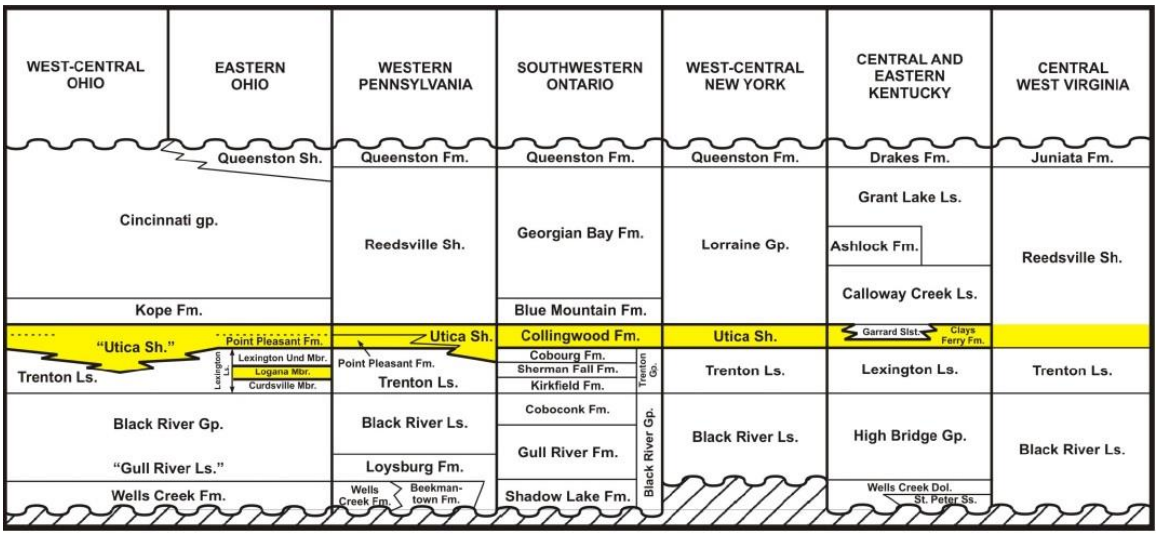

Figure 2: Correlation of the Utica Shale across the Appalachian Basin (Patchen et al., 2006).

The subsurface position of the Utica Shale and Marcellus Shale from New York into Pennsylvania is shown in Figure 3. A similar cross section extending from Ohio to Pennsylvania is shown in Figure 4. The Utica Shale is much deeper than the Marcellus. The depth of the Utica Shale decreases to the west into Ohio and to the north into Ontario to less than 2000 feet below sea level. It deepens to about 14,000 feet below sea level in western Pennsylvania and to approximately 12,000 feet in northeast Pennsylvania (Fig. 5). The depth of the Utica Shale in my study area is approximately 12,000 feet and the shale interval dips due south.

The vertical distance between the Utica Shale and Marcellus Shale is about 1800 feet in western New York and about 5000 feet in south-central Pennsylvania. Most rock units in the Appalachian Basin are thicker towards the east and thinner towards the west. In addition, there are considerable differences between the Marcellus Shale and Utica Shale in terms of their stratigraphy, depositional environment, thermal maturity, etc.

Because the depth of the Utica Shale can exceed 14,000 feet in some areas, recent exploration efforts have mostly focused on the shallower and more economical Marcellus Shale Formation.

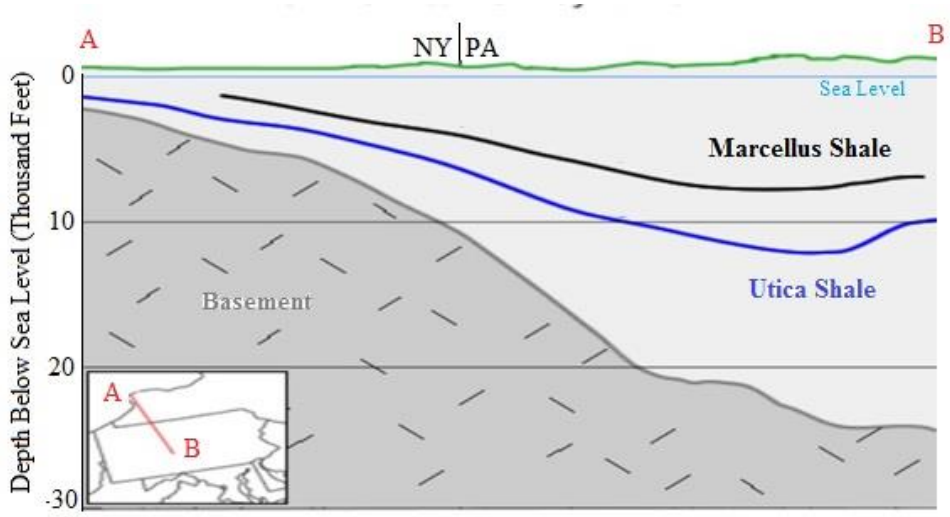

Figure 3: Cross Section of the Utica and Marcellus Shale in New York to Pennsylvania (modified by geology.com).

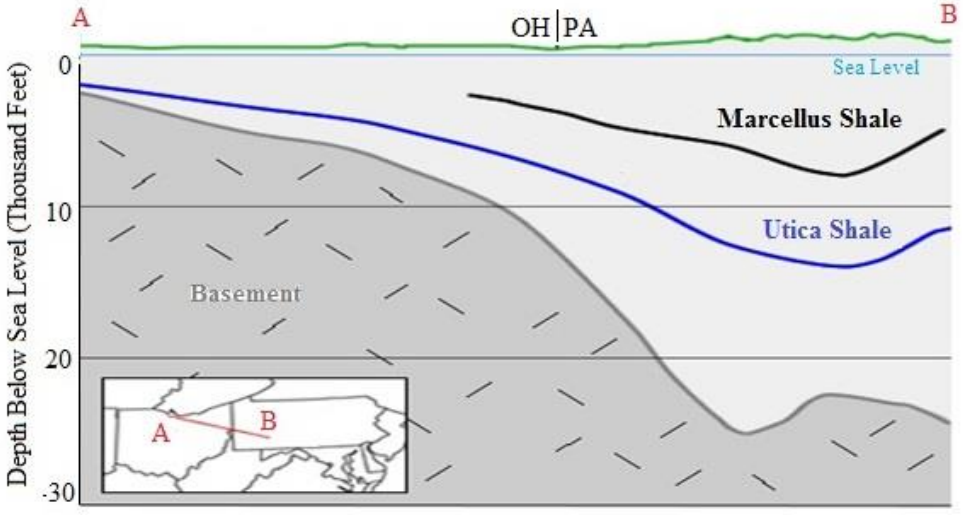

Figure 4: Cross Section of the Utica and Marcellus Shale in Ohio to Pennsylvania (modified by geology.com).

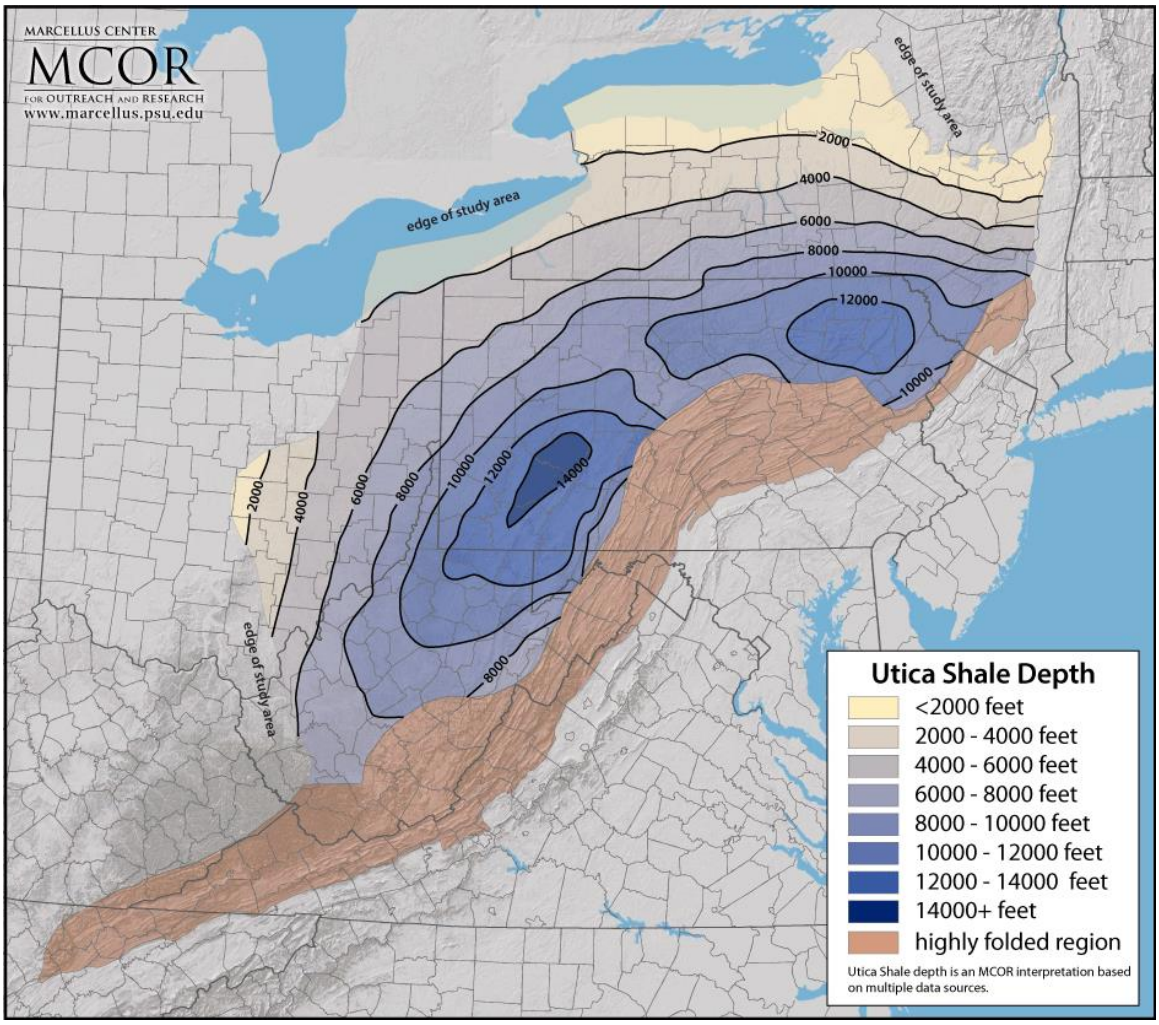

Figure 5: Depth in feet to the base of the Utica Shale (Marcellus.psu.edu).

The thickness of the Utica Shale is variable and ranges from more than 500 ft in northwest Pennsylvania to 100 ft in Ohio (Fig. 6). The thickness generally increases to the east and decreases to the northwest. In my study area, the thickness interval is approximately 250-350 ft (76 to 106m).

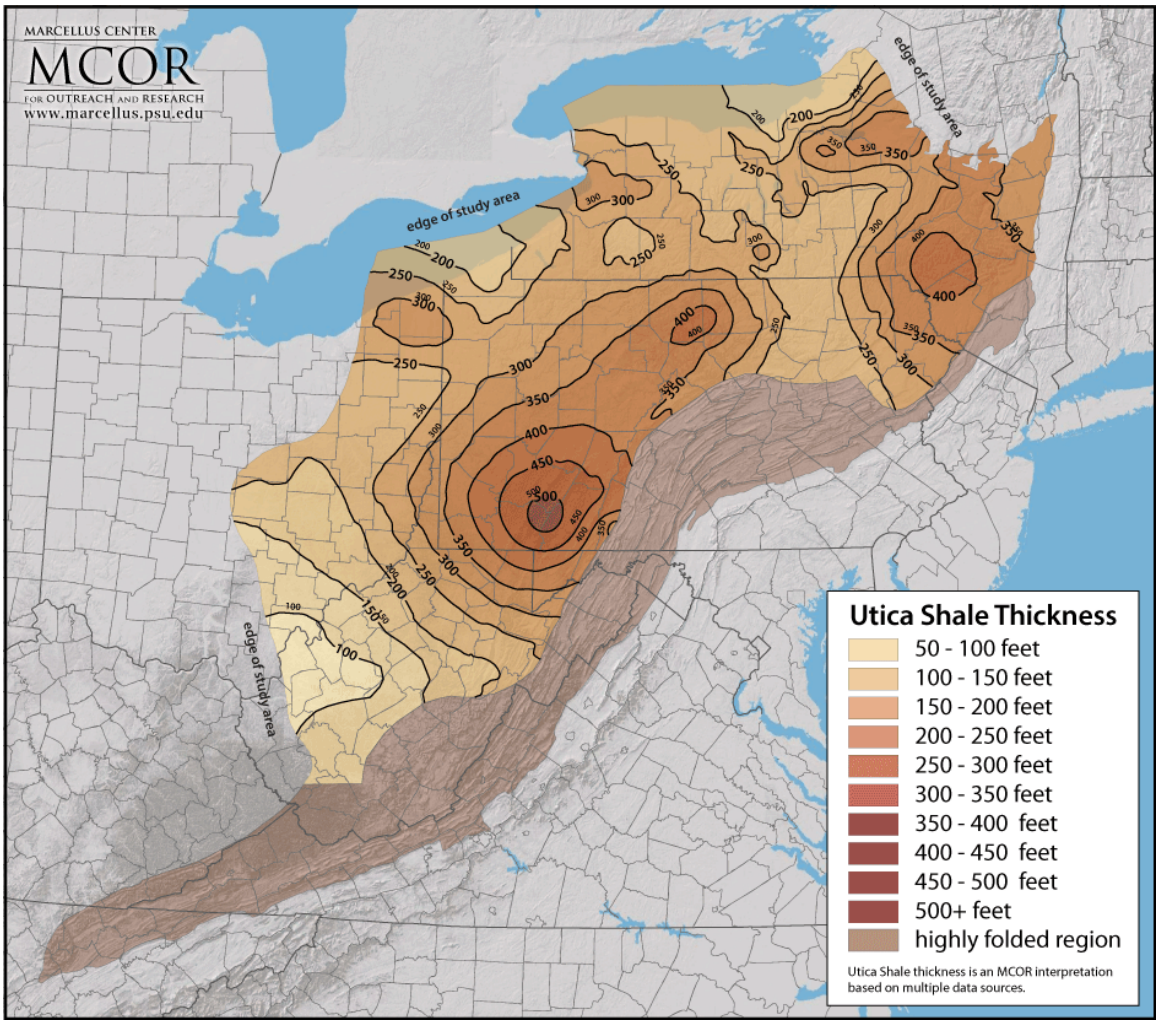

Figure 6: Thickness of the Utica Shale in the northern Appalachian Basin (Marcellus.psu.edu).

Stratigraphy of the Utica Shale

The Middle-Upper Ordovician Utica Shale is bounded below by the older Trenton/Black River Group strata and above by the younger Lorraine Formation (Fig. 7). Middle Ordovician stratigraphy shows connections between shallow shelf carbonates of the Trenton Group, thin-bedded dark shales of the Dolgeville Formation, and the overlying Utica Shale.

The evolution of the Appalachian basin during Trenton time results in the appearance of low-relief carbonate buildups of the Trenton platform which extends across the Utica sub-basin. Carbonate production kept pace with the increase of water depth due to marine transgression. During this transgression, significant paleoclimate change and increasing abundance of fossiliferous carbonates were present (Keith, 1989). Extensive carbonates developed on the Trenton platform in Ohio, Michigan, Ontario, and New York resulting in extensive argillaceous carbonates. The shale appearance during this time marks a significant paleogeographic change during Trenton Time (Kolata et al., 2001).

The Trenton shelf is characterized by upward shallowing cycles, having vertical dimensions of 9.84 to 19.68 feet (Baird et al., 1992). These cycles originated as tabular bedded, inter-layered shale-limestone facies. This interval also contains ash layers. The limestone beds are closely spaced and amalgamated above this tabular bedded interval. This amalgamated structure is rich in skeletal packstones dominated by brachiopods. Storm scour structures characterize the upper part of the cycles and include bed-amalgamated, nodular facies. Muddy carbonate intervals are also deposited within these cycles. These cycles may be either tectonic or eustatic in origin. In terms of sequence stratigraphy, lower-energy aggradational accommodation characterizes the tabular-

bedded interval. Overlying amalgamated beds indicate increasing energy level. Lastly, an interval of condensed sections indicates transgressive conditions (Baird et al., 1992).

Abrupt facies transitions of Trenton Limestone into Utica Shale can be recognized (Kay, 1953). Phosphorite-rich zones deposited below this transition appear as the "Thruway Unconformity" between the Trenton Limestone and Utica Shale. Black, laminated shale successions characterize the exposures above this transition. This section also includes micritic layers of rock succession with widely spaced tabular structures (Kay, 1953).

The Taconic orogeny increased its intensity during the deposition of the Utica Shale and resulted in a series of shallow-water platforms. Significant volumes of black shale deposition during this period suggest the formation of a new carbonate platform. At the edges of Taconic subsidence, the accumulation of carbonate deposition and sediment influx was at maximum rate. At the more distal parts of the platform, sediment accumulation rate decreased because of the constant sea-level and resulted in the deposition of cleanest carbonates (Patchen et al., 2006). During the deposition of the Utica Shale, rapid rise in sea-level or increased subsidence in the platform replaced the carbonate deposition with the Utica Shale. More open-marine ramp environments followed the Utica Shale deposition time when the Taconic orogeny lessened. The depositional pattern of the central Appalachian Basin depocenter trends to the north, and the last carbonate deposition is named the "Kope" interval.

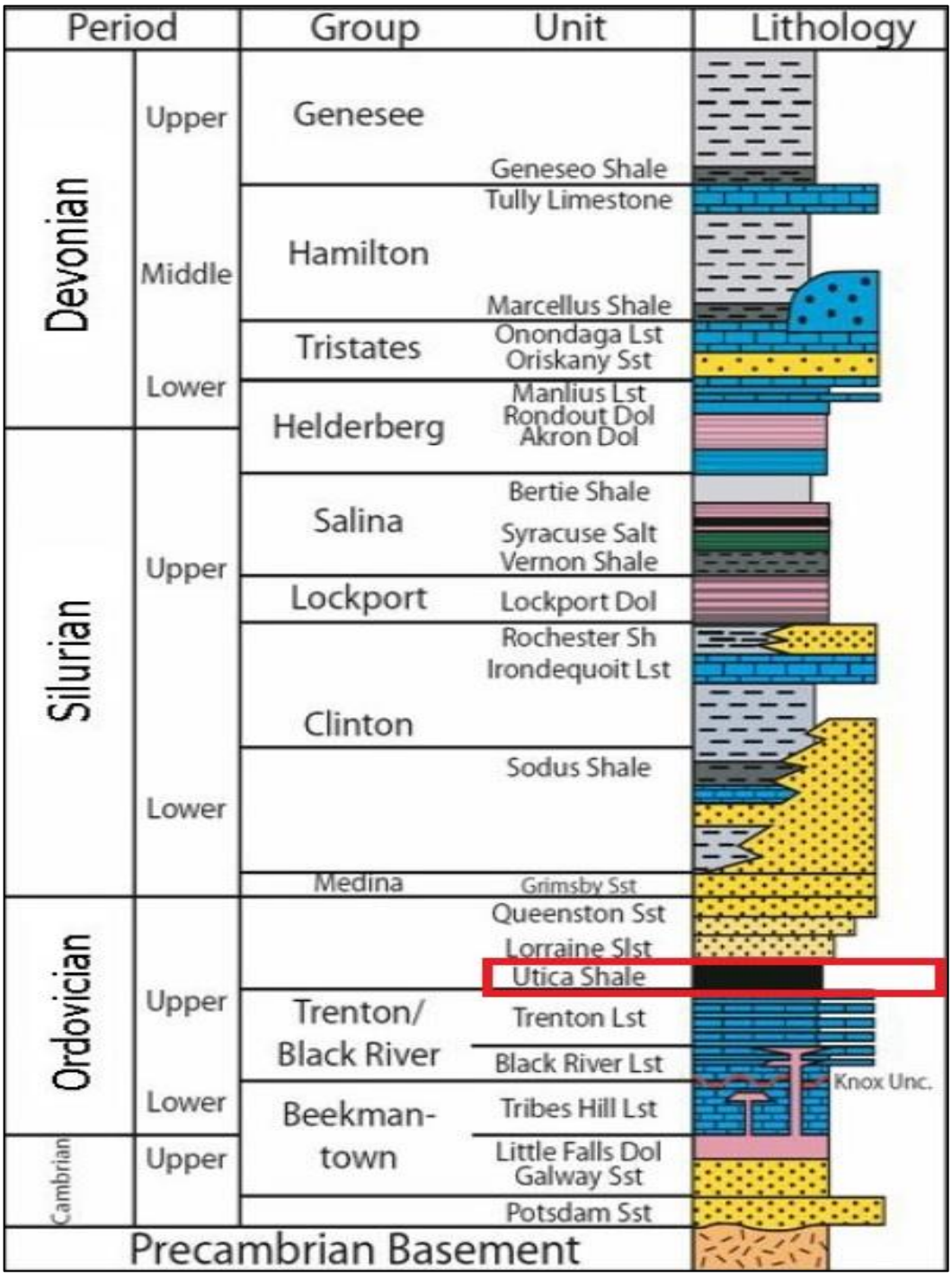

Figure 7: Stratigraphic column for the study area (Nyahay et al., 2007).

The Utica Shale belongs to the Utica sequence (Wallace and Roen, 1989), which includes the Utica Shale and its correlatives: the Antes Shale, the lower part of the Reedsville Shale, the lower part of the Martinsburg Shale, the Point Pleasant Formation, and the basal part of the undivided Cincinnatian Series (Fig. 8).

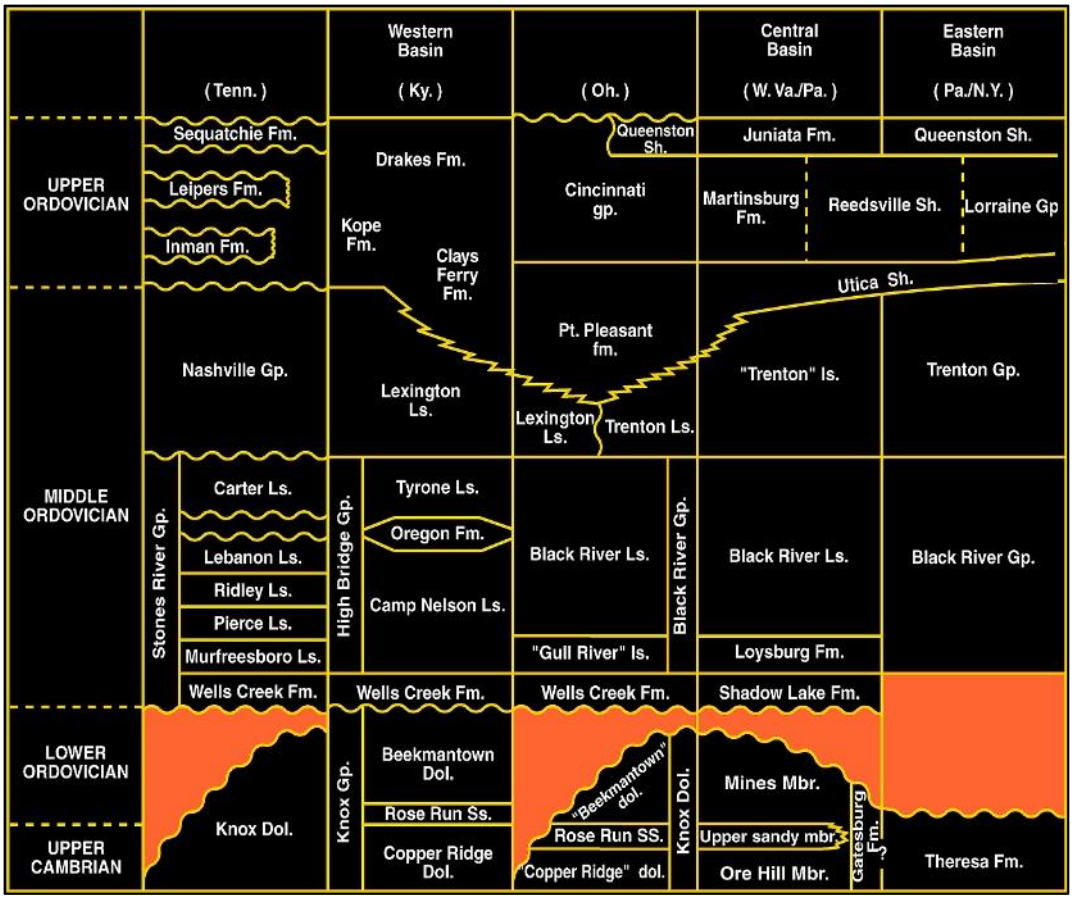

Figure 8: Utica Shale and its correlatives (Wickstrom et al., 1992).

The Utica Shale was formed from the erosion of the Taconic Mountains at the end of the Ordovician. The Utica Shale was deposited during the Taconic orogeny in an environment where a shallow-marine carbonate platform transitioned into a siliciclastic foreland basin. Subsidence of the eastern portion of the foreland basin caused a

progressive change from carbonate to siliciclastic sedimentation. The package of strata consists of three successions namely; siliciclastic-free carbonate rocks, argillaceous carbonate rocks, and clastic wedge deposits (Lehmann et al., 1995).

The Black River Group is a siliciclastic-free limestone succession which includes supratidal micrite to shallow subtidal biomicrite facies (Anderson et al., 1978). The Black River facies consist of clean carbonate mudstones, argillaceous carbonate mudstone, clean carbonate grainstones and packstones, argillaceous carbonate grainstones and packstones, calcareous shale and interbedded limestone, and shale. Argillaceous carbonate rocks are associated with the Trenton group. Lithofacies deposited during Trenton time consisted of clean or argillaceous carbonate grainstones, packstones, wackestones, shale, and calcareous shale with interbedded limestone (Patchen et al., 2006). The Trenton includes deeper marine argillaceous limestone interbedded with shale.

The Utica Shale is characterized as a black, organic-rich shale that consists of three members. In ascending order, these members are the Flat Creek Member (oldest), Dolgeville Member, and the Indian Castle Member (youngest) (Fig. 9). Although there are some different ideas about the division of the Utica Shale members, the stratigraphic convention of Smith and Leone (2010) is used here.

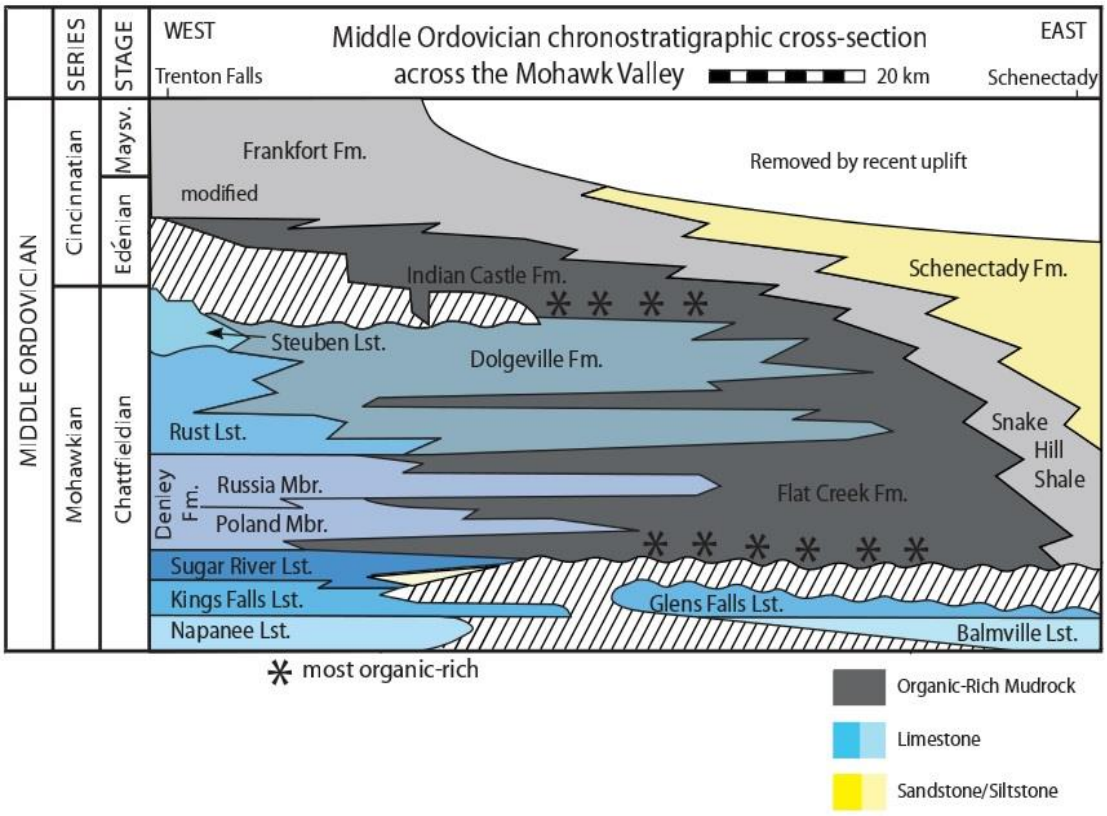

Figure 9: Middle Ordovician chronostratigraphic cross section showing members of the Utica (Goldman et al., 1999, Smith and Leone, 2010).

The Flat Creek member of the Utica Shale is time-equivalent to the Trenton limestone and is an organic-rich calcareous shale. The lower part of the Flat Creek is the most organic-rich interval. The upper Flat Creek member grades laterally into limestone (Fig. 10). The Dolgeville member is an interbedded limestone and shale which is also time-equivalent to the Trenton limestone (Fig. 11). The Utica Shale is divided by the Dolgeville member into two tongues. The lower tongue is the Flat Creek member, and the upper tongue is the Indian Castle Member (Goldman et al., 1999). The Indian Castle member is an organic-rich, fissile black shale (Fig. 12) (Smith and Leone, 2010).

Figure 10: Flat Creek Member in Florida, Montgomery Co. (Martin et al., 2008).

Figure 11: Dolgeville member in Little Falls, NY (Martin et al., 2008).

Figure 12: Indian Castle member in Little Falls, NY (Martin et al., 2008).

Depositional Environment of the Utica Shale

The Middle-Upper Ordovician Utica Shale is bounded below by the Trenton/Black River Group strata and above by the Lorraine Formation (Fig. 7). The Middle-Late Ordovician Black River group represents a basin architecture change from a passive regime to a compressive regime. The Taconic Arc collision is the key factor that created this change. Because transgression occurred during this period, the architecture is characterized by a shallow-water carbonate ramp that created considerable carbonate buildup (Keith, 1989). The Utica Shale sub-basin was surrounded by carbonate platforms during Trenton time. After Trenton time, deposition occurred in a restricted sub-basin. The intensity of the Taconic orogeny was the mechanism responsible for depositing the Utica Shale because there was a rapid rise in sea level and/or increased subsidence (Patchen et al., 2006). Following the orogenic events, because the Utica Shale was deposited during Ordovician greenhouse times, characterized by low-amplitude eustatic

sea level changes, the main force responsible for the deposition of the Utica Shale is assumed to be increased subsidence rather than eustatic sea level change (Fig 13) (Smith and Leone, 2010).

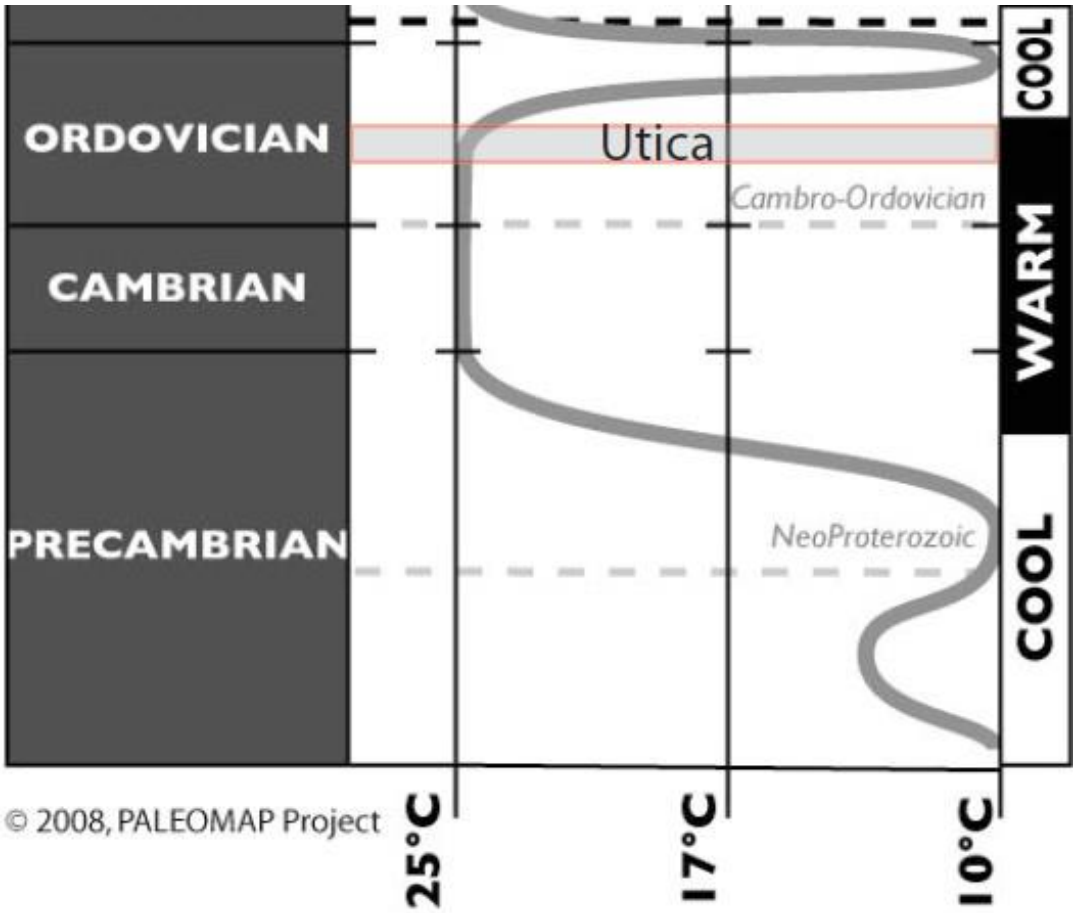

Figure 13: Utica Shale paleomap (Scotese, 2003).

Although the depositional environment of the Utica Shale has been interpreted as a deep-water basin, recent stratigraphic work indicates the presence of a shallow, low-oxygen environment (Smith and Leone, 2010). Fresh water flow from land and conditions along the margin of newly developing tectonic foreland basins combined to create anoxic environments.

Tectonic Setting of the Utica Shale

The Lower Ordovician stratigraphy of the Appalachian basin represents a uniform sequence of dolomitic carbonates deposited in a passive Laurentia margin in shallow water environments. The transition between the Early-Middle Ordovician times resulted in interbedded calcareous and detrital facies by uplift and erosion. This stratigraphy reflects the mobilization of Laurentia by the Taconic Orogeny when complex facies patterns replaced the simple-pattern of platform margin sedimentation. Taconian tectonism, therefore, clarifies the relationship between sedimentation and tectonism along the Appalachian Basin (Etthenson, 1991), and allows the tectonic setting of the Utica Shale to be explained by foreland basin tectonic models.

The tectonic scenario of foreland basins consists of four major processes: collisional braking, active deformational loading, active tectonism halting, and lithospheric relaxation. In the first stage, overthrust and bulge migration created a major unconformity (Jacobi, 1981), and foreland basins experienced rapid subsidence caused by the active tectonism and deformational loading (Fig. 14). During the early phases, the basin had minor clastic influx and sedimentation and basin fill was composed of organic matter and clay. These conditions precede the development of transgressive carbonate sequences (Walker et al., 1983). Following rapid subsidence, the deposition sequence was characterized by organic-rich, dark shales. The basin deepened because active tectonism became dormant. Center and proximal margins of the foreland basin were characterized primarily by clastic sediments. In the distal margin, in contrast to the previous stage, regressive carbonate sequences are observed (Walker et al., 1983). As the basin fills with clastic sediments, a period of equilibrium and rebounding takes place. Terrestrial deposits are deposited as redbeds. The Middle-Upper Ordovician stratigraphy of the Appalachian

basin follows the tectonic development of the lithospheric flexure model that is explained above. The Taconian orogeny Trenton Limestone is the initial transgressive carbonate platform and underlies the organic-matter rich Utica Shale. The Queenston Delta is deposited above the Utica Shale as a result of an unloading-type relaxation (Ettensohn, 1991).

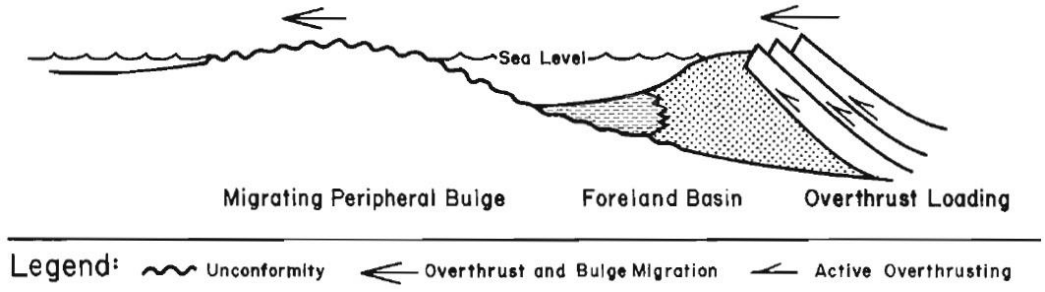

Figure 14: Schematic diagram of development of foreland basin (Quinlan and Beaumont, 1984).

The Utica Shale is an organic-rich mudrock that is deposited primarily on the cratonward side of the Appalachian basin (Fig. 15). Clastic influx cannot extend to the far side of the basin which results in a rich concentration of organic matter. This mudrock was deposited in anoxic water conditions that were 10 to 50 m deep (Tyson and Pearson, 1991).

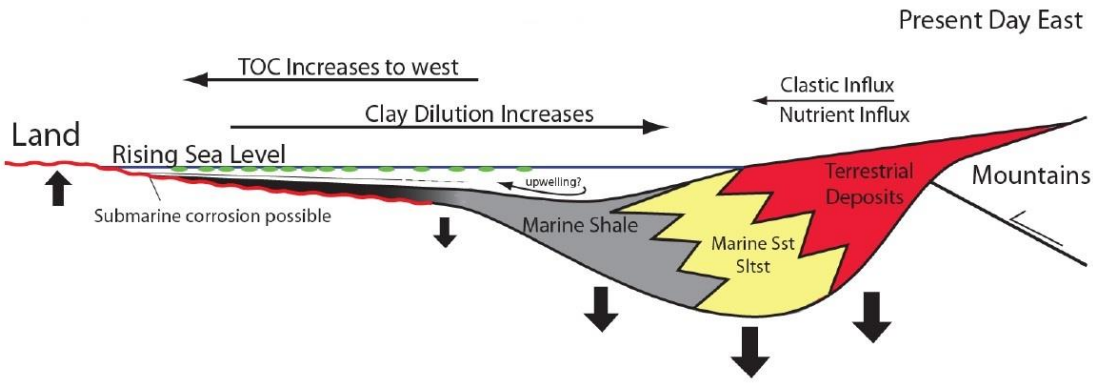

Figure 15: Depositional environment of organic rich mudrocks in New York (Smith and Leone, 2010).

Total Petroleum System of the Utica Shale

The Utica Shale total petroleum system was discovered in the late 1880s in central Ohio (DeBrosse and Vohwinkel, 1974). Discovered oil and gas resources in the basin represent only 15 to 20 percent of the remaining reserves (Ryder, 2008). Reservoirs of the total petroleum system are generally at depths of less than 6,000 ft. There are also scattered gas fields in the total petroleum system which occurs in the deeper parts of the basin in central Pennsylvania about 7,000 and 12,000 ft. During the late 1990s, most active petroleum exploration has targeted gas accumulations in hydrothermal or fractured dolomite in the Upper Ordovician Trenton and Black River Limestone of south-central New York (Smith, 2006).

Interest in the Utica Shale has increased due to recent estimates of potential natural gas production. The Utica Shale extends throughout the Appalachian Basin, and has thickness ranging from 350 to 700 feet (Fig. 6). In order to produce commercial amounts of natural gas from any tight shale, the shale needs to be mature. Cracking of the reservoir is also required to release the hydrocarbon. However, increasing maturation

causes a loss of carbon and hydrogen from shale because of hydrocarbon generation. Therefore, increasing thermal maturity decreases Total Organic Carbon (TOC). TOC values (in wt percent) for the Utica Shale are generally greater than 1-percent, and TOC values increase in the southern portion of the Appalachian Basin which is where the Utica Shale also thickens (Fig 16). Utica Shale TOC measurements for core and outcrop samples are expressed as (Nyahay et al., 2007);

- Indian Castle < .5%
- Dolgeville .5-1.5%
- Flat Creek 1.5-3%

The Utica Shale is characterized by Type II Kerogen, which is typically prone to oil generation. Oil-source rock correlations of samples from Utica Shale reservoirs in Ohio and from group of oils from Cambrian and Ordovician reservoirs suggest a positive oil-source rock correlation. Alkane distributions of these samples indicate odd-numbered n-alkanes between nC11 and nC19 (Ryder et al., 1998). The Trenton Limestone is also characterized by an important source rock of this group; however, this source rock occurs mostly in the thrust belt fields of southwestern Virginia and eastern Tennessee.

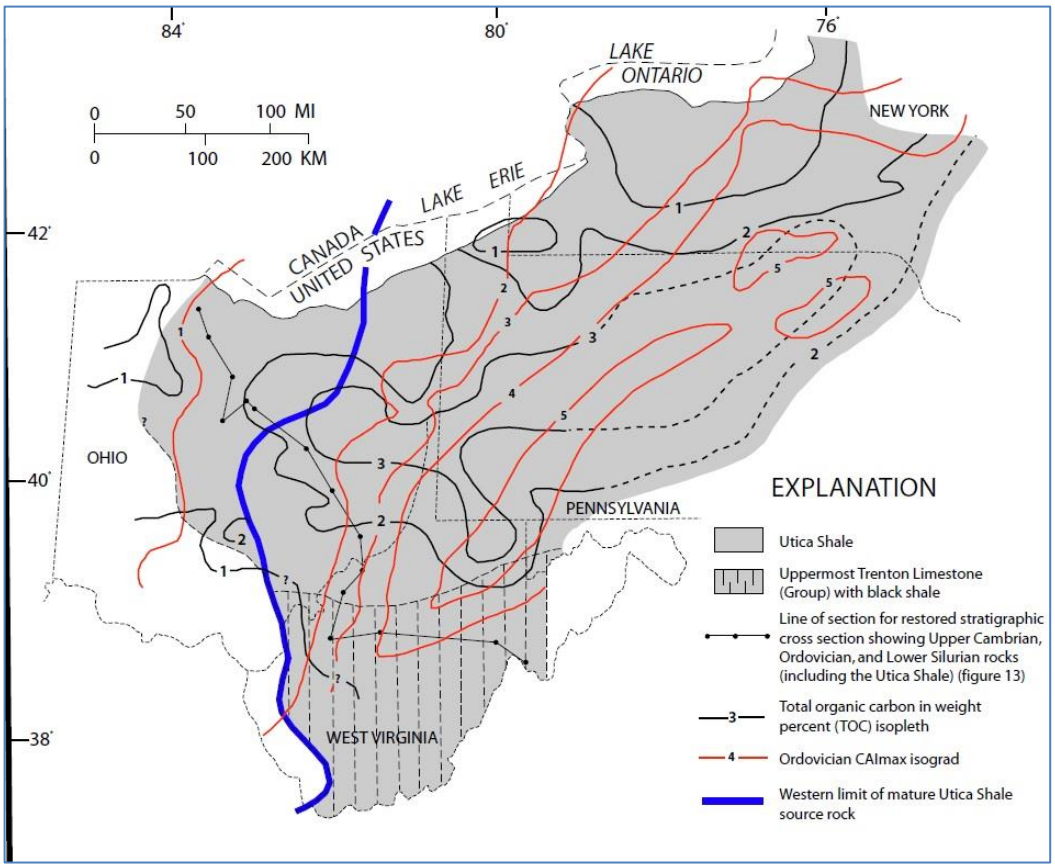

Figure 16: Distribution of weight percent total organic carbon (TOC) content in the Utica Shale (Ryder, 2008).

Nyahay, et al. (2007) evaluated the thermal maturity of the Utica Shale in New York and found it to be within the range of dry gas generation. Burial history and thermal history models of the Utica Shale indicate that Utica Shale entered the oil window in the Late Devonian (~ 385 Ma) and entered in the gas window in Middle Mississippian time (~ 330 Ma). Vertical and lateral hydrocarbon migration occurred in the Utica Shale until the early phases of post-Paleozoic uplift and erosion. There are also multiple pathways that migration has followed which involve secondary porosity and dissolution zones along the Knox unconformity (Ryder, 2008).

In terms of reservoir rock characteristics of the Utica Shale total petroleum system, the Upper Ordovician Black River/Trenton Limestone and Upper Ordovician Queenston Sandstone are evaluated in the 2002 USGS assessment. The majority of the Black River/Trenton Limestone reservoirs are characterized by hydrothermal dolomite by the alteration of limestone host rock to dolomite in the fault zones. These hydrothermal dolomite reservoirs are characterized by vuggy and fracture porosity (Smith, 2006) and initial reservoir pressures are less than 0.43 psi/ft (Nyahay et al., 2007). The sandstone reservoirs in the Queenston Sandstone are characterized by fine-grained quartz with permeability values of about 0.20 milidarcies and porosity of about 3 to 4 percent. There are also some secondary reservoirs which are considered to be negligible.

The traps in the Utica total petroleum system are either stratigraphic traps or structural traps. Stratigraphic traps include some unconformity traps and sedimentary-facies pinchouts. Structural traps are characterized by low-amplitude anticlines and faults. The Salina Group that contains halite and anhydrite is the regional seal of the Utica total petroleum system (Ryder, 2008).

According to recent mineralogical and lithological data, Thériault (2012a, b) divide the Utica Shale into two units (lower and upper). The lower group shows a mineralogical composition similar to the underlying Trenton Group. The mineralogy of the upper Utica Shale represents a transition into the overlying Lorraine Group. The thicknesses of these units are similar; however, there are some significant differences.

Lorraine shales are calcite-poor with quartz and feldspar dominance; whereas, the Utica Shale is rich in calcite. Calcite content decreases from the Trenton Group to the base of the Utica Shale, then increases up to the middle part of the Utica Shale, and lastly

decreases to its minimum value at the base of Lorraine Group. There is an inverse trend of quartz and feldspar to the calcite (Thériault, 2012b) (Fig. 17).

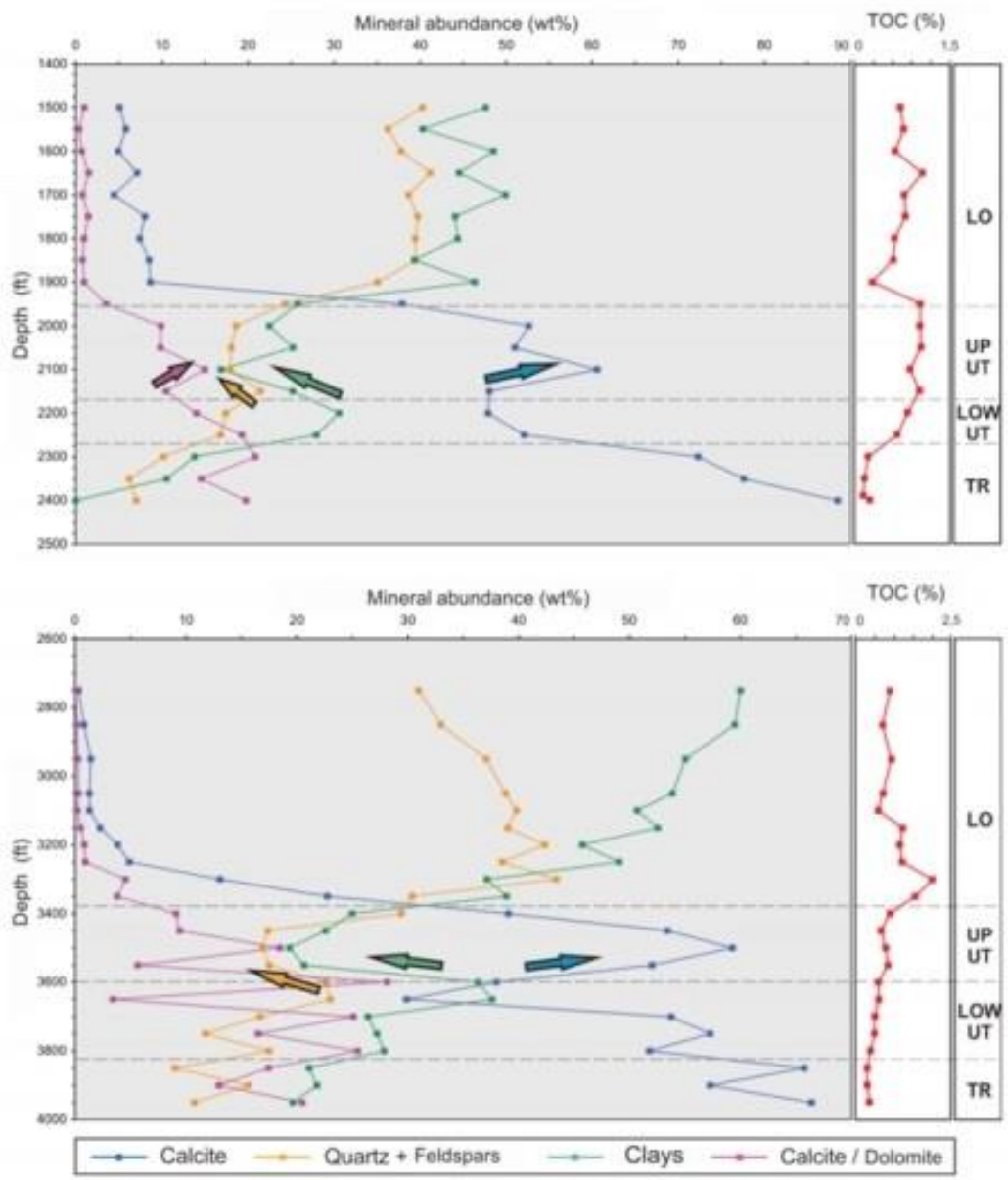

Figure 17: Vertical mineral trends for the Trenton (TR) to the Lorraine (LO) groups (modified from Thériault, 2012a).

Biostratigraphic Setting of the Utica Shale

The transition from a carbonate ramp to a black-shale basin corresponds to the biostratigraphic setting of the Utica Shale. The replacement of graptolite-rich Utica Shale is regionally diachronous where there are set of graptolite biozones within the black shales (Riva, 1969). The black shale deposition starts with the deposition of the Dolgeville Formation where it is composed of Utica and Trenton beds and shows the transition of facies. There may also be a deposition of lowstand fans during the relative drop in sea level (Baird and Brett, 1994). The Indian Castle Member of the Utica Shale overlies this succession as alternating black shales. There are four graptoloid biozones that represent the biostratigraphy of the Utica Shale (Fig. 18) (Goldman et al., 1999).

THE CORYNOIDES AMERICANUS ZONE

The initial observance of graptoloids in the upper Middle Ordovician rocks represents a gradual succession of species. The succession includes Corynoides americanus, Climacograptus caudatus, Dicranograptus nicholsoni, Normalograptus brevis and Lasiograptus harknessi. These fossils show the change of depositional environment from carbonate shelf to deep basin.

THE ORTHOGRAPTUS RUEDEMANNI ZONE

The base of this zone is characterized by the disappearance of the C. americanus zone and the appearance of a low-diversity fauna. This zone characterizes the shallow basin during this interval and there is no evidence of any facies shift.

THE CLIMACOGRAPTUS SPINIFERUS ZONE

The set of black-shale depositions mark this zone with several new species, including some spiniferus and Climacograptus caudatus species.

THE GENICULOGRAPTUS PYGMAEUS ZONE

The K-bentonite rock study shows the discontinuity within the Utica Shale marked by the C. spiniferus/G. pygmaeus boundary.

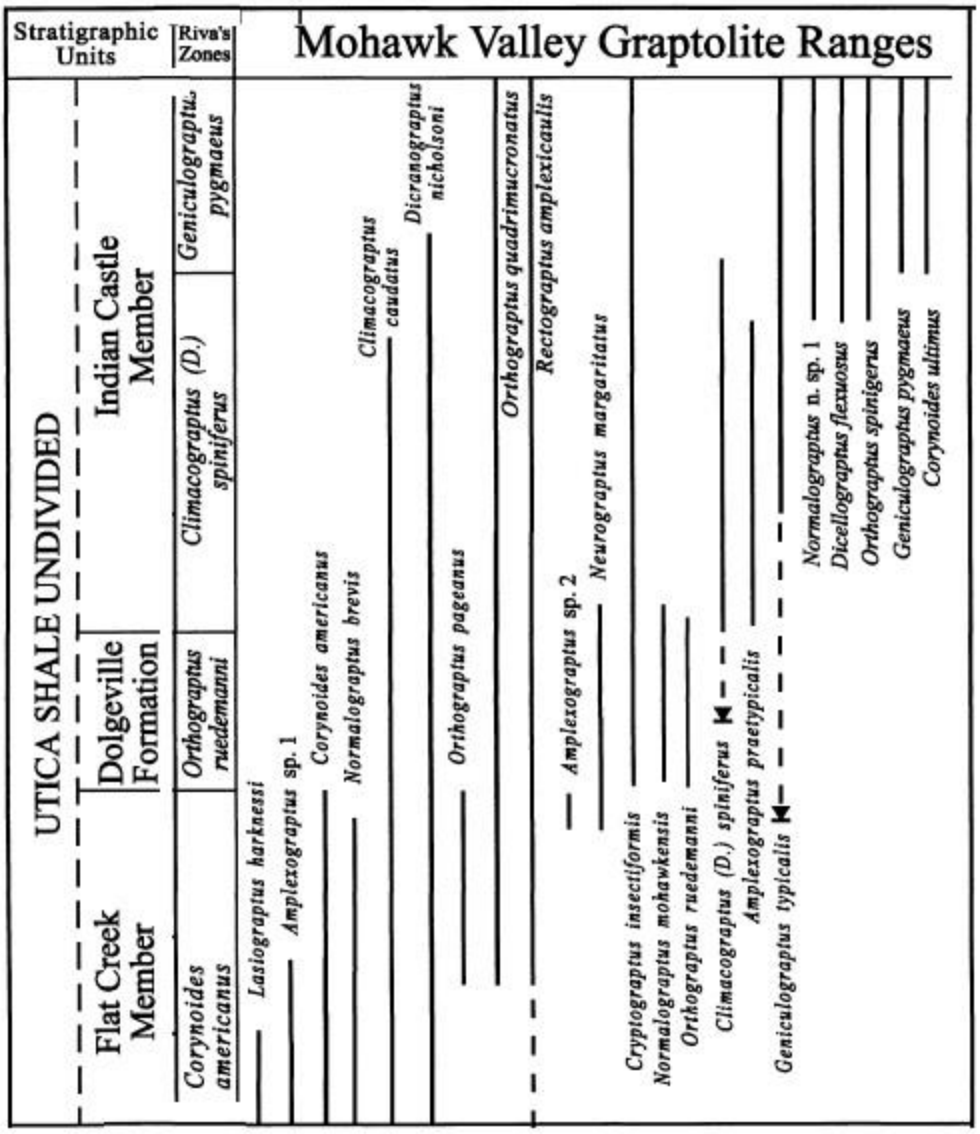

Figure 18: Stratigraphic ranges of Utica Shale graptolites in the Mohawk Valley (Riva, 1969).

The faunal turnovers that define the biozones indicate maximum flooding surfaces. The graptoloid distribution occurs laterally across the basin, and parasequences are missing in the shallower parts of the basin. There is a well-defined synchrony between the Utica Shale graptolite fauna and the sedimentary facies (Goldman et al, 1999).

CHAPTER 2 RESEARCH DATABASE

Introduction

Key database elements used in this research included digital well logs, synthetic seismogram-based time-to-depth calibration, and 3C3D data to initiate an integrated reservoir characterization of the Utica Shale in Bradford County, Pennsylvania. In order to define this exploration target within the P-P seismic data and converted-wave seismic (P-SV) volumes, all three data components were integrated.

Well Data

Well top information obtained from the IHS website (ihs.com) is an important part of my research database. This information includes the interpreted stratigraphic picks (in measured depth) of the Utica Shale Formation and its neighboring geologic units in Bradford County, Pennsylvania. This database is summarized in Table 1. The associated well locations relative to 3C3D study area are represented in Figure 19.

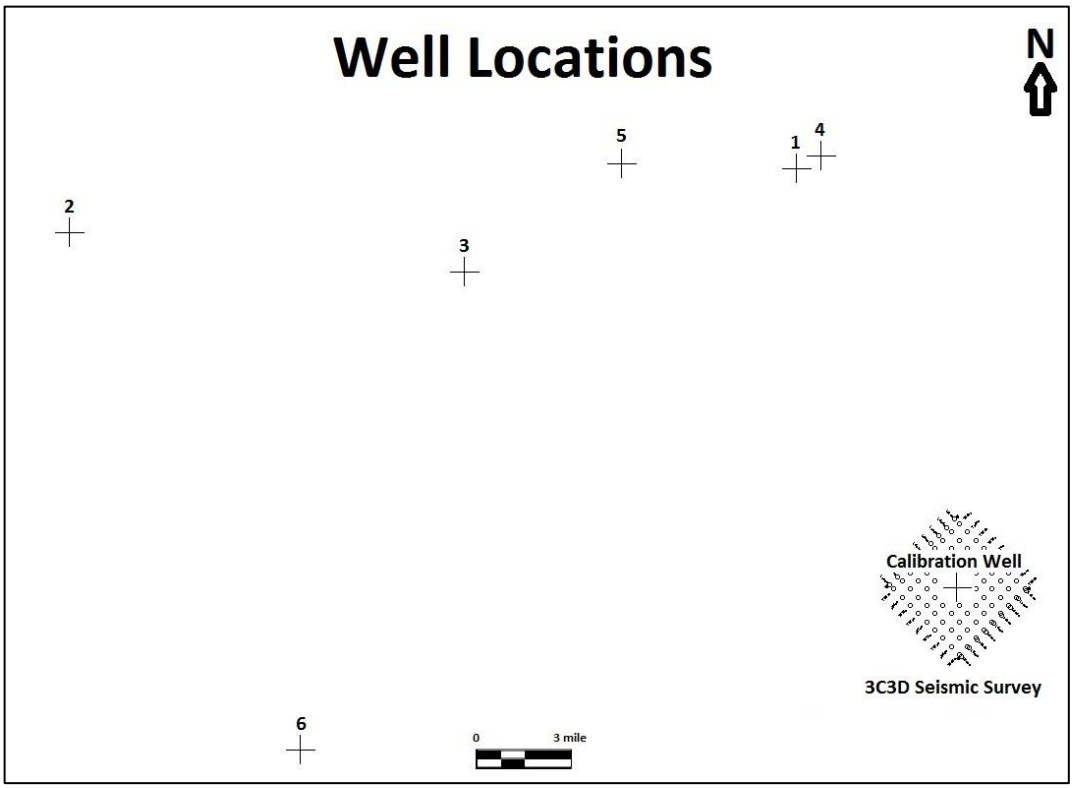

Figure 19: Well locations having Utica Shale depth information with respect to the 3C3D survey.

Although the location of the control wells with respect to the 3C3D survey can be considered as "too far away", the stratigraphic picks for the Utica Shale, Trenton Limestone, and Queenston Sandstone Formations at these wells were used to create regional contour maps that extended into the 3C3D survey. This mapping allowed an estimation of the depth to Top Utica Shale, which was then used to estimate the two-way time position in P-P wave and P-SV wave seismic data volumes.

Time-to-Depth Calibration Using Synthetic Seismograms

Dipole-sonic log data were used for time-to-depth calibration. These data enabled me to measure the P-wave (P-P), fast-S (P-SV_1), and slow-S (P-SV_2) velocities and to estimate P-SV anisotropy. Depth profiles of P-P and P-SV wave velocities were created by velocity logs recorded in the calibration well. Combining these velocity logs with the density log enabled me to create synthetic seismograms.

The calibration well positioned at the center of the seismic image space was used for depth registering two-way time-based P and S seismic data to depth-based stratigraphic interpretations and digital well logs. However, the calibration well at the center of 3C3D survey (Fig. 20) terminated at the base of the Onondaga Limestone (6382 ft). In order to make a constrained estimation of the deeper Utica Shale Formation (approximately 12,000 ft) we used the P-P and P-SV calibration results from Hardage et al., 2012, then assumed an increasing linear time-depth function (velocity) to the deeper estimated Utica Shale Formation. As a result, I will describe my interpreted Utica Shale horizon as a "near Utica Shale horizon".

3C3D Seismic Data

The 3C3D multicomponent seismic data were acquired in Bradford County, Pennsylvania. The seismic survey represents an orthogonal brick pattern (Fig. 20). There are thirteen receiver lines deployed northwest-to-southeast at intervals of 880 ft (268 m). 3C microelectromechanical systems (MEMS) formed a 2mi - 2mi (3.2 km – 3.2 km) square with 97 receiver stations spaced at intervals of 110 ft (33.5 m) on each receiver line. Explosive charges of 2.2 lbs buried a depth of 20 ft (6 m) were used as energy

sources to generate P and S data across this 3C3D survey. Source stations were spaced 220 ft (67 m) apart with a gap of 880 ft (268 m) between source line segments. There were 41 source lines spaced at intervals of 660 ft (201 m) to form a southwest-to-northeast orientation of brick pattern source stations. Trace gathers created from responses from vertical, radial-horizontal, and transverse-horizontal surface geophones are displayed on Figure 21.

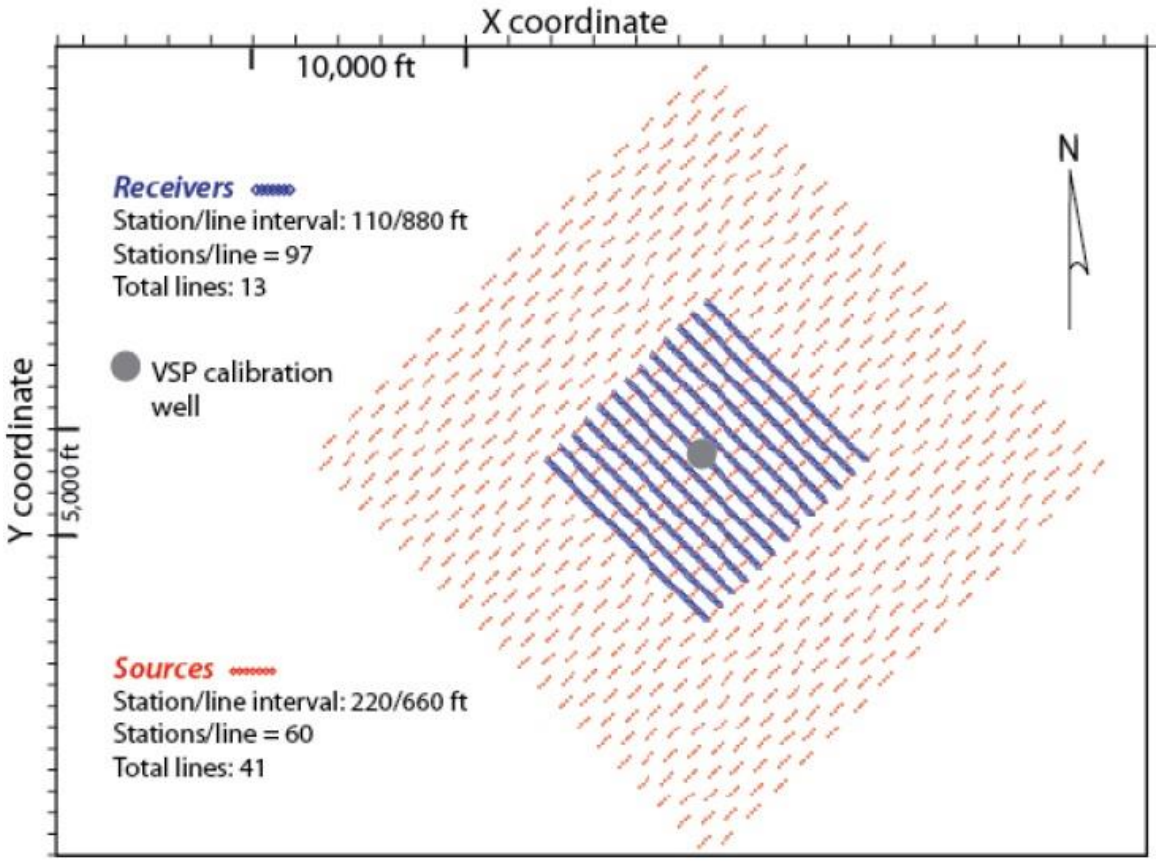

Figure 20: Map of the 3C3D study area showing the seismic acquisition survey (Hardage et al., 2012).

These data give a first look at the quality of the seismic data. The Utica Shale is estimated to be around 1.7s in P-P image time. This examination of trace gathers led to an

observation that the signal-to-noise ratio of 3C3D data at that time is good enough for a valuable multicomponent seismic data evaluation across the Utica Shale.

The identification of a package of reflectors associated with the Utica Shale and its deep geology has been completed in P-P and P-SV data volumes. The mapping of reflections related to the top and bottom of the Utica Shale has been completed. Interpretation and characterization of 3C3D data volumes are discussed in Chapter 3.

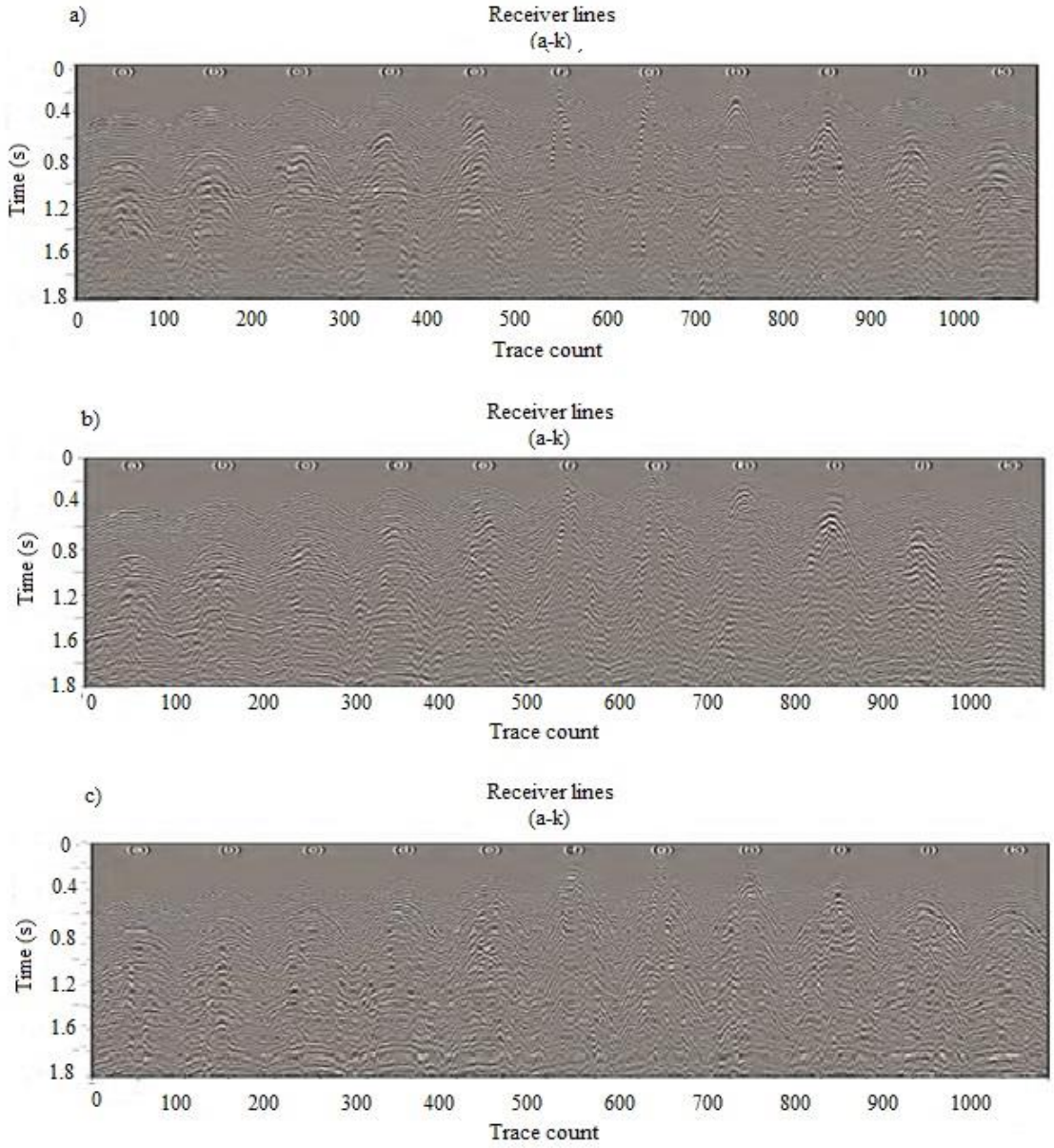

Figure 21: Trace gathers of responses of (a) vertical geophones, (b) radial-horizontal geophones, and (c) transverse-horizontal geophones from the 3C3D data (Hardage et al., 2012).

CHAPTER 3 INTERPRETATION OF MULTICOMPONENT SEISMIC DATA

Introduction

Three time-migrated seismic data volumes were utilized for this study. They were the conventional P-wave volume (P-P), a fast-S converted-shear (P-SV_1) volume, and a slow-S converted-shear (P-SV_2) volume. If azimuthal anisotropy is present in the rock formation, two separate shear waves, S1 and S2, are created by shear-wave splitting in a phenomenon called birefringence. There is a time delay between these two shear waves which indicates the amount of anisotropy, with S1 being the faster S-wave. S1 polarization is generally parallel to maximum stress. The use of multi-component seismic data allows fractures to be identified and improves interpretation of features caused by heterogeneity (Sandanayake and Bale, 2011).

Both P-SV volumes were created by CCP (common-conversion point) procedures. CCP imaging is valid if the velocities of the downgoing P mode and the upgoing SV mode are different. Prestack migration of P-SV reflections was implemented to construct converted-mode images (Hardage et al., 2012). Each data volume consisted of 30,448 data traces. Each data trace was 4 seconds long. Image bin dimensions were 110-ft x 110-ft (33.5-m x 33.5-m). The seismic images spanned an area of approximately 9.3 mi^2 (23.8 km^2).

Well data including the Utica Shale tops, Trenton Limestone tops, and Queenston Sandstone tops were valuable for depth registering these P and S seismic data.

Seismic Data Quality

Initial examinations of the P-P, P-SV_1, and P-SV_2 data volumes are important indicators of the quality of each seismic data set. Examples of P-P, P-SV_1, and P-SV_2 data volumes are illustrated in Figure 22, 23, 24, respectively. All data volumes are distorted by migration irregularities along the edges of their image space. However, S-wave data volumes are more distortion than the P-wave volume. Regardless, the study area has good seismic data quality over 95% of the P-P image space and over 60% of good image space in the P-SV data sets. Figure 22-24 show these edge effects for the P-P, P-SV_1, and P-SV_2 data volumes, respectively.

The migration data processing phase of the Utica Shale (deep seismic reflection data) can produce migration artifacts at the edge of seismic data. The reason for the migration effects can be explained by poor signal penetration because of the truncations on the stack section. Because the signal-to-noise ratio is dramatically decreased at the edges of the seismic data, it is not possible to map key geologic horizons near the outer boundaries of the data volumes, which limits the interpretation of deep geology. Another possible reason for the migration edge effects can be explained by strong lateral velocity variations, when the deep seismic reflection data were processed, velocity picking controls the quality of a seismic image. Weak reflections at the edges of seismic data may indicate the presence of subsurface faults, but these dipping layers may be artifacts produced during the acquisition or processing phases of seismic data (Calvert, 2004).

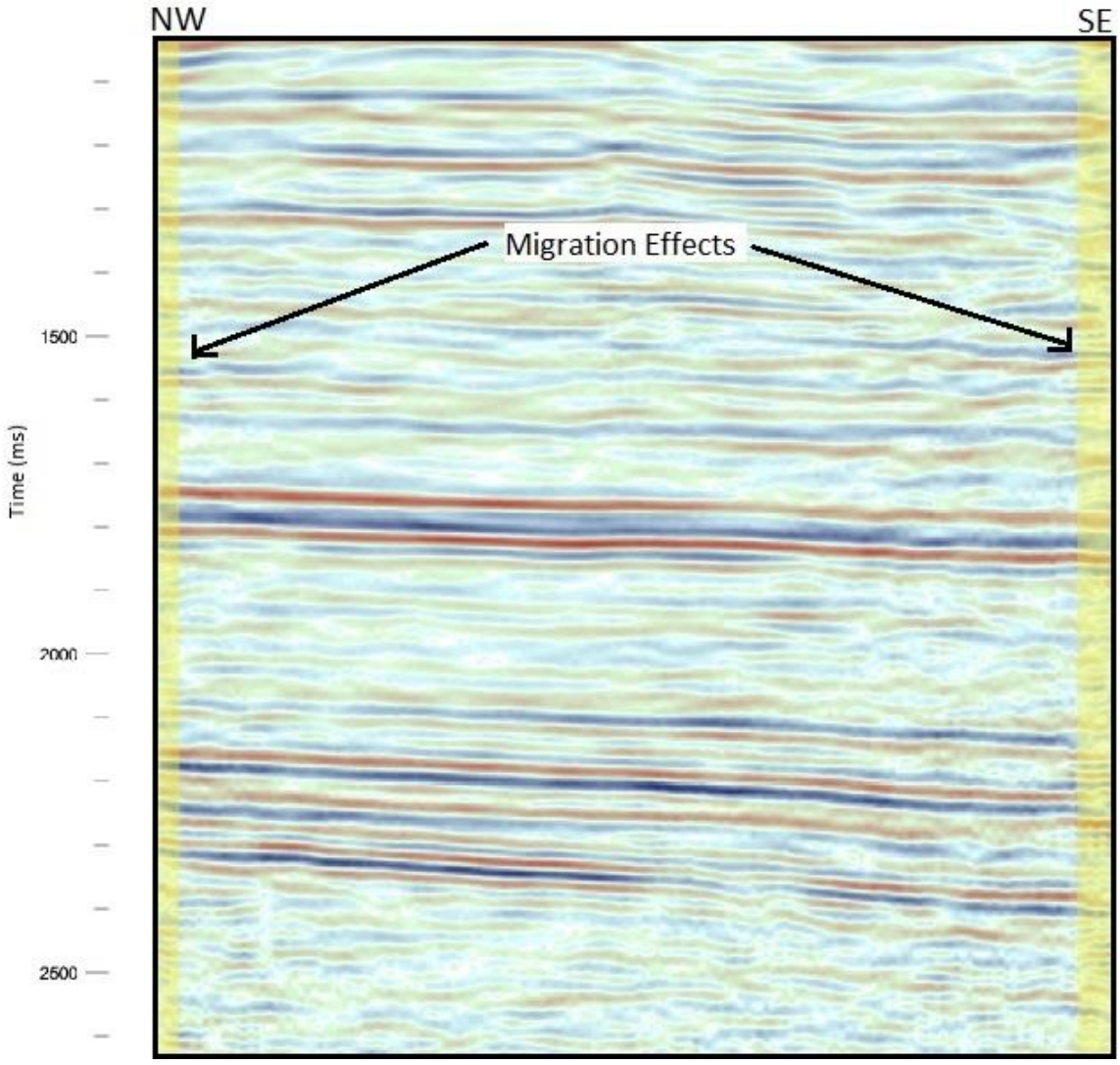

Figure 22: Migration effects (shaded areas) along the edges of the P-P image space.

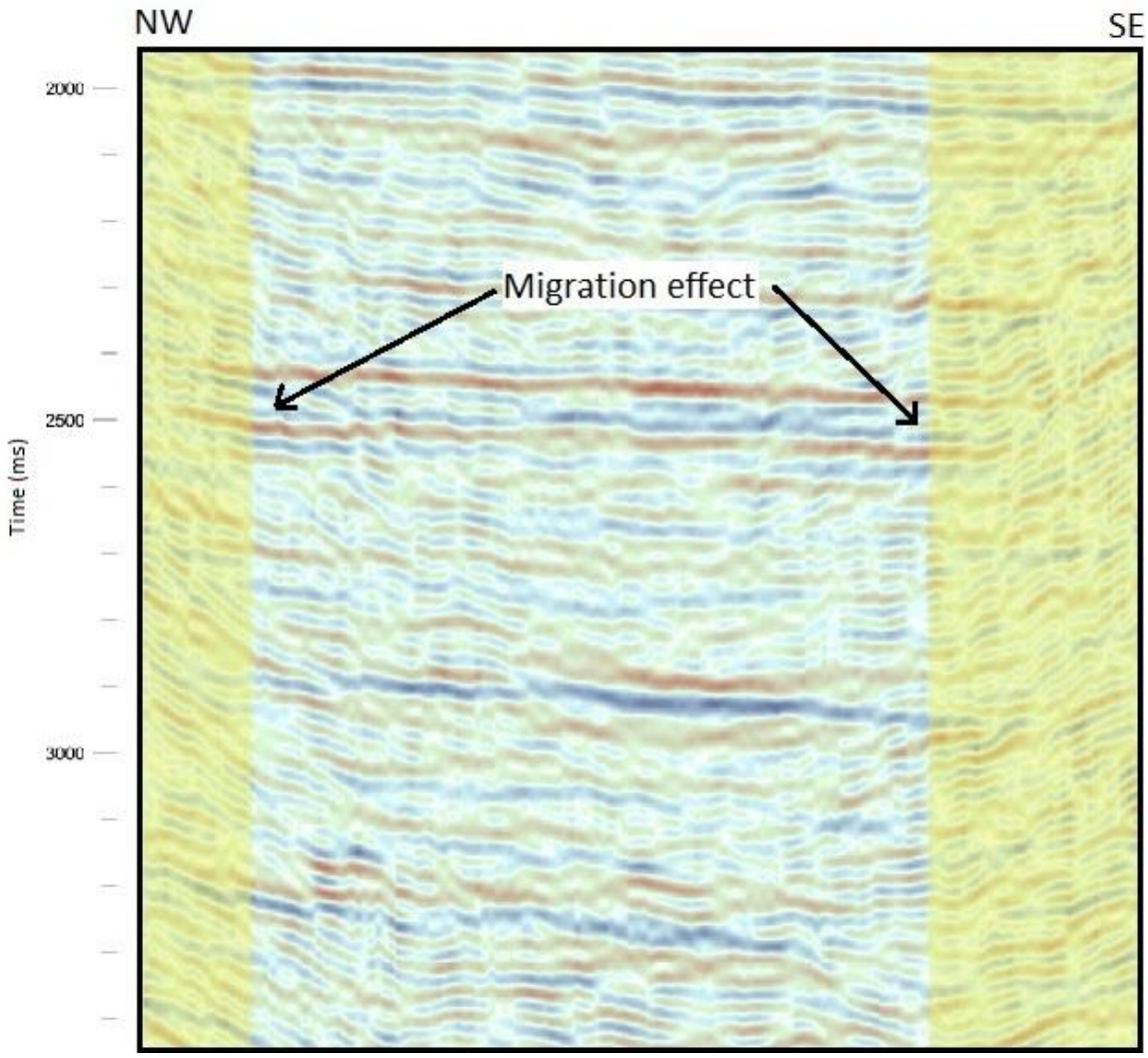

Figure 23: Migration effects (shaded areas) along the edges of P-SV_1 (fast-S) image space. Note the increase in reflection dip inside the shaded areas.

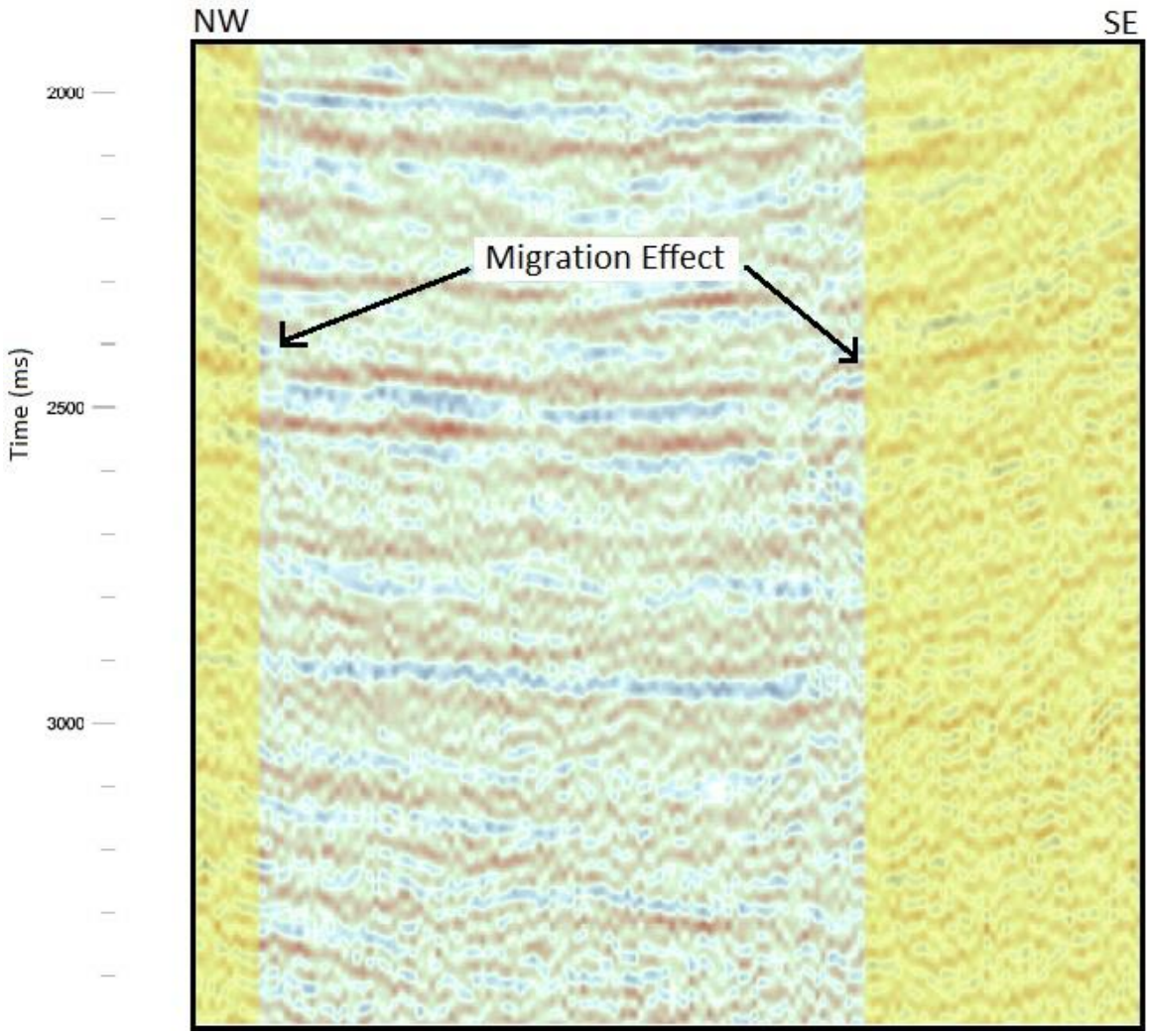

Figure 24: Migration effects (shaded areas) along the edges of P-SV_2 (slow-S) image space. Note the increase in reflection dip inside the shaded areas.

Frequency Spectra Analysis

Spectral analysis of P-P, P-SV_1, and P-SV_2 data characterizes the frequency content of each seismic data volume. The P-P data volume has a flat frequency spectrum between 10 and 40 Hz that reduces to -60 dB at 100 Hz (Fig. 25). The P-SV_1 data volume has a flat frequency spectrum between 10 and 30 Hz and reduces to -50 dB at 60 Hz (Fig.

26). The P-SV_2 data volume has a flat frequency spectrum between 10 and 30 Hz and reduces to -40 dB at 50 Hz (Fig. 27).

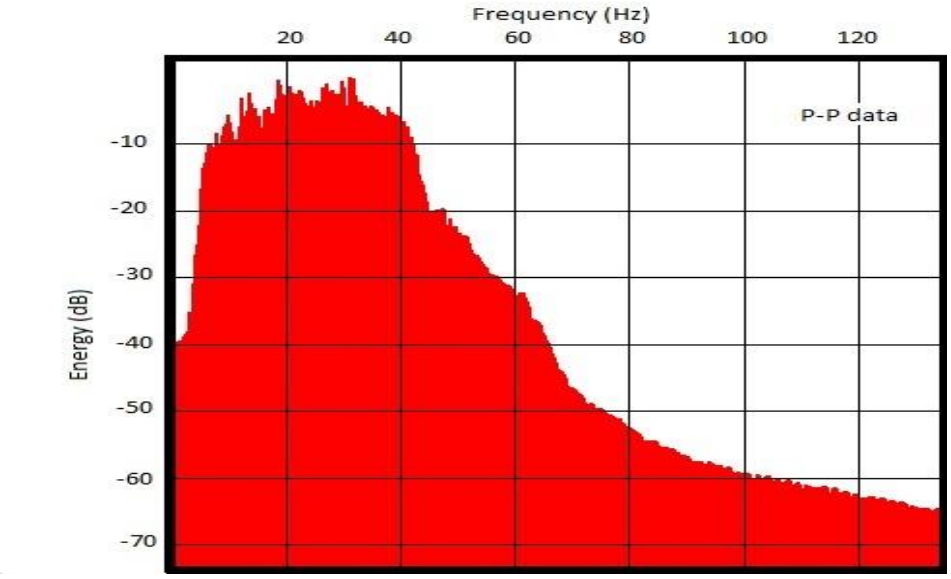

Figure 25: Frequency spectrum of P-P data.

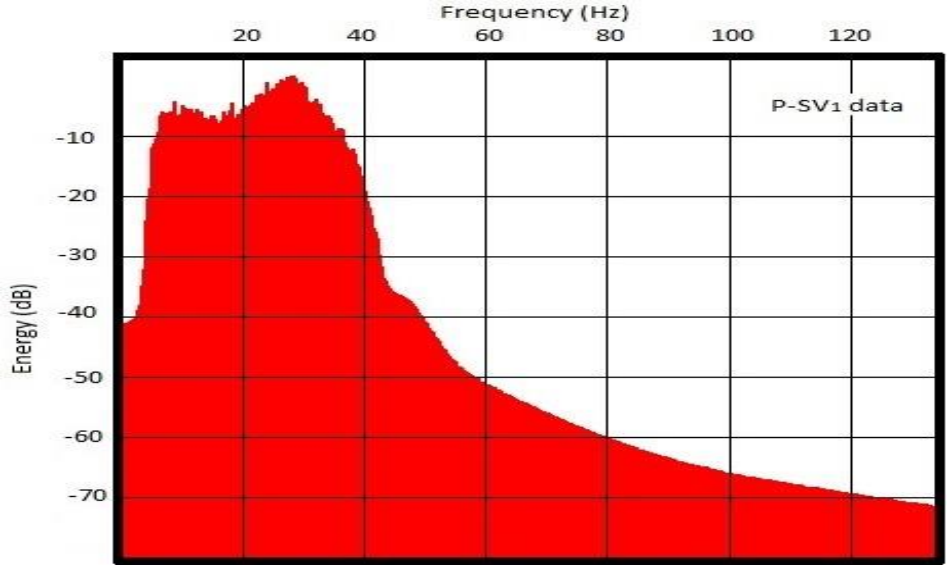

Figure 26: Frequency spectrum of P-SV_1 data.

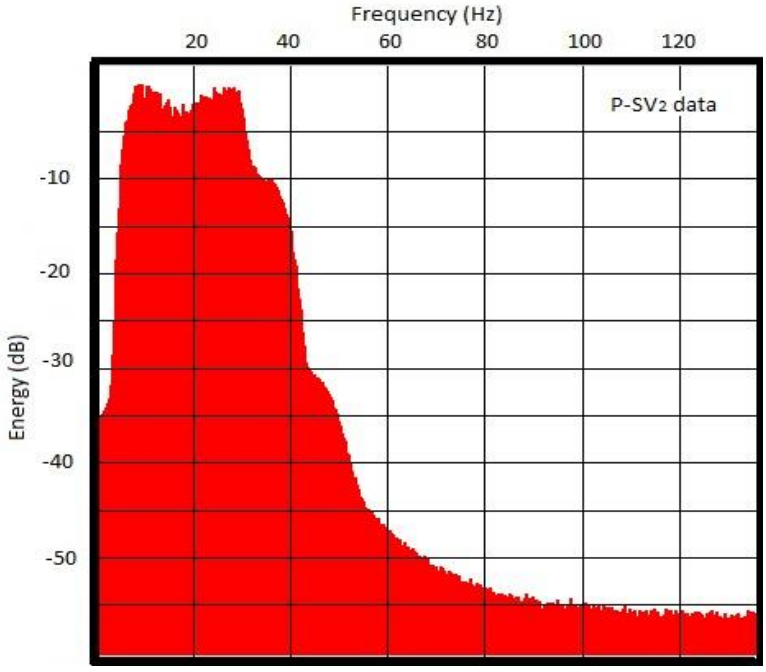

Figure 27: Frequency spectrum of P-SV_2 data.

These analyses reveal important information about the vertical (resolution) limits of the data volumes. Vertical resolution limits are determined by a relationship between velocity (V), frequency (f), and wavelength (λ) of the seismic wavelet at a particular interval. An entire stratigraphic unit (top-to-bottom) can be successfully resolved (mapped) in seismic data when the unit thickness is less than ¼ wavelength of the seismic wavelet. The detection limit, a more subtle expression, is 1/32 wavelength for a stratigraphic unit (Sheriff and Geldart, 1995).

$$\lambda = V/f$$

Equation 1: Wavelength calculation

In the study area, the average P-wave internal velocity for the Utica Shale Formation is estimated to be 15,750 ft/s (~4,800 m/s) and the dominant frequency is about 30 Hz (Fig. 25). Using the formula above we determine λ is approximately 530 ft (~160 m) for this interval (Eq. 1). Therefore, the resolution limit in P-P data for the Utica Shale is about 130 ft (~40 m) and the detection limit is about 16 ft (~5 m). This analysis pushes the limitations of the seismic data because the Utica Shale is deposited relatively deep.

P-P Depth Registration of Geologic Horizons

Multicomponent seismic interpretation of the Utica Shale and its deep geology was aided by integrating available well information and previous studies (Hardage et al., 2012). It is important to select which geologic stratal surfaces are key elements of the geologic horizons. The key horizons were selected as Trenton Limestone, Queenston Sandstone, and Basement. The seismic signature of the Trenton Limestone cannot be observed with these data, but the Trenton Limestone is deposited just under the Utica Shale (Fig. 7). The Queenston Sandstone can be important for hydraulic fracturing purposes. The Basement surface also cannot be ignored when interpreting the Utica Shale and its deep geology.

Well information obtained from the IHS database (ihs.com) included stratigraphic tops interpreted for the Utica Shale, Trenton Limestone, and Queenston Sandstone Formations. This information provides important first impressions about the position of key geologic horizons in 3C3D image space. The position of the Top of Precambrian basement data was obtained from the Pennsylvania Department of Conservation and Natural Resources database. This database shows basement contours for Bradford County

that allowed me to estimate the position of the Basement surface in 3C3D image space (Fig. 28). The regional structural contours of Basement surface range between 14,760-21,300 ft (4,500-6,500 m). Within the 3C3D survey, the Top of Precambrian basement was mapped across the study area, and then converted to depth structure by using synthetic seismograms to establish time-to-depth calibrations. The Basement surface is presented in Figure 30. It is noted that both the structure contours of the Precambrian basement (Fig. 28) and the Top of Precambrian basement surface interpreted from the seismic volumes (Fig. 29) dip to the south-southeast, adding to our confidence that the horizons mapped in the seismic data represent key geologic horizons within the study area.

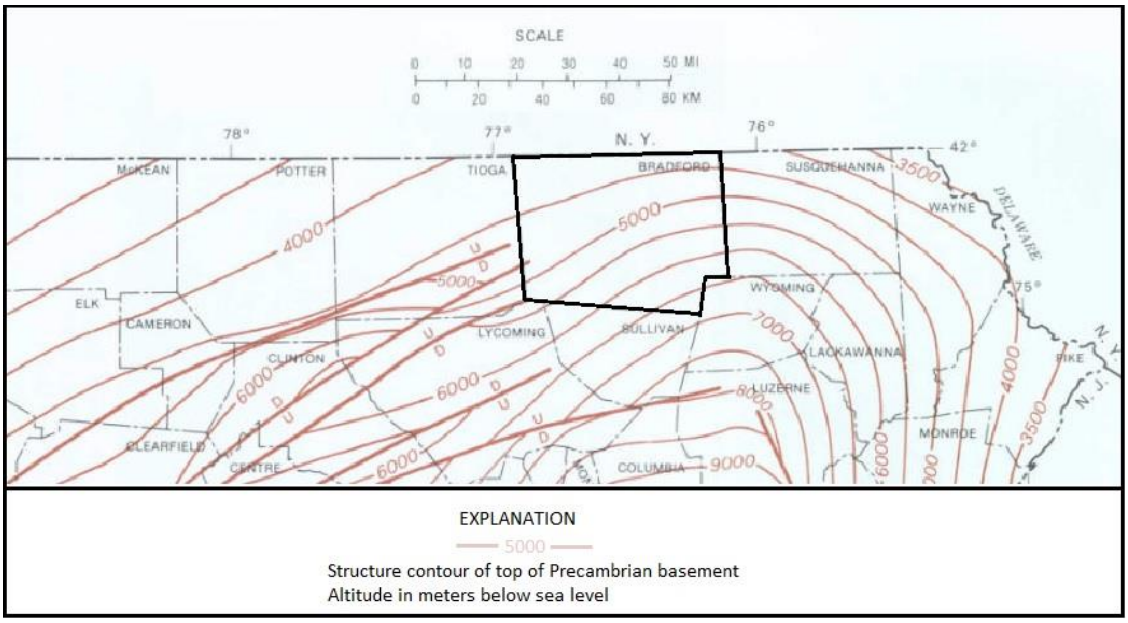

Figure 28: Structure contours on subsurface Precambrian basement in Pennsylvania (modified from DCNR). Outlined area is Bradford County, Pennsylvania.

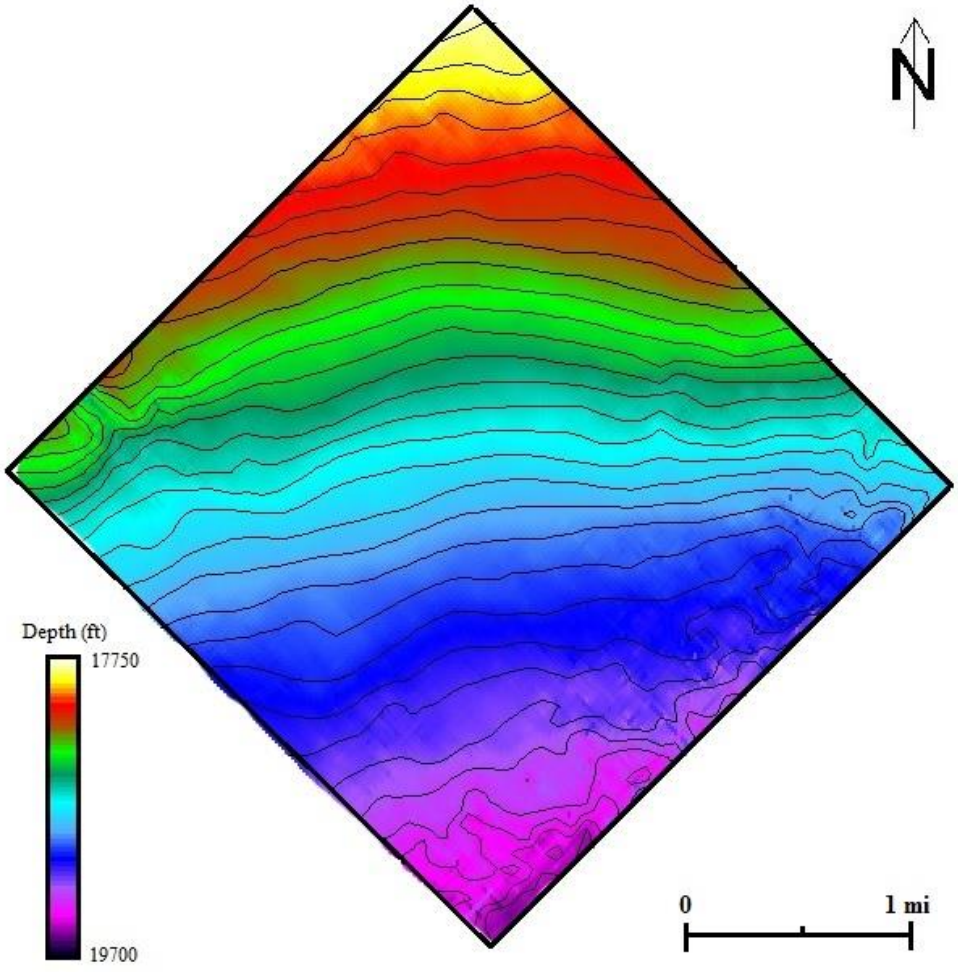

Figure 29: Structural contour map of the top Basement surface (Contour interval is 50 feet).

Time-to-Depth Calibration

It is necessary to determine which reflection events correlate with the key geologic horizons analyzed in this study. A reliable time-to-depth calibration from a previous study (Hardage et al., 2012) was used as an interpretation starting point for the shallower seismic horizons. Synthetic seismograms were generated using density and sonic logs for matching real data extracted from near the calibration well. A time-to-

depth function was created for the P-P and P-SV modes, respectively. Each function was applied to the calibration well and its corresponding seismic mode (P-P or P-SV). The individual P-wave data and S-wave modes are interpreted by using their respective time-to-depth functions. Because, the calibration well is terminated at the Onondaga limestone, time-to-depth calibration of P and S seismic data is only allowed down to the Onondaga limestone and is considered to be reliable (Figs. 30-32) (Hardage et al., 2012).

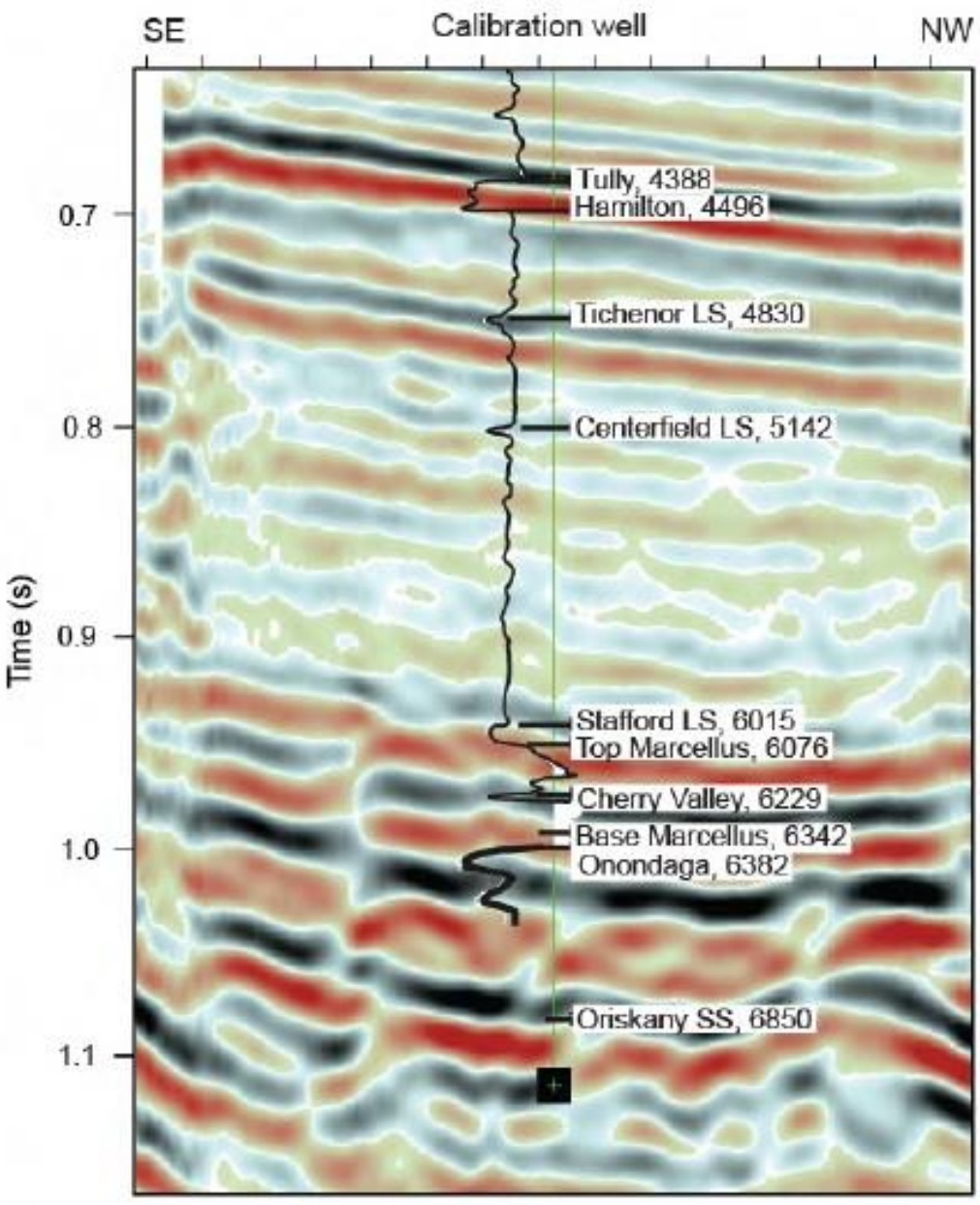

Figure 30: Time-to-depth calibrated geologic horizons in P-P image-time space (Hardage et al., 2012).

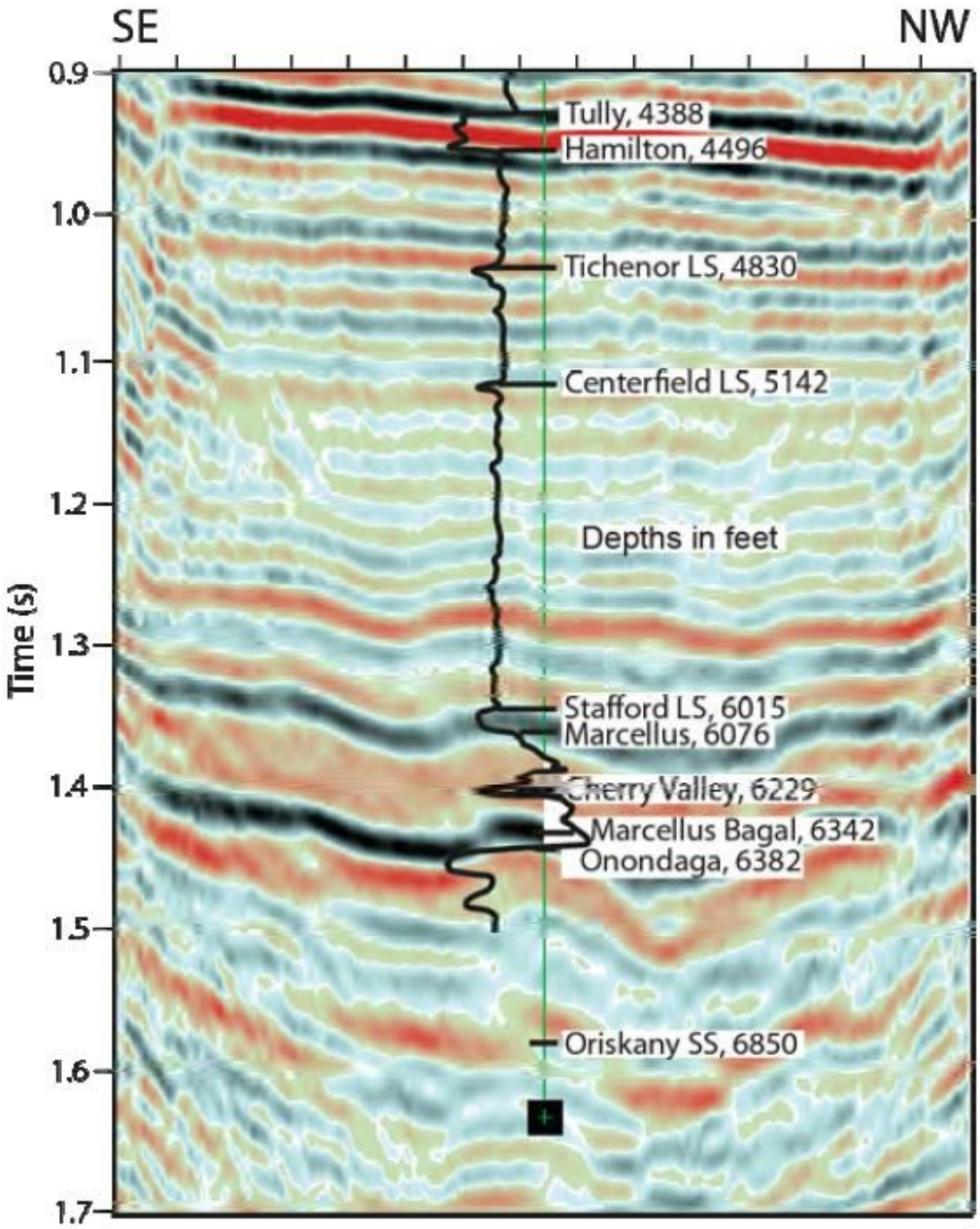

Figure 31: Time-to-depth calibrated geologic horizons in P-SV_1 image-time space (Hardage et al., 2012).

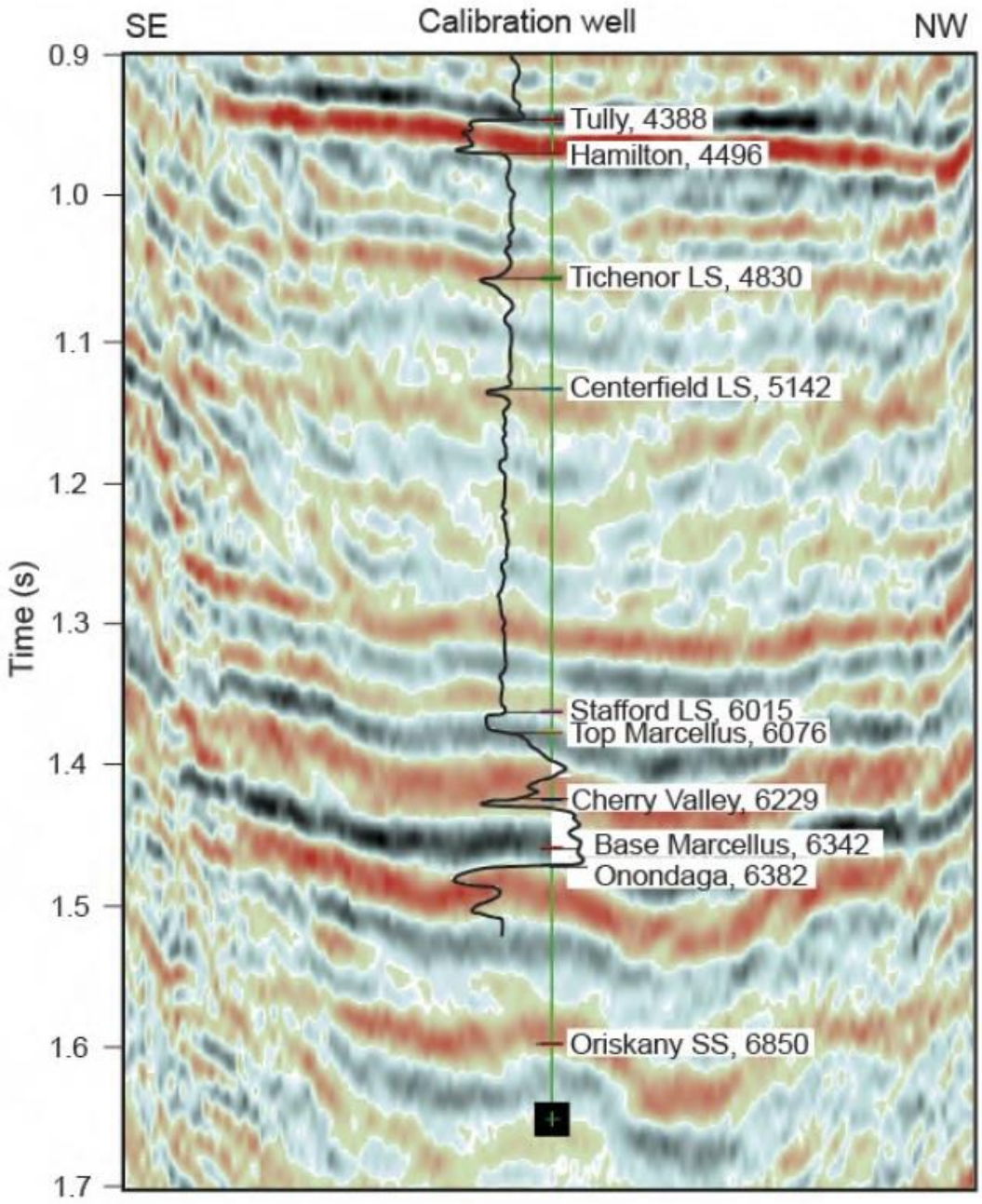

Figure 32: Time-to-depth calibrated geologic horizons in P-SV_2 image-time space (Hardage et al., 2012).

Seed Horizons

Seed horizons are interpreted as chronostratigraphic surfaces along mappable seismic reflection events. These chronostratigraphic surfaces are assumed to be deposited at a common geologic time. Important points when interpreting these geologic time horizons are the interpreter's confidence in selecting targeted geologic horizons in a seismic data volume and the validity of the interpretation of that particular reflection event. If the reflection event has good signal-to-noise ratio, interpreted horizons are easily mapped and are more relevant to chronostratigraphic surfaces.

Interpreted profiles along inline and crossline directions are separated by Δx and Δy, respectively. The important point when determining an appropriate, Δx and Δy is based on the confidence of the interpreter. To prevent interpreted geologic horizons from jumping to an incorrect reflection event, key horizons in the data volumes were interpreted along every profile. This approach increases the confidence and validity of my interpreted horizons.

In order to construct compatible stratigraphic correlations between P-P, P-SV_1, and P-SV_2 data volumes, P-wave and S-wave horizons were mapped separately. Some uncertainty is introduced because of the distortion of the seismic images near the edges of the image space. Thus interpreted geologic horizons along profiles were terminated before reaching the data volume edges. This requirement was more common with the interpretation of P-SV_1 and P-SV_2 data volumes than with the interpretation of the P-P volume.

The objective of this study is to evaluate the Utica Shale and its deep geology. Because there is only time-to-depth calibration to a total depth of 6382 ft in the calibration well, the identification of the Utica Shale within each seismic volume had to

be estimated using interpolation of known depth to Top of the Utica Shale and estimating which reflector corresponded with these first approximations. The resulting calibrated key geologic horizons for the P-P data volume is presented in Figure 33.

The interpolated locations of the Queenston Sandstone, Utica Shale, Trenton Limestone, and Basement surface are important tools for seismic interpretation of the deep geology. If seismic reflectors can be matched to those approximated interpretations, it would be clear that the interpreted key geologic horizons are within a reasonable range of these selected horizons.

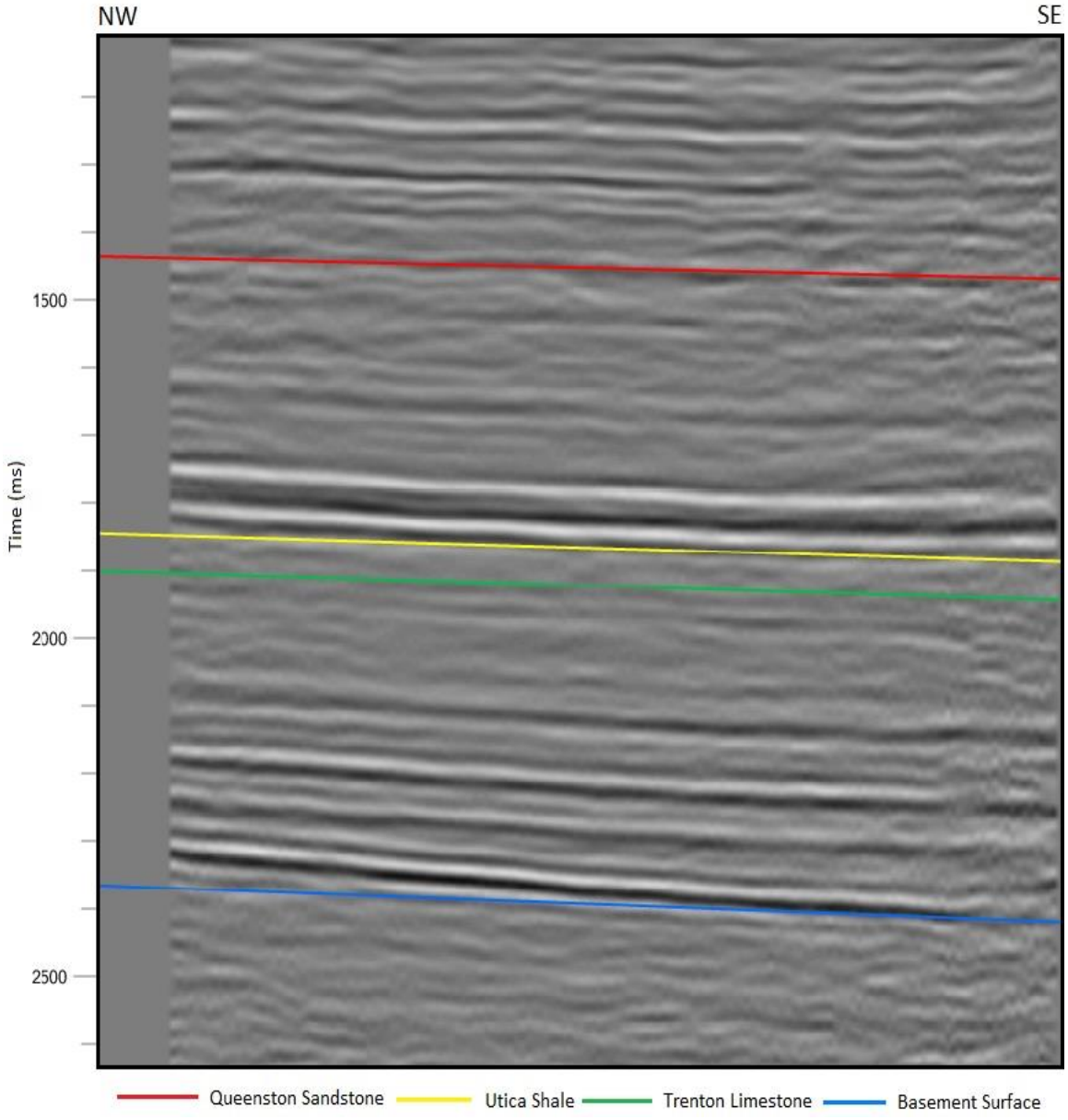

Figure 33: Geologic key horizons obtained from IHS converted to P-P time.

The procedure to convert the 3C3D depth-based P-P horizon to a time horizon is based on a single velocity function. P-wave depth registered horizons are converted to time by using a depth-to-time conversion function. The position of the Utica Shale and its

deep geology are determined by an extrapolation of time-to-depth curves. It is based on the assumption that the velocity change with respect to depth is assumed to be linear below the base of calibration well (Onondaga limestone) and the Utica Shale. This single function is used only to approximate the positions of geologic horizons. As a result, time-converted geologic horizons are approximately correct. Therefore, the interpreted geologic horizons are considered only as approximate definitions of the targeted horizons.

Equivalent P and S Horizons in Image Time Spaces

It is crucial to determine which S reflection is time equivalent to a targeted P reflection event. Without establishing S-to-P registration, P and S seismic attributes cannot be calculated across targeted stratigraphic depth intervals.

My approach to create time-equivalent P and S data volumes was done by working in section views of the data volume. In other words, my approach is based solely on visualization of P and S data volumes. The equivalent P-P time image and its companion P-SV_1 time image is illustrated in Figure 34.

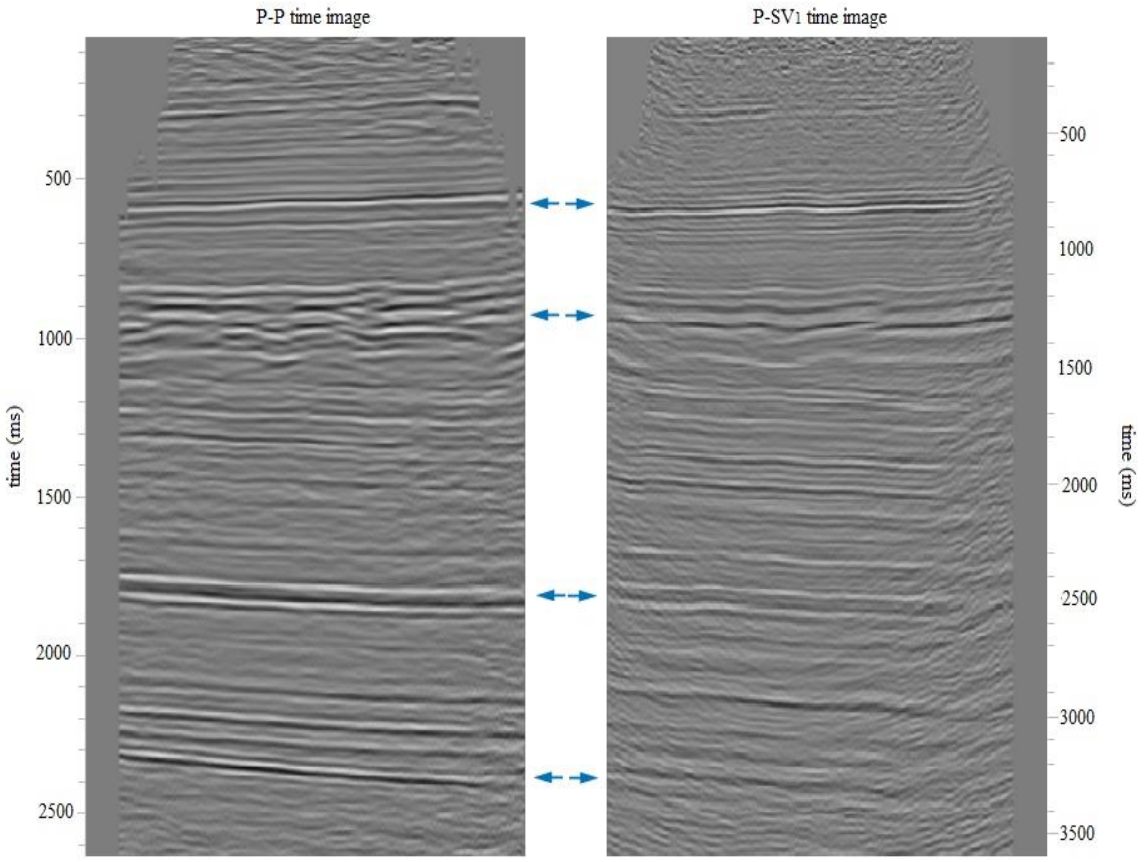

Figure 34: Equivalent geologic horizons in P-P and P-SV_1 image spaces. Note the different time axis.

The comparison of P-P and P-SV_1 image times has similar geologic features as indicated by blue arrows. These arrows mark characteristic features that exist in both data sets. These reflections represent the same geologic horizon in P-P and P-SV_1 image spaces and increase the confidence of the interpretation. Another helpful comparison between two data sets can be achieved using fault surfaces. However, there are no significant faults at the study location.

Utica Shale Interval

It is essential to accurately interpret the correlated P-P and P-SV horizons associated with the Utica Shale and Trenton Limestone in order to characterize the Utica Shale interval. Examples of these correlated surfaces are illustrated in Figure 35.

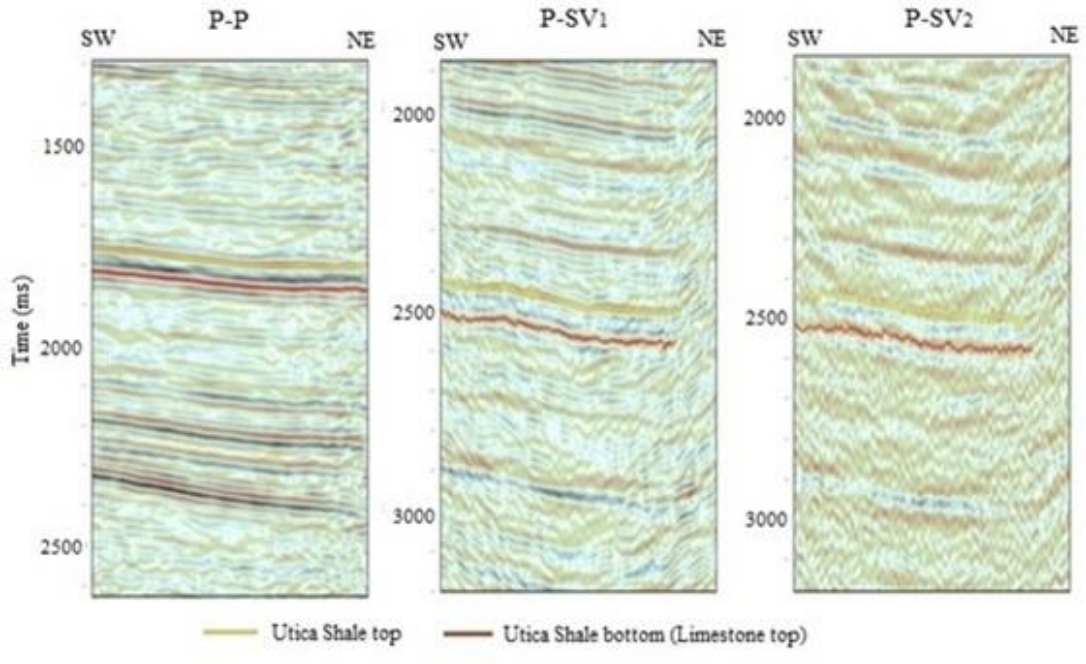

Figure 35: Profiles showing P-P, P-SV_1, and P-SV_2 images of the Utica Shale interval.

The reflections associated with the top and base of the Utica Shale is characterized by bold reflection events in all three data volumes. The top of the Utica Shale is a large negative amplitude event that laterally spans the entire section of the P-P data volume. A decrease in acoustic impedance crossing from the Queenston Sandstone into the Utica Shale produces a trough at the top of the Utica Shale. It can also be emphasized that the distance between Utica Shale and Trenton Limestone is large enough to avoid tuning effects.

The Utica Shale is confidently mapped across the P-P data volume. However, because of the migration effects that exist on the edges of the P-SV data volumes, it is difficult to trace the Utica Shale to the edges of P-SV profiles. These migration effects are considered as “poor data” in the P-SV data volumes.

The synthetic seismogram based time-to-depth calibration well at the center of the 3C3D seismic data space is used to make depth registrations of the top and bottom of the Utica Shale. Extrapolated formation tops of the Utica Shale and the Trenton Limestone are used as an input to calculate the thickness map of the Utica Shale. This approximation yields the thickness change of the Utica Shale across the study area and gives a reliable check for the time-to-depth calibration analysis. As a result, a thickness map of the Utica Shale can be constructed. Figure 36 illustrates the thickness map created for the Utica Shale.

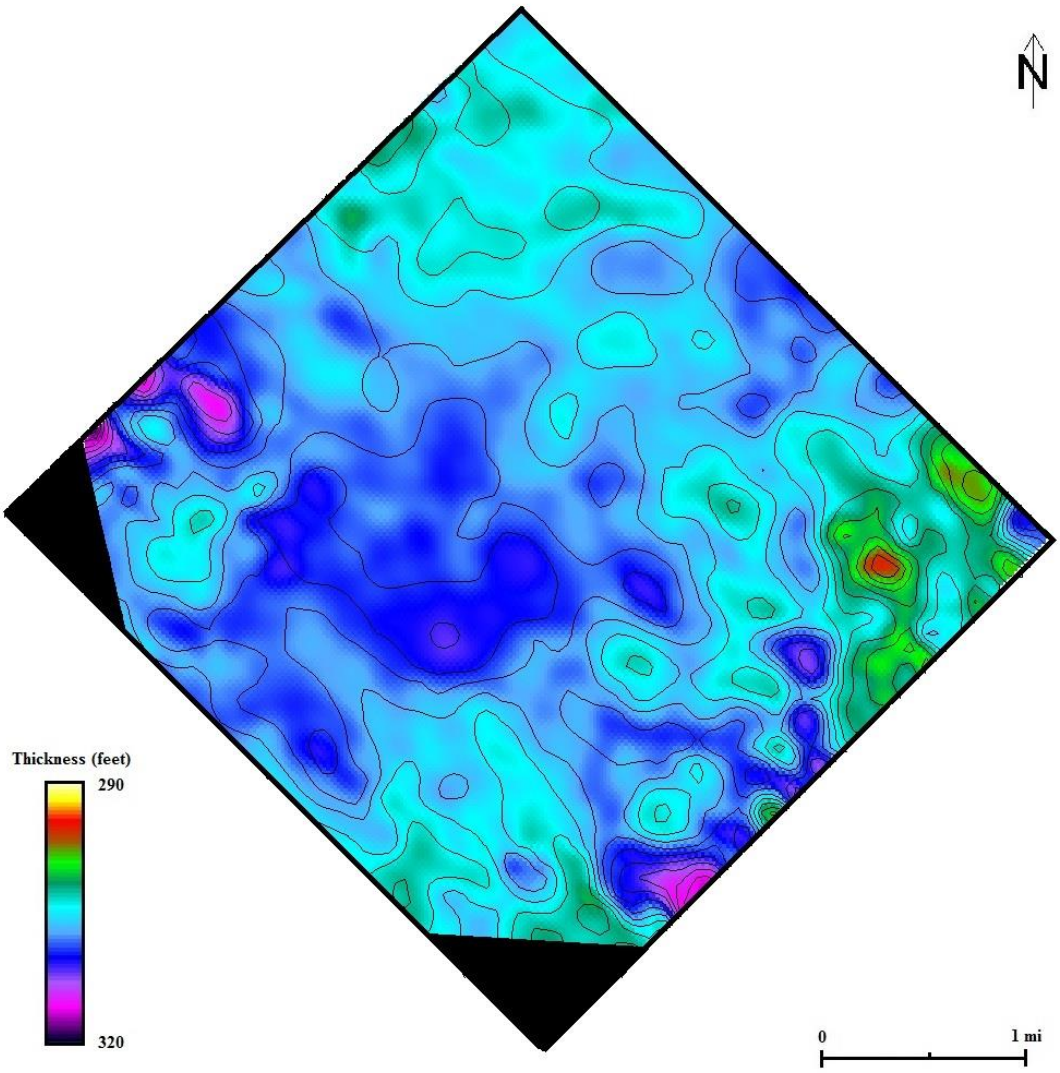

Figure 36: P-P map of Utica Shale thickness (Contour interval is 2 feet).

Because the thickness map of the Utica Shale is calculated by the approximated positions of the Utica Shale and the Trenton Limestone, it is helpful to make general observations about the thickness behavior of the Utica Shale across the 3C3D seismic data spaces. According to the Utica Shale thickness map (Figure 6), the

Utica Shale is approximately 300 feet thick across Bradford County, thus the calculated map in Figure 38 matches this expected behavior fairly well.

Frequency spectra calculated in the Utica Shale interval in P-P, P-SV_1, and P-SV_2 data volumes are displayed on Figures 37, 38, and 39, respectively.

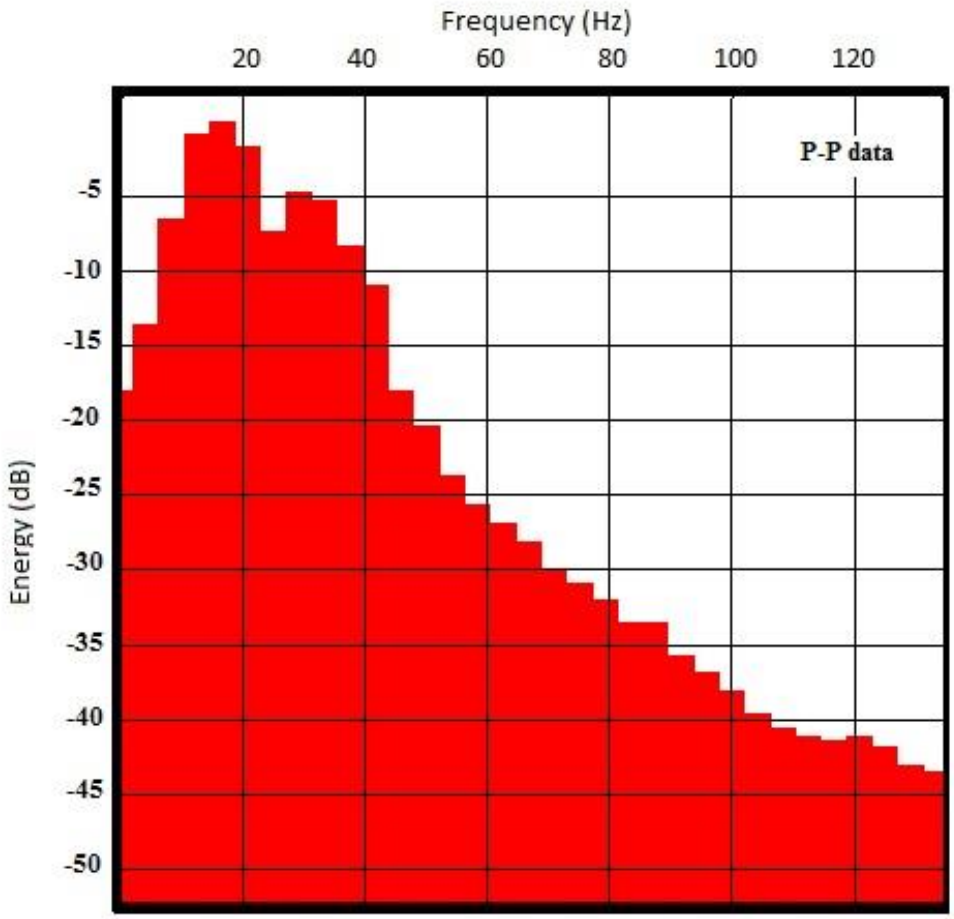

Figure 37: P-P frequency spectrum across the Utica Shale interval (1700-1900 ms).

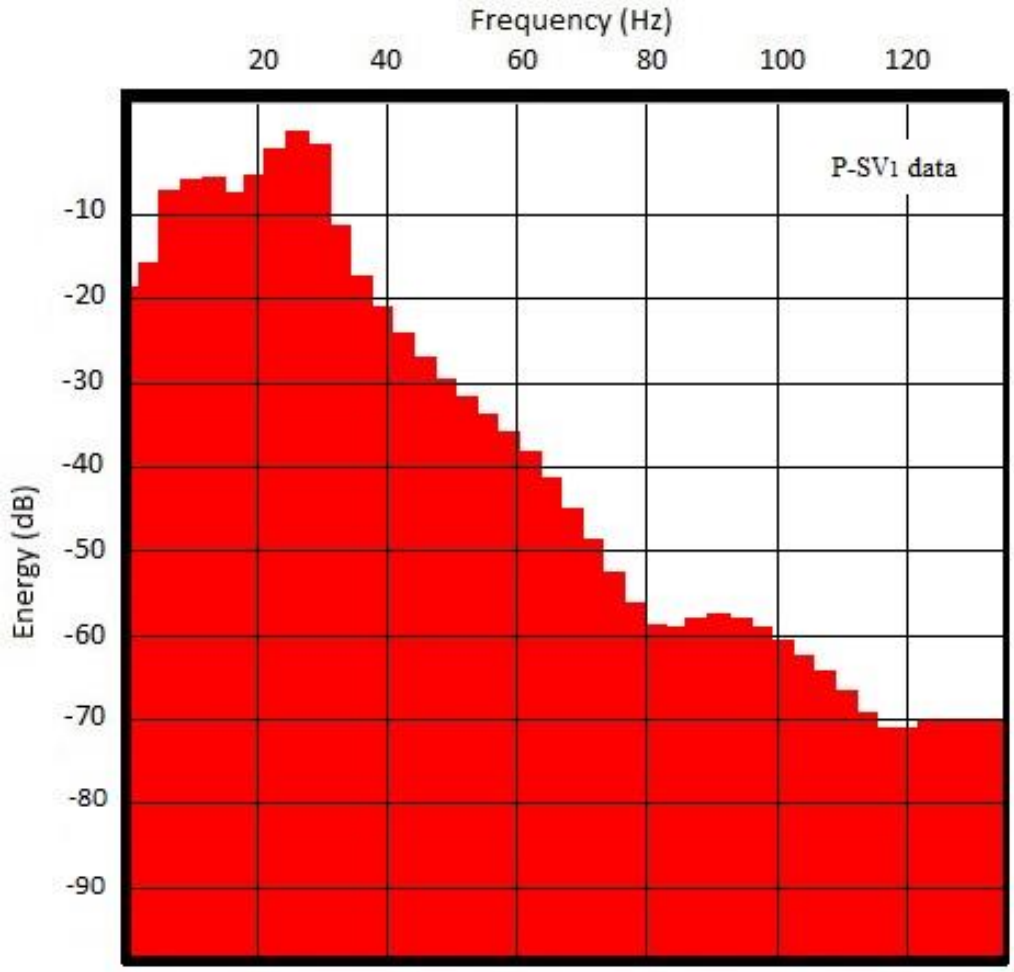

Figure 38: P-SV1 frequency spectrum across the Utica Shale interval (2300-2600 ms).

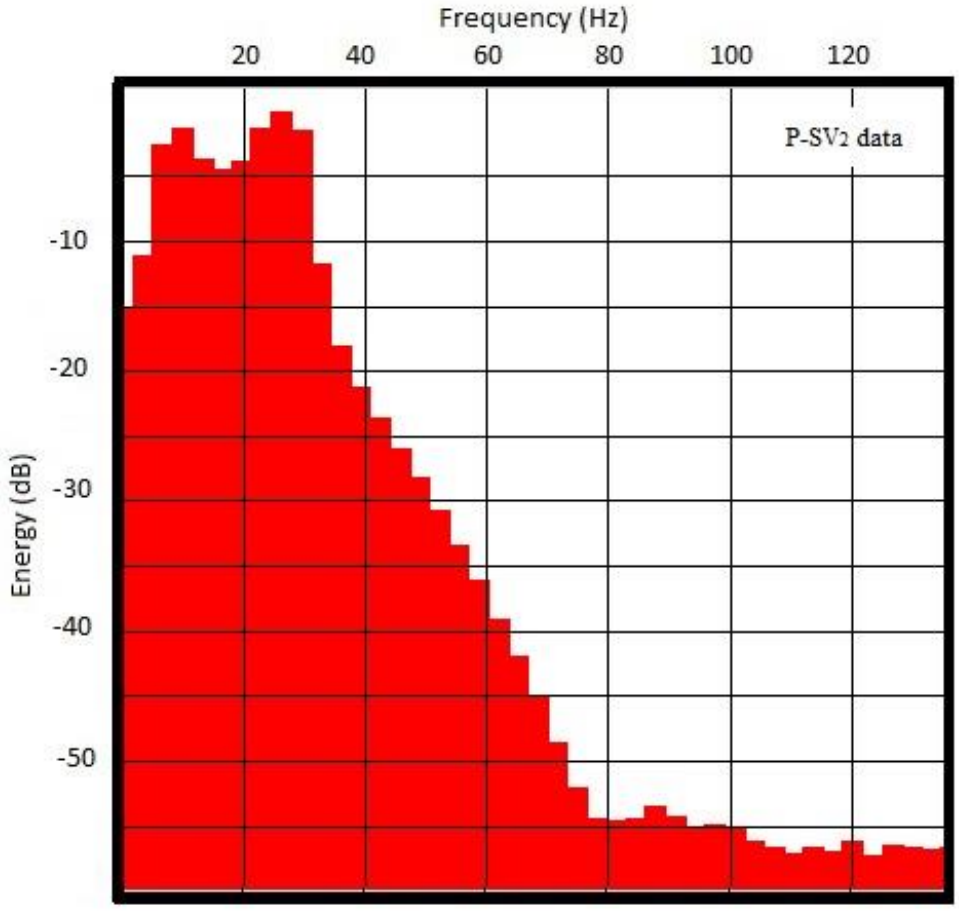

Figure 39: P-SV2 frequency spectrum across the Utica Shale (2300-2600 ms).

Using an energy reduction of 20 dB to define the high-end of signal frequency, these spectra confirm the signal frequency content of P-P data across the Utica Shale interval span a range of 10-48 Hz and both P-SV_1 and P-SV_2 data have a signal bandwidth of 7 to 38 Hz. Thus even though P-SV data have lower frequencies than P-P data, P-SV data provide better resolution than P-P data because P-SV wavelengths (V_{sp}/f_{sp}) are shorter than P-P wavelengths (V_p/f_p). Thus, P-SV data provide important information when analyzing anisotropy. The azimuthal anisotropy analysis displayed by

fast-S and slow-S modes should enable fractures and horizontal stress fields to be characterized across the Utica Shale.

Utica Shale Structural Interpretation

The Utica Shale interval is delineated as “near Utica” in P-P and P-SV data volumes. This is because of the reasons explained earlier in this chapter. However, it is important to emphasize that time structure maps constructed from these “near Utica” horizons are useful for estimating the structural trend of the Utica Shale across the study area.

The time structure maps of Utica Shale are presented in Figures 40 thru 42. P-P and P-SV data volumes indicate that no significant faults cut through the Utica Shale. The structural dip of the Utica Shale is due south. Although natural fracture patterns may be below seismic resolution limits within the Utica Shale, the generated structure maps provide insight into Utica Shale fracture systems. The analyses of these natural fracture patterns are important for the hydraulic fracture treatments and fluid injection operations.

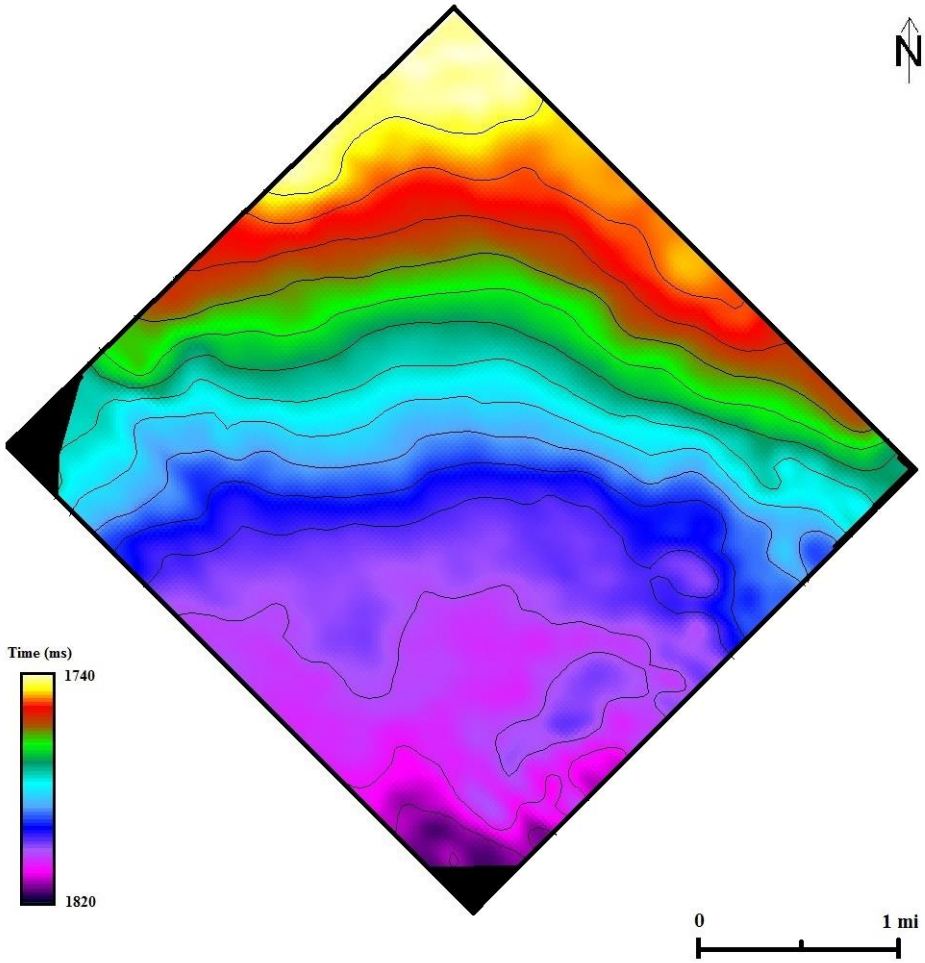

Figure 40: P-P two-way time structure of the top Utica Shale (Contour interval is 5 ms).

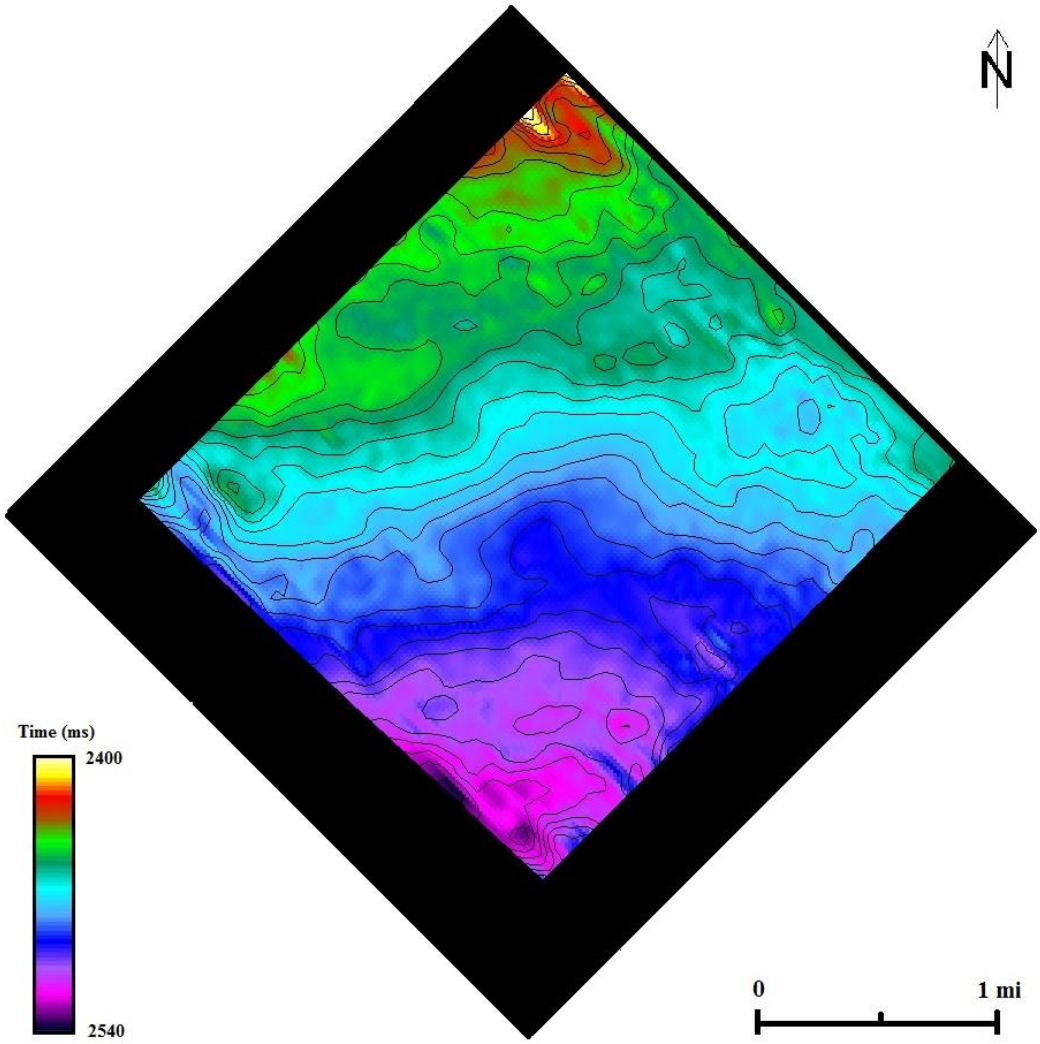

Figure 41: P-SV_1 two-way time structure of the top Utica Shale (Contour interval is 5 ms).

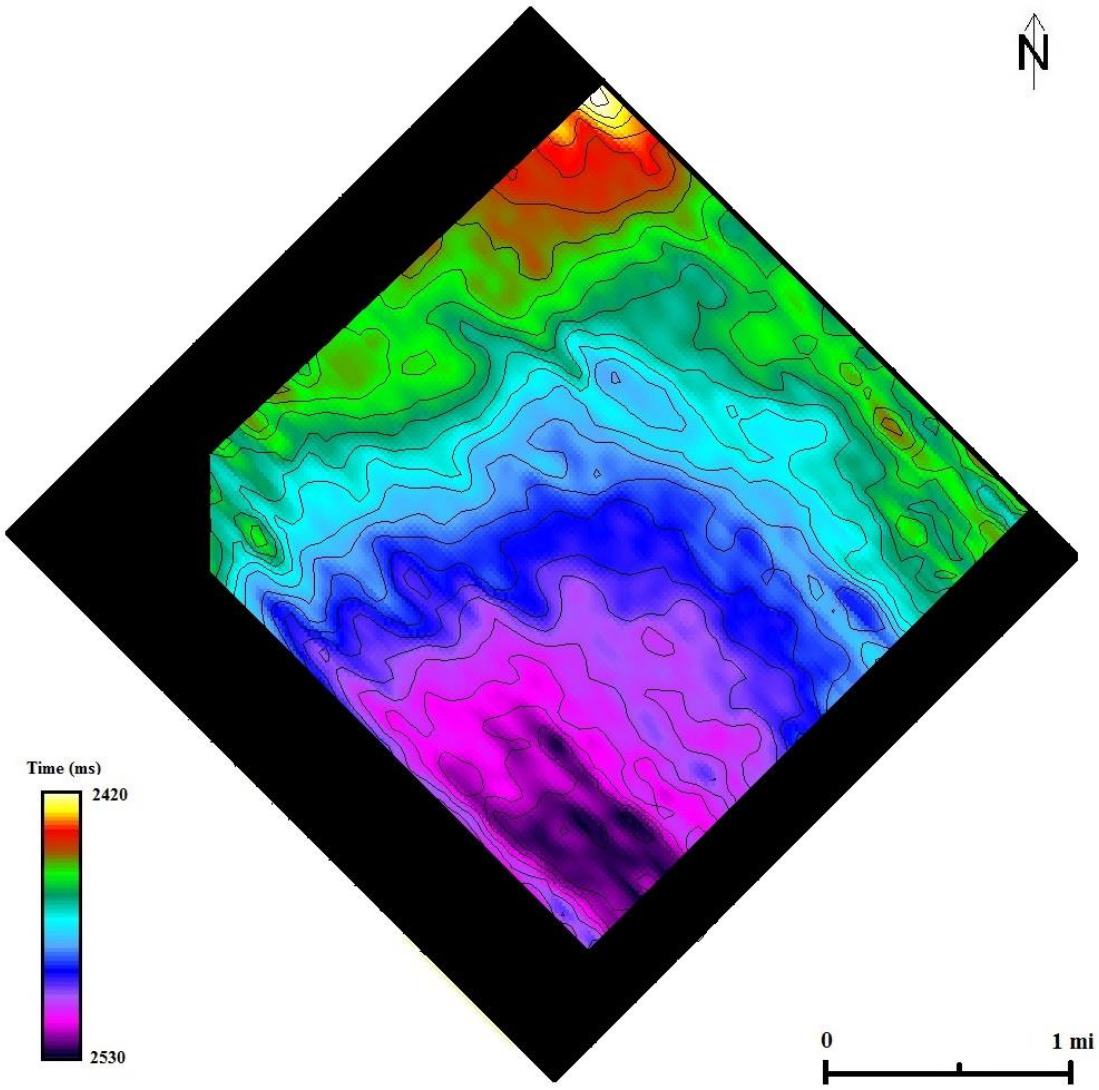

Figure 42: P-SV_2 two-way time structure of the top Utica Shale (Contour interval is 5 ms).

My first approach to understand the Utica Shale structural fabric was based on previous work. Recent studies indicate that the fracture planes in the Utica Shale indicate a dominant northeast orientation and a secondary east orientation (Ellison, 2014). This study was done in the Ohio region, but it gives helpful information for the estimation of structural trends (Fig. 43).

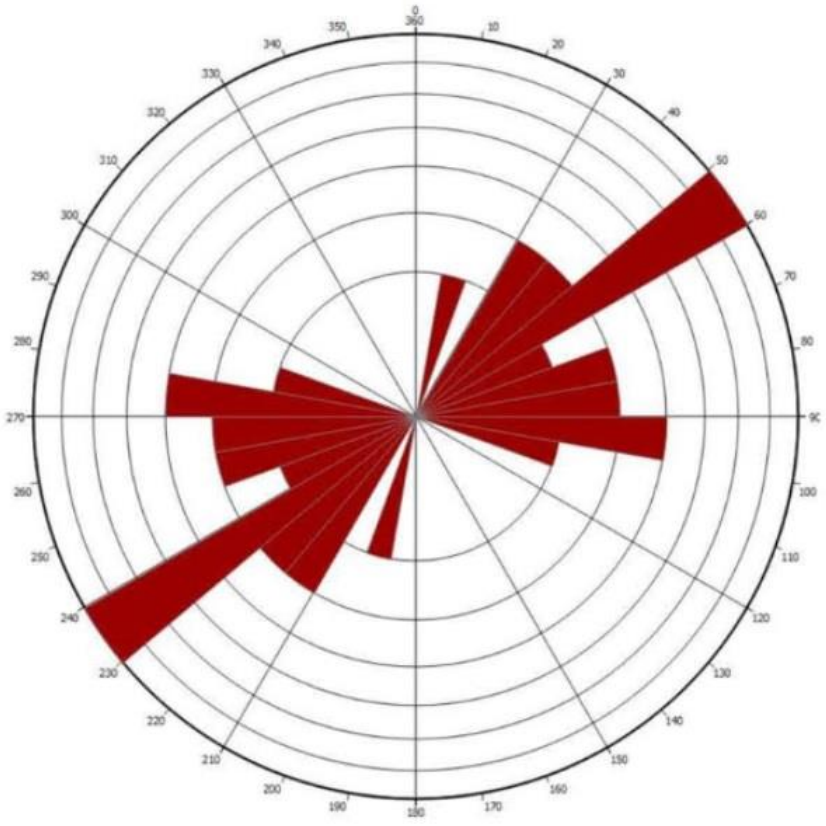

Figure 43: The Rose diagram of the Utica Shale indicating a dominant northeast orientation and a secondary east orientation (Ellison, 2014).

My second approach for understanding the Utica Shale structural trends was based on seismic attribute analysis. Analysis of time-slices generated for the Utica Shale

interval for P-P (1600-2000 ms), P-SV_1 (2300-2700 ms), and P-SV_2 (2300-2700 ms) was used to map quasi-linear features that might relate to fractures or subtle faults. All structural lineations were picked in P-P, P-SV_1, and P-SV_2 time-slices and the aim was to determine if some of the lineations indicate the structural trend of the Utica Shale. Examples of the lineations are expressed in Figure 44.

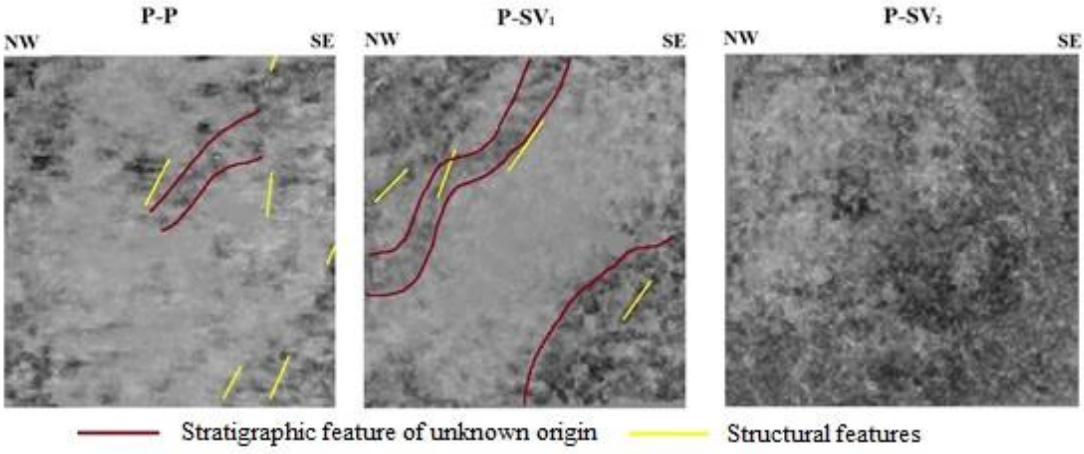

Figure 44: Interpreted stratigraphic and structural features within the Utica Shale in P-P, P-SV_1, and P-SV_2 images.

Two conclusions can be made regarding these depth-equivalent time-slices. First, there is a stratigraphic feature of unknown origin. The interesting point about this feature is that it is more resolvable in the P-SV1 image than in the P-P or P-SV_2 images. The P-P image can barely resolve this feature, and there is no clear evidence in the P-SV2 image. This observation supports the fact that one or more key depositional features not seen by one wave mode may be seen by another wave mode (Hardage et al., 2006). Second, there is a lateral-migration of this stratigraphic feature in the P-P and P-SV1 images. The resolution and the position of this interpreted stratigraphic feature would appear

differently in converted-wave data if the V_p/V_s ratio used to process the data is slightly in error (Frasier and Winterstein, 1990).

The structural trends of linear features in the Utica Shale, based on interpreted time slices, are represented in Figure 45. A dominant northeast and east orientation is observed. Some lineations are parallel to the inline direction of the seismic survey. This orientation may be the result of acquisition footprints created by data-acquisition geometry.

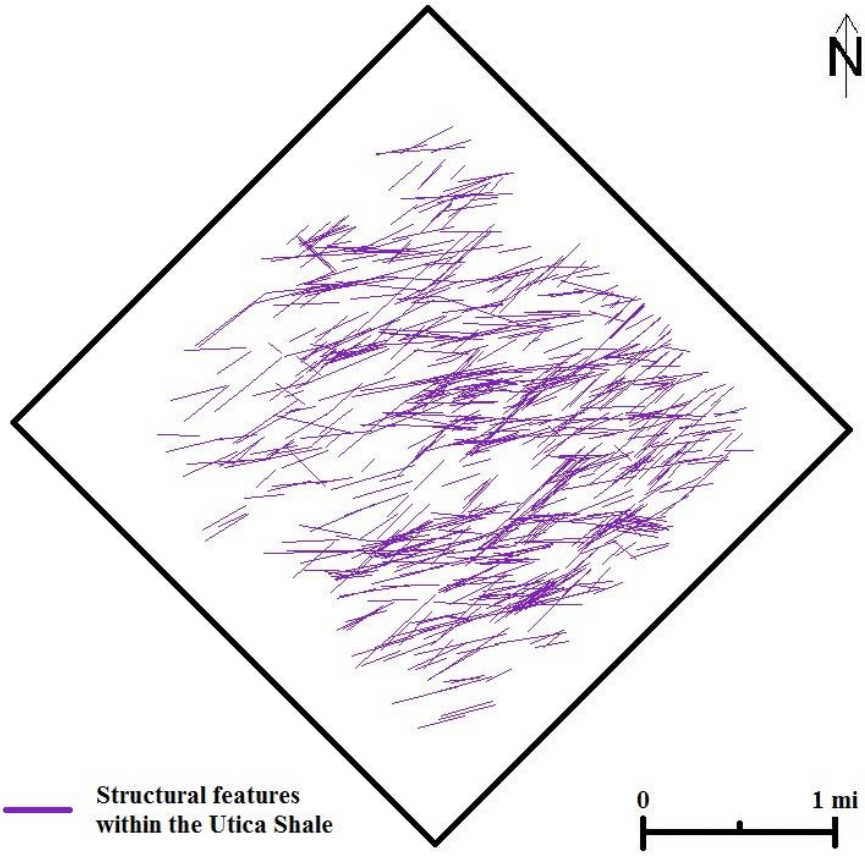

Figure 45: Interpreted linear structural features within the Utica Shale. There are dominant north-east and east orientations.

A negative aspect of this interpretation is that because the Utica Shale is relatively deep, the natural fracture pattern is below the resolution limits within the Utica Shale. Because the size of 3C3D seismic survey is limited (9mi^2, 23 km^2), it is hard to demonstrate that these interpreted structural complexities are related to any specific regional orogenic event (for example, Taconian or Acadian).

In order to understand the Utica Shale interval structural complexities in more detail, I evaluated amplitude attribute maps that generated from the P-P, P-SV_1, and P-SV_2 seismic data volumes.

Amplitude Attributes across the Utica Shale Interval

Amplitude attributes are useful when identifying lithology, porosity, channel sands, and unconformities. In stratigraphic studies, lateral changes in amplitude can reveal missing stratigraphic features. For example, concordant beds have maximum amplitudes, but chaotic beds have the lowest.

RMS (root-mean-square) amplitude is calculated as the square root of the average of the squares of the amplitudes that is found in the specified window (Eq. 2). Because this analysis is bounded between the Utica Shale top and the Trenton Limestone top, the amplitude information is directly related to the Utica Shale interval and may indicate sand rich environments as increases in seismic amplitudes.

$$RMS = \sqrt{\frac{1}{N}\sum_{i=1}^{N} a_i^2}$$

Equation 2: RMS amplitude calculation where N is the number of samples, and a_i is the amplitude.

Horizon-based RMS amplitude attributes were generated across the entire Utica Shale to evaluate the Utica Shale in terms of structural patterns. These RMS amplitude maps can possibly provide additional information about fracturing, faulting, or jointing systems within the Utica Shale interval. To construct these maps, P-P, P-SV_1 and P-SV_2 RMS amplitudes were calculated from the top of the Utica Shale to the base of the Utica Shale.

P-P root-mean-square (RMS) reflection amplitudes across the Utica Shale interval are shown in Figure 47. The black areas across the RMS amplitude map indicate the no-lease properties where the release of seismic information is forbidden. P-P reflection amplitudes show a random distribution across the image area and there are no inferable stratigraphic features or structural trends. At the edges of the image space, there are some uncommon amplitude behaviors because of the edge-related migration artifacts.

P-SV_1 and P-SV_2 RMS amplitude maps have similar patterns as shown in this P-P reflection amplitude map (Figs. 47-48.). Random distributions of amplitudes are also observed in these maps. Unfortunately, these results may indicate the fact that because the depth of the Utica Shale is relatively deep (12,000 feet), RMS amplitude maps are not as valuable as they are for shallower targets.

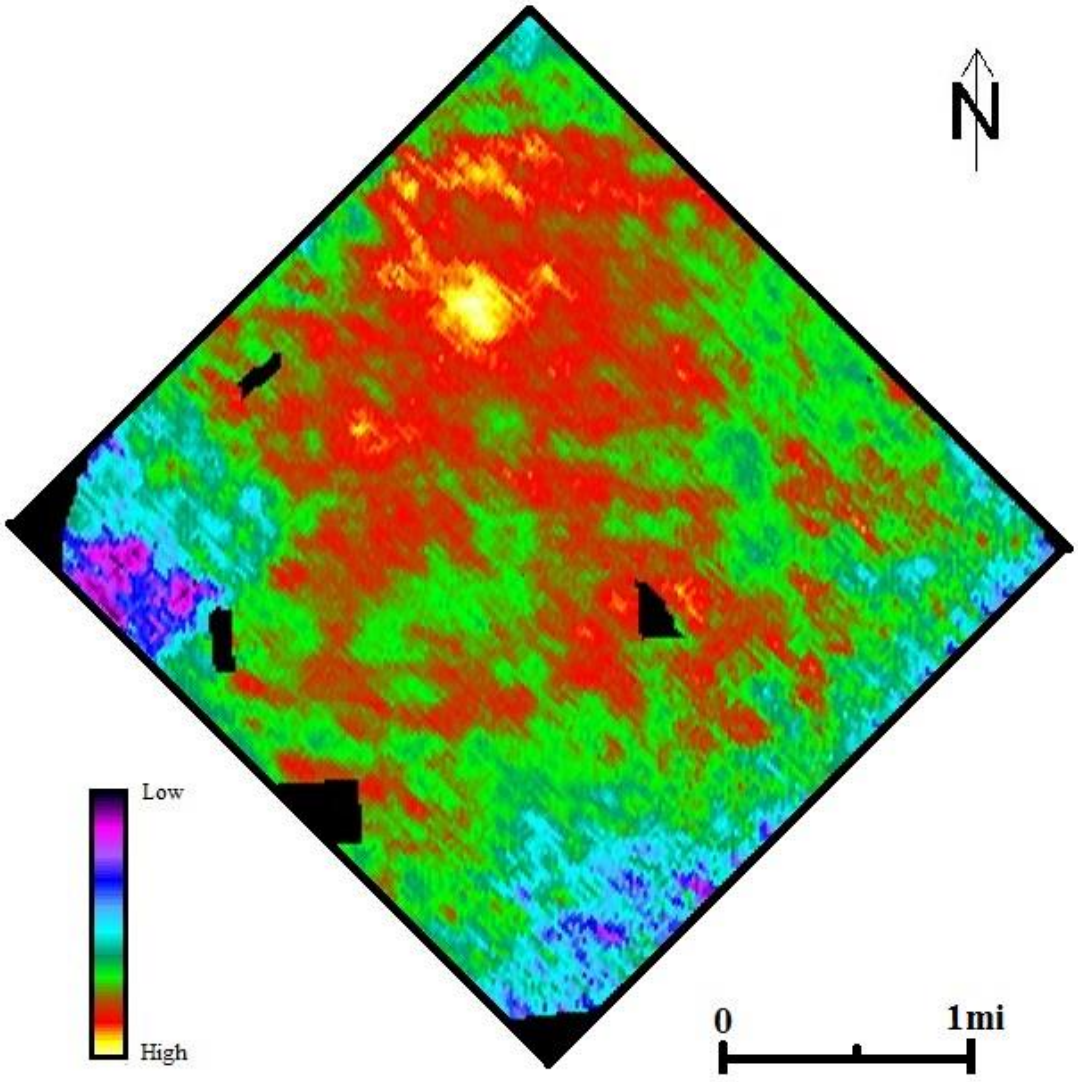

Figure 46: P-P RMS amplitude across the Utica Shale interval.

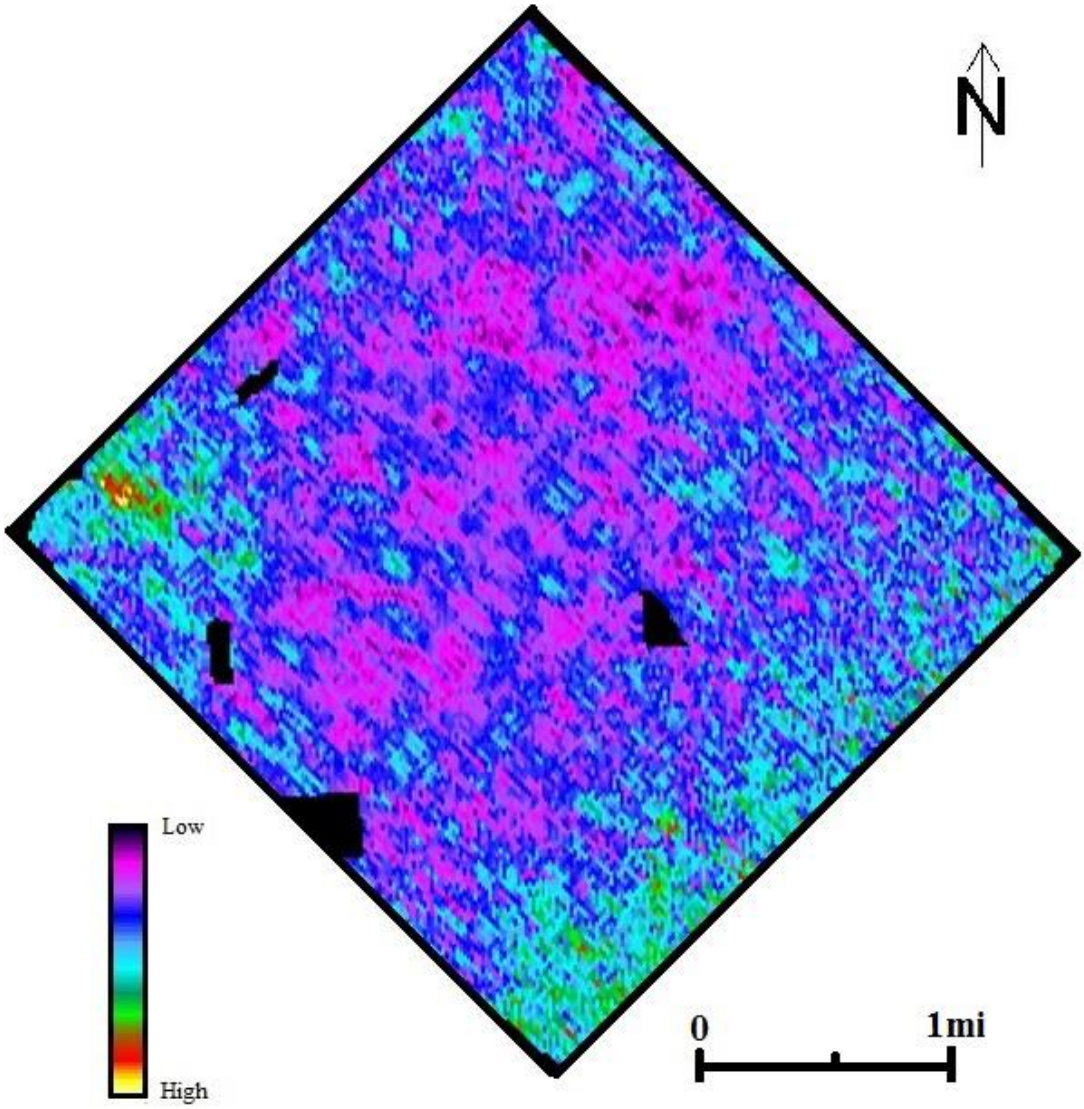

Figure 47: P-SV_1 RMS amplitude across the Utica Shale interval.

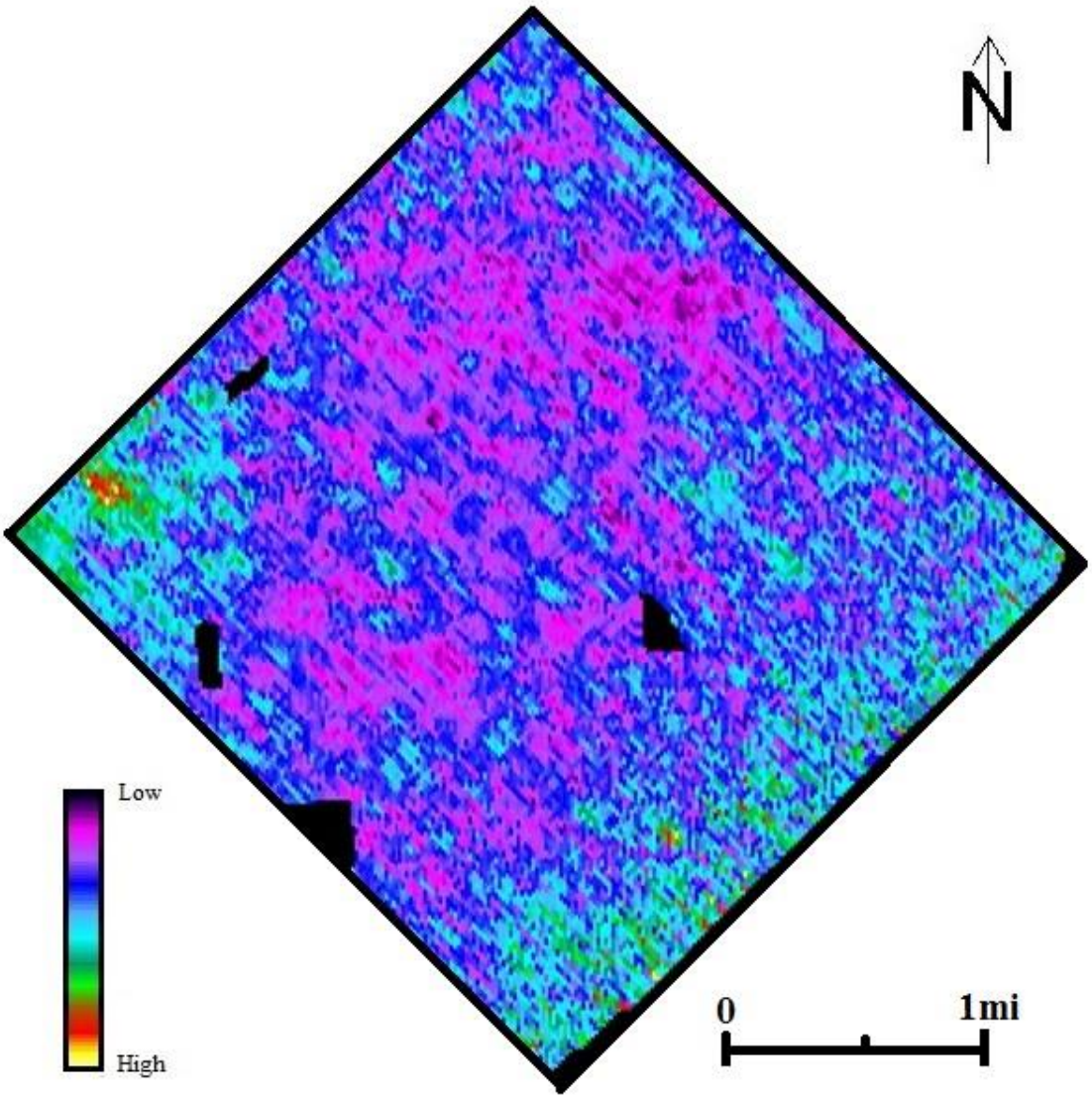

Figure 48: P-SV_2 RMS amplitude across the Utica Shale interval.

Each RMS amplitude map showed random distributions of amplitudes across the seismic image similar to the effects exhibited in Figure 46 through 48. There were no inferable stratigraphic features or structural trends. These random amplitude effects may occur because the depth of the Utica Shale is too deep for detailed amplitude analysis.

Stratal Surfaces of the Utica Shale

The stratal slicing method was used to understand the depositional systems within the Utica Shale interval. This method is based on the fact that the time interval between two seismic reflection events can be divided by variable-thickness intervals that also represent surfaces of constant geological time. It should also be noted that this method is valid if there are no truncations or discordant reflections along seismic reflections (Zeng, 2006). In my stratal slicing effort, these sub-intervals were uniformly spaced to create 4000 constant-geological-time horizons within the Utica Shale. This procedure divided the Utica Shale interval into 4000 chronostratigraphic surfaces with fixed time increments between adjacent surfacesas demonstrated by Zeng (2006). Therefore, the geologic time across each sub-interval is reasonably constant.

This method also has advantages in terms of resolution. Because the natural fracture pattern is below the resolution limits of the Utica Shale. (Eq.1, frequency is 30 Hz, velocity is 4,800 m/s, and wavelength is 160m), a stratal slicing method may provide detectable structural and stratigraphic features within the Utica Shale Formation.

This stratal slicing method was applied from the Queenston Sandstone to the Basement surface in order to verify any missing stratigraphic or structural features between these key geologic horizons. Semblance maps were generated from the stratal slices. Semblance analysis is sensitive to lateral changes in seismic data caused by

variations in structure, stratigraphy and lithofacies. The principle focus was on the Utica Shale interval. P-P, P-SV_1, and P-SV_2 semblance maps for the Utica Shale are represented in Figure 49.

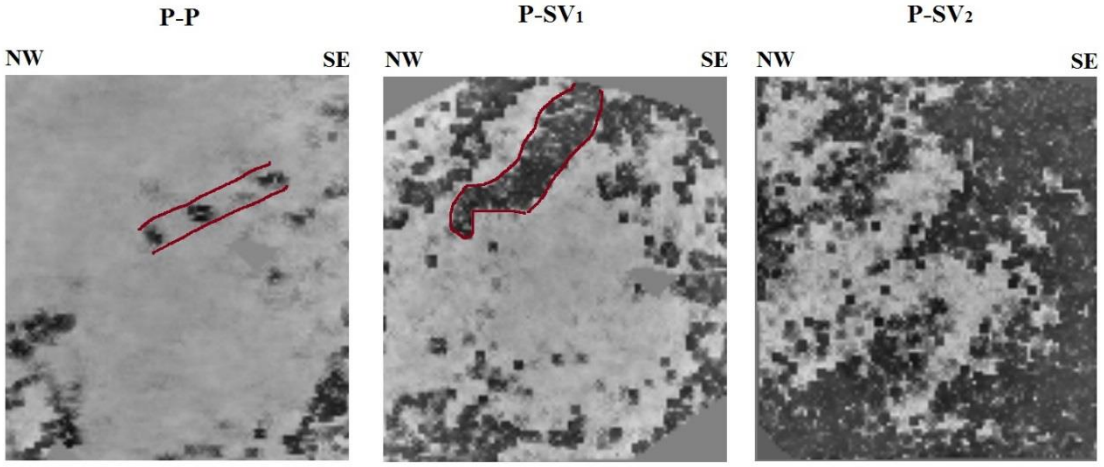

Figure 49: Semblance maps generated after time slicing of the Utica Shale interval in P-P, P-SV_1, and P-SV_2 data volumes. Note that the outlined surface that could be interpreted as a stratigraphic feature, possibly a turbidite.

Semblance analysis indicates an interesting stratigraphic feature within the Utica Shale. This stratigraphic feature correlates with the interpretation of the time-slices in Figure 45. A possible origin of this feature may be turbidites within the Utica Shale. Because the depositional environment of the Utica Shale is shallow-water, it is possible that turbidites were generated even in gentle slopes.

There is again a lateral-migration of the stratigraphic feature in the P-P and P-SV_1 images. As noted the position of the feature in P-SV_1 image space is controlled by the selected V_P/V_S ratio used in data processing. Incorrect values of V_p/V_s will position features at different locations in conventional (P-P) and converted (P-SV_1) images (Frasier and Winterstein, 1990).

V_P/V_S Ratio Analysis for the Utica Shale

V_P/V_S ratio analysis is used for rock type identification (Domenico, 1984). The behavior of a V_P/V_S ratio indicates large-scale changes in rock type. Laboratory measurements of various rock types show that each rock type has a different V_P/V_S ratio. The range of V_P/V_S in typical rocks is presented in Table 2 (Domenico, 1984).

The reasonable range for the Utica Shale V_P/V_S ratio is between 1.70-3.00. In order to relate the V_P/V_S ratio across the Utica Shale interval, I used the relationship:

$$\frac{Vp}{Vs} = 2\left[\frac{\Delta ts}{\Delta tp}\right] - 1$$

Equation 3: V_p/V_s ratio calculation based on two-way arrival time in P-P and P-SV times (Hardage et al., 2012)

In this equation, Δt_S is the isochron thickness of the Utica Shale interval measured in P-SV time and Δt_P is the isochron thickness of the Utica Shale interval measured in P-P time.The calculated V_P/V_{S1} and V_P/V_{S2} ratios for the Utica Shale in the study area are presented in Figure 50 and Figure 51, respectively.

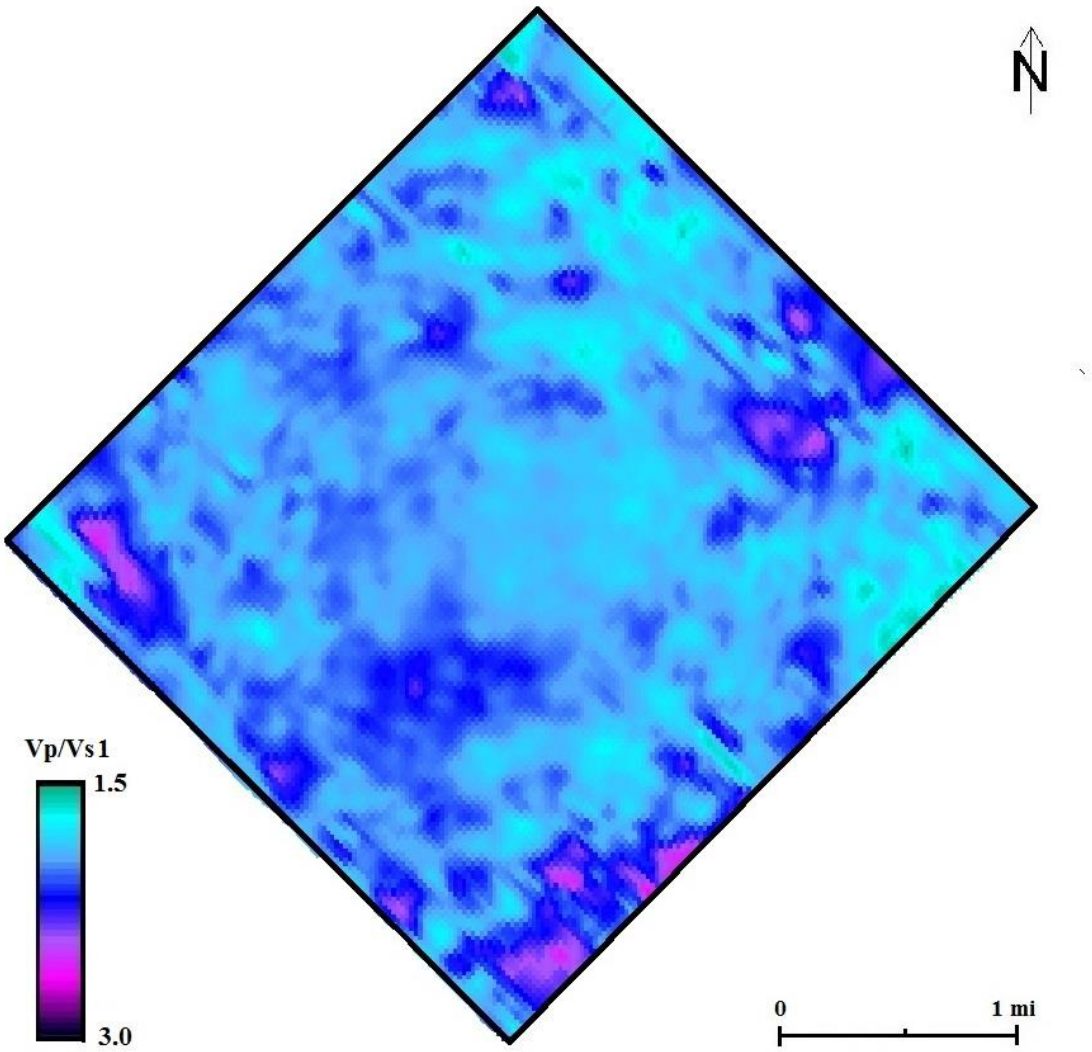

Figure 50: V_P/V_{S1} ratio of the Utica Shale within the study area.

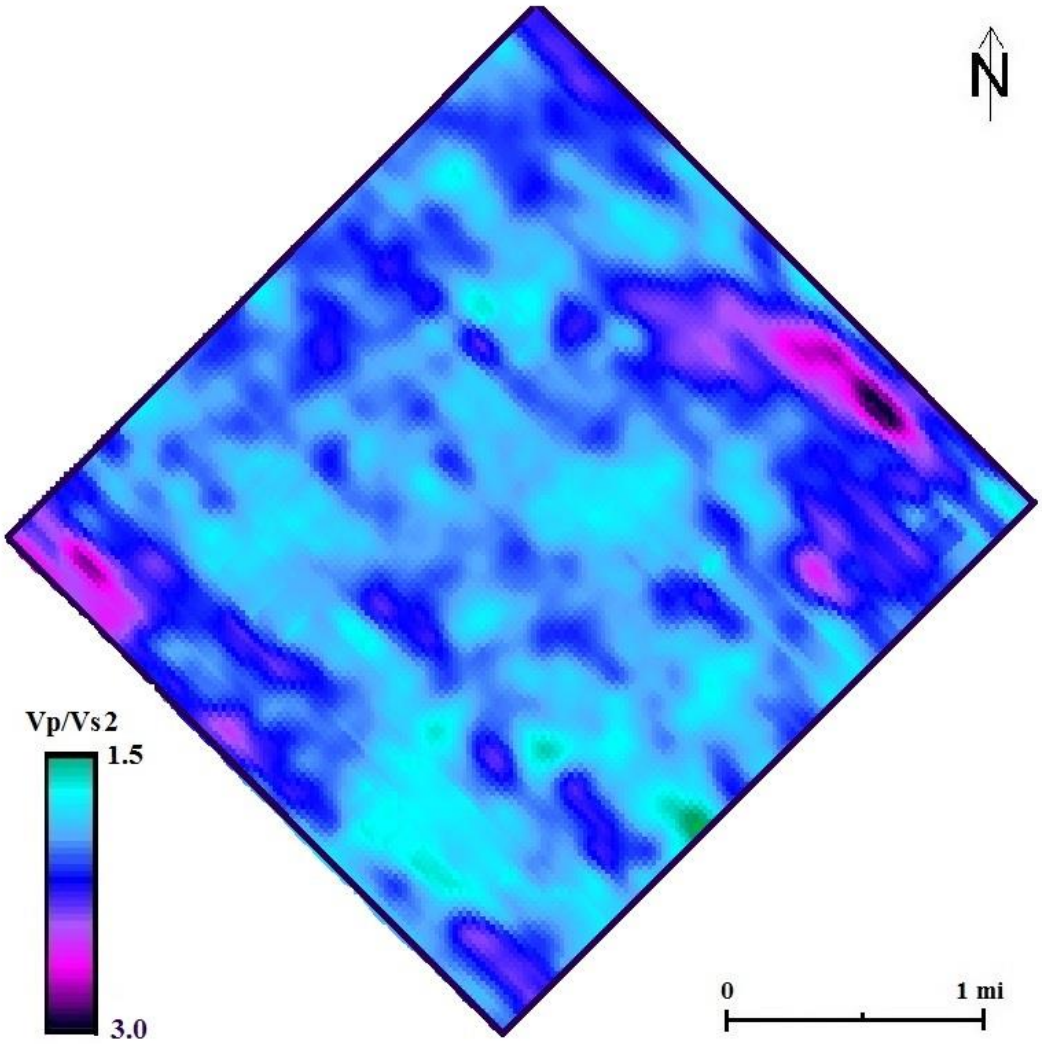

Figure 51: V_P/V_{S2} ratio of the Utica Shale within the study area.

V_P/V_S ratios for the Utica Shale are in the range determined by laboratory measurements on rock samples range (Table 2). These results also support the validity of my interpreted time-structure maps. Because the calculated V_P/V_S ratios are numerically correct, the time-structure maps created for the Utica Shale interval are reliable.

Utica Shale S-Wave Anisotropy

Stress fields across a targeted interval cause that interval to be an anisotropic seismic propagation medium. The azimuth-dependent difference in propagation velocities of S-waves is known as S-wave anisotropy. The quantity of S_{ANI} is defined in Equation 4,

$$S_{ANI} = (\Delta T_2 / \Delta T_1) - 1$$

Equation 4: Calculation of S-wave anisotropy

ΔT_1 is the time thickness of the interval on a fast-S image, and ΔT_2 is the time thickness of the interval on a slow-S image (Hardage et al., 2012).

Time-delay analyses of depth-equivalent horizons in S_1 and S_2 data were helpful for identifying time differences across stratigraphic intervals. These magnitudes of time differences were assumed to be a measure of stress fields. Time-delays measured across the Utica Shale interval are presented in Figure 52. Time delays of the S2 mode relative to the S1 mode are quite small, in the range of 0.82 % to -0.38 %. It may thus be inferred that there is little anisotropy within the Utica Shale Formation in my study area.

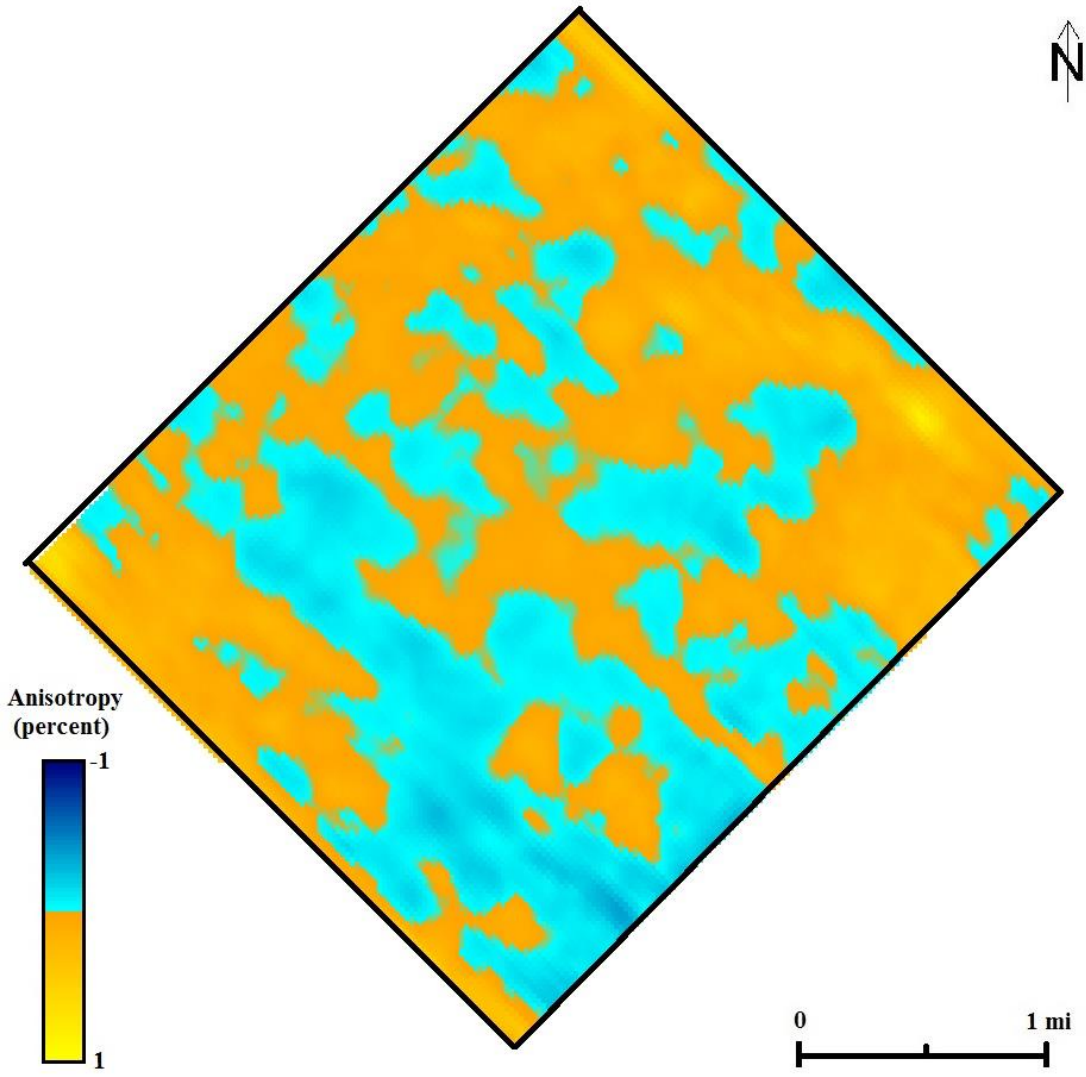

Figure 52: S-wave anisotropy across the Utica Shale interval.

Trenton Limestone Structural Interpretation

It is also important to analyze the structural behavior of the Trenton Limestone to determine if that horizon relates to any critical features of the Utica Shale. Time structure maps of Trenton Limestone are presented in Figures 53 to 55 and show that the structural dip of the Trenton Limestone is due south. According to the time structure maps and the Utica Shale maps (Figs. 40-42), the structural dip of deep formations is due south.

Although there are interpreted stratigraphic/structural features across the Utica Shale (Fig. 49), semblance map of the Trenton Limestone does not show these features (Fig. 56). The reason can be explained by the seismic resolution limits discussed in Utica Shale Structural Interpretation chapter. Therefore, semblance maps of the Trenton Limestone cannot be used to find missing stratigraphic/structural features.

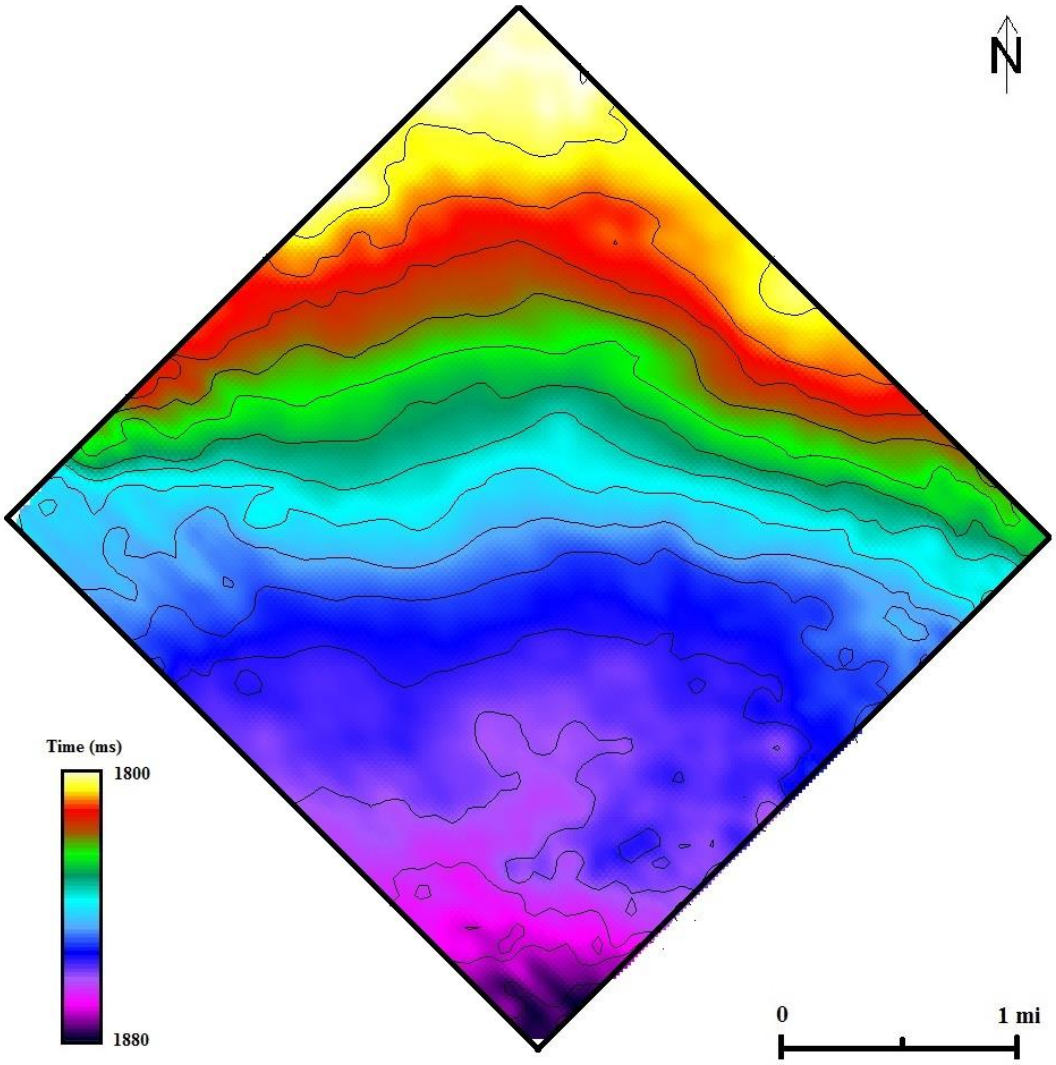

Figure 53: P-P two-way time structure of the top Trenton Limestone (Contour interval is 5 ms).

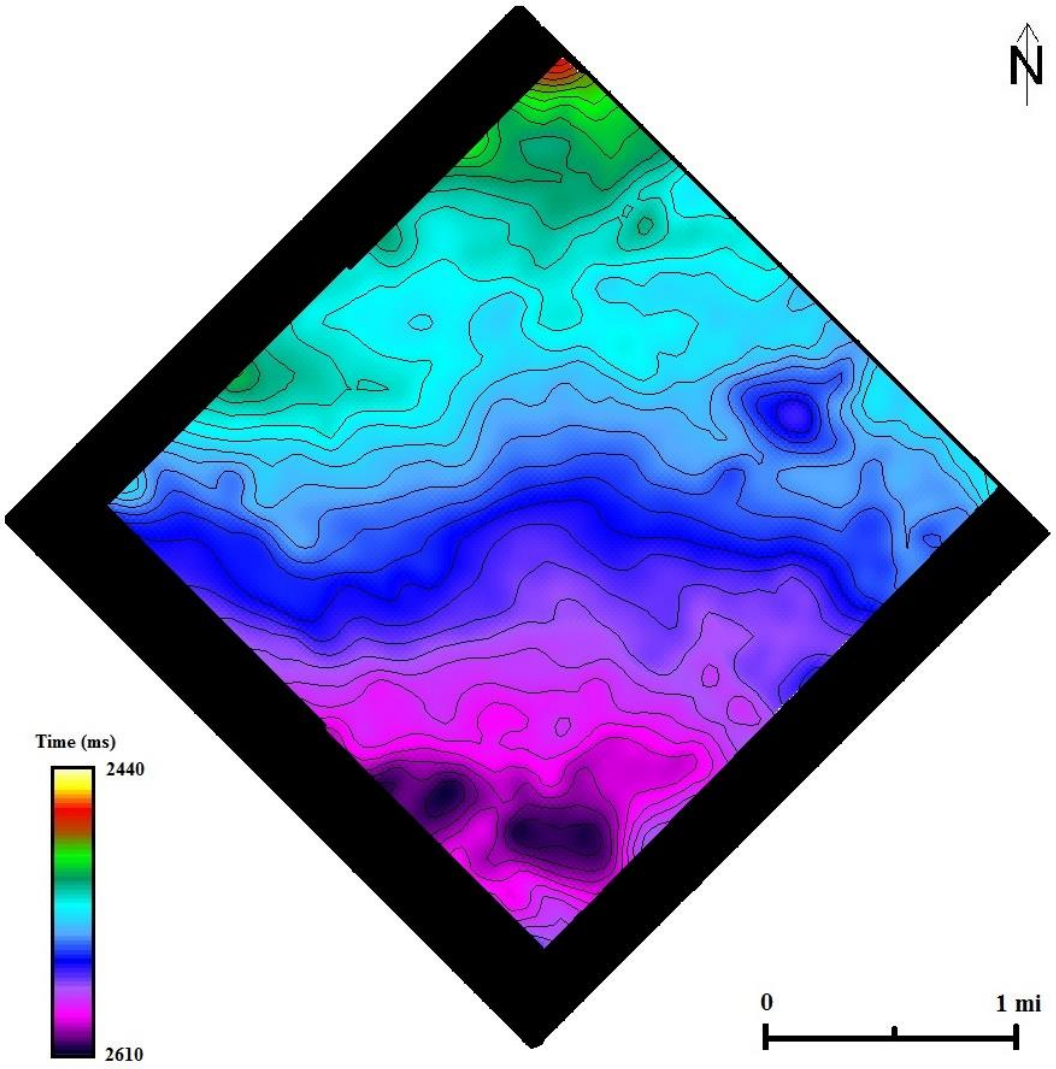

Figure 54: P-SV_1 two-way time structure of the top Trenton Limestone (Contour interval is 5 ms).

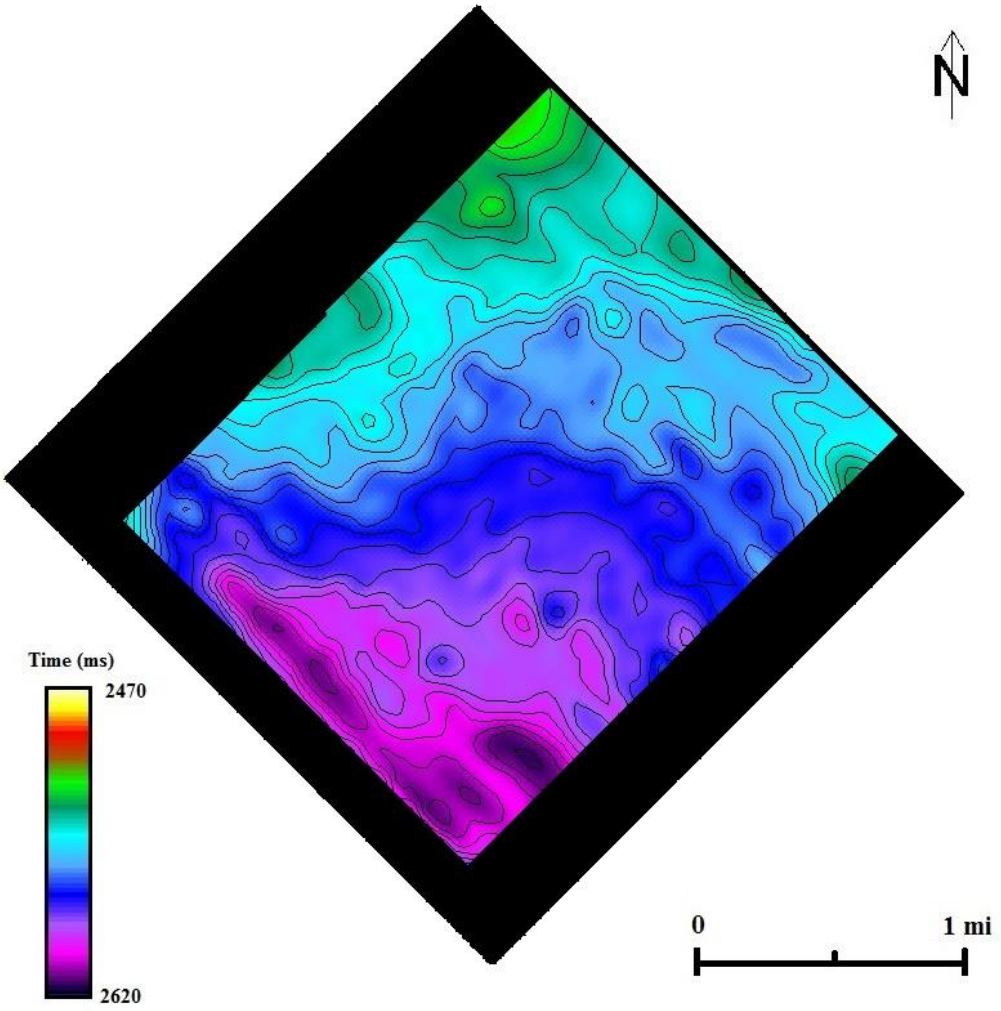

Figure 55: P-SV_2 two-way time structure of the top Trenton Limestone (Contour interval is 5 ms).

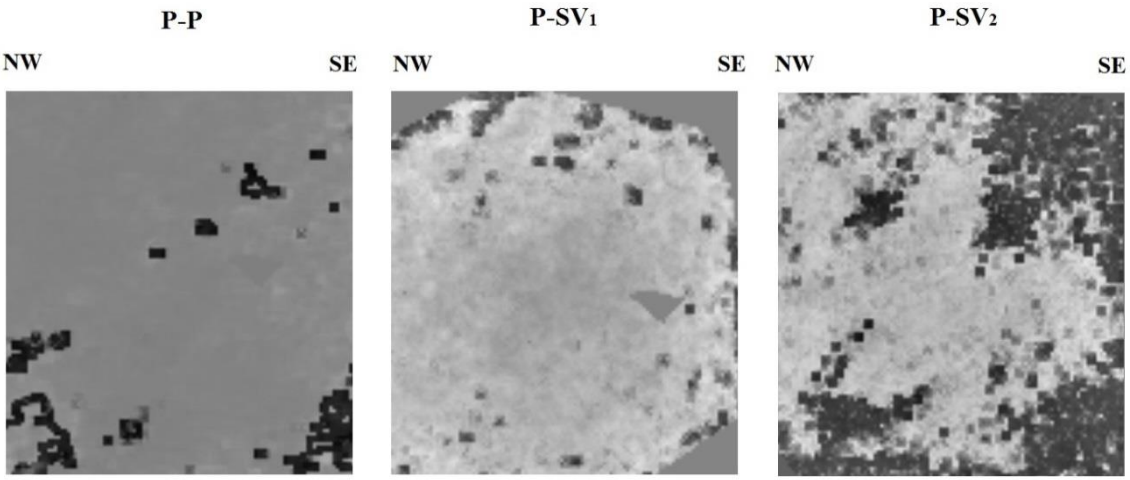

Figure 56: Semblance maps of the Trenton Limestone interval in P-P, P-SV_1, and P-SV_2 data volumes.

Queenston Sandstone

It is essential to interpret any sandstone-prone interval above the Utica Shale to evaluate this unit as a possible storage reservoir for hydrofracking fluids. A structural interpretation of the Queenston sandstone is important to determine if there is any evidence of fault zones, because faults can create escape routes for injected fluids. I find evidence of no fault zones across the Queenston sandstone. The interpreted P-P, P-SV_1, and P-SV_2 time images are represented in Figures 57, 58, and 59, respectively.

Across the 9.3 mi^2 (23.8 km^2) area of seismic image space, the Queenston Sandstone is structurally low in the south portion of the image space and dips gently to the south based on the time-based interpretations. Semblance maps for Queenston Sandstone are presented in Figure 60. Semblance maps of the Queenston Sandstone failed to find any missing stratigraphic/structural features.

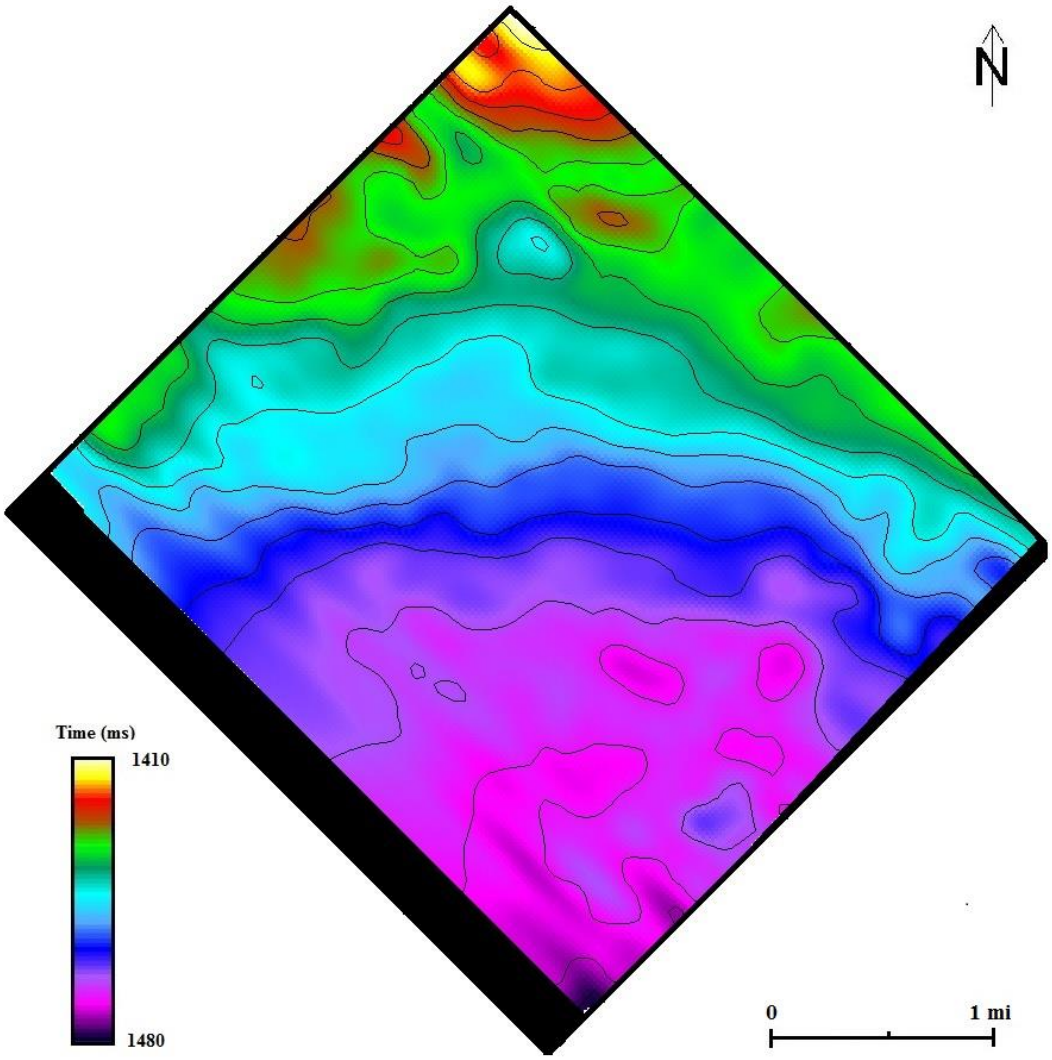

Figure 57: P-P two-way time structure of the top Queenston Sandstone (Contour interval is 5 ms).

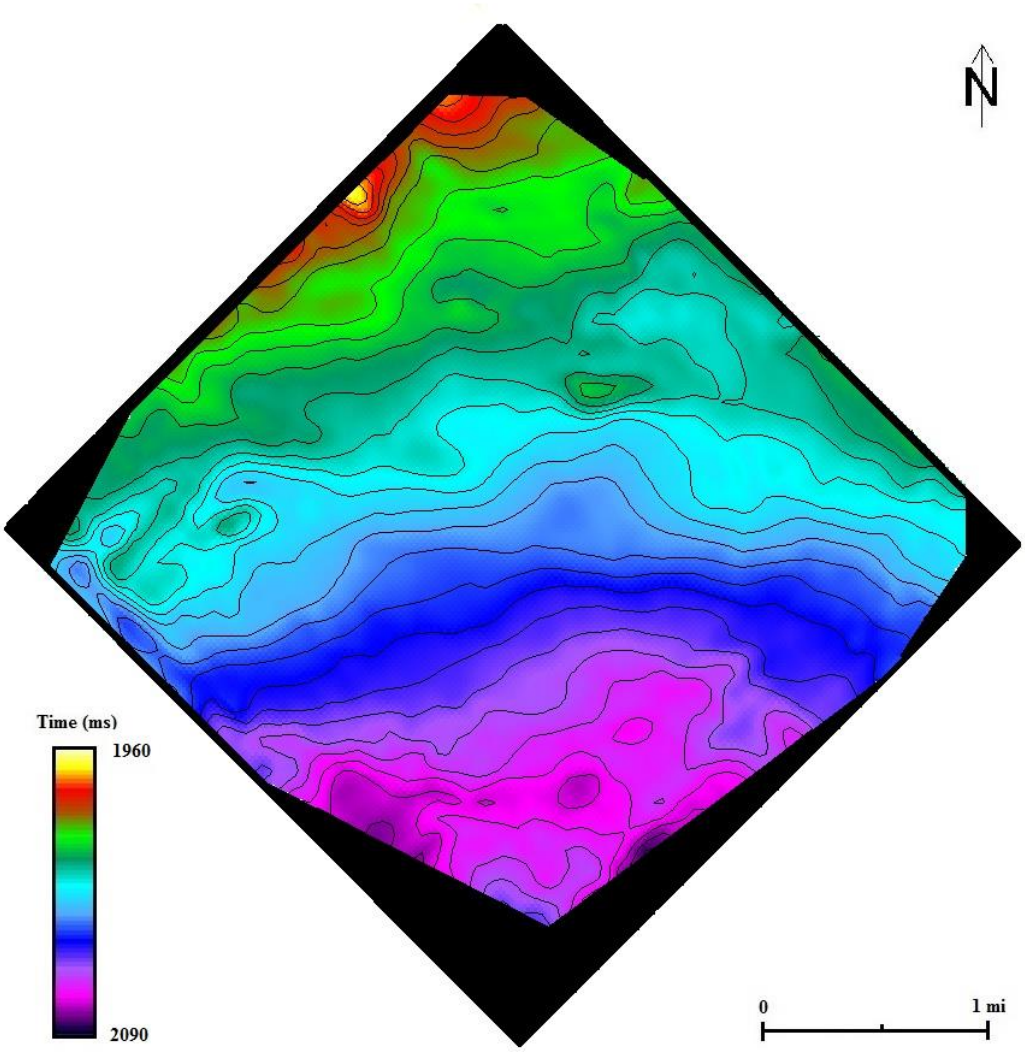

Figure 58: P-SV_1 two-way time structure of the top Queenston Sandstone (Contour interval is 5 ms).

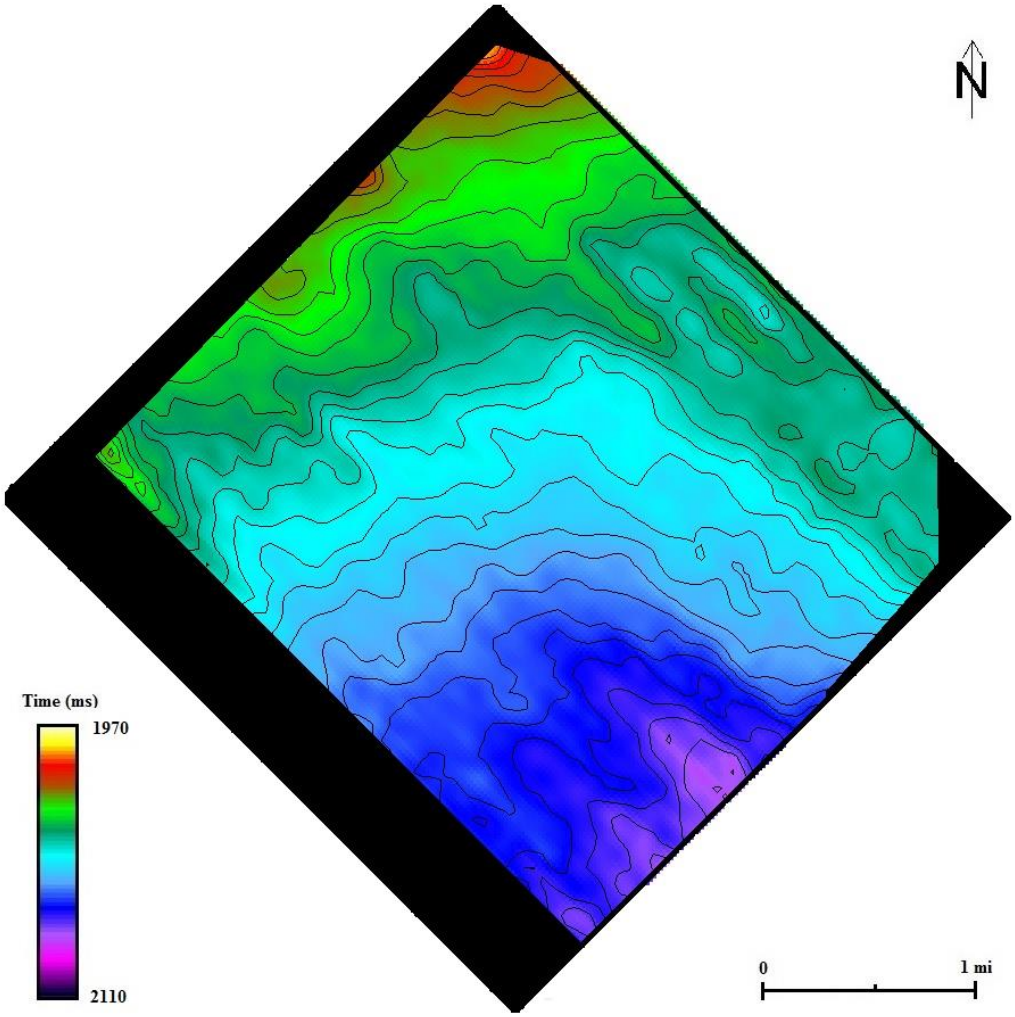

Figure 59: P-SV_2 two-way time structure of the top Queenston Sandstone (Contour interval is 5 ms).

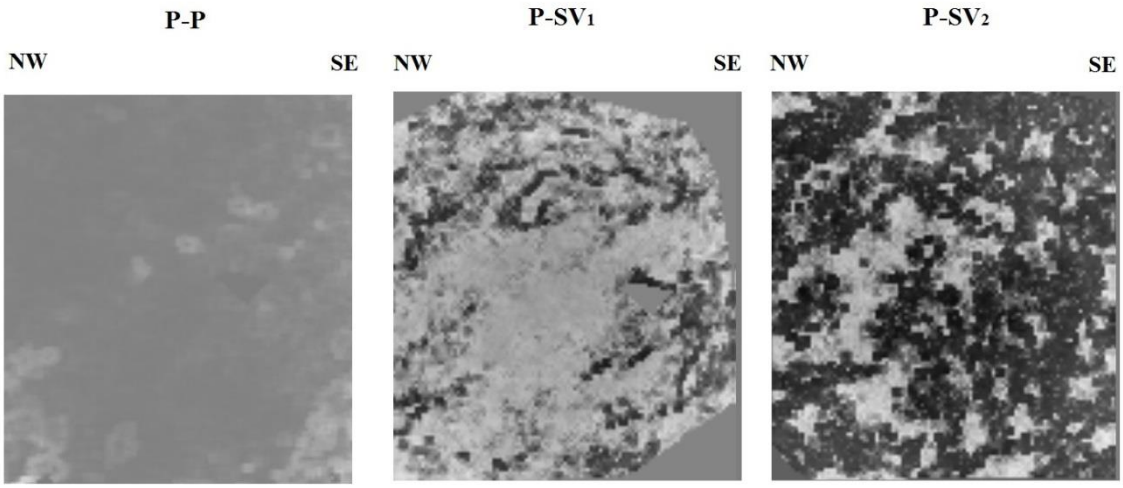

Figure 60: Semblance maps of the Queenston Sandstone interval in P-P, P-SV_1, and P-SV_2 data volumes.

CONCLUSION

My objective was to evaluate the Utica Shale Formation in terms of its stratigraphic and structural behavior. I did an intense study of the Utica Shale using 3C3D seismic data, digital well logs, and synthetic seismograms. My evaluations of the Utica Shale in seismic time windows represent best guesses for the depth position of the Utica Shale in P-P and P-SV time space images. The Utica Shale is approximately positioned at a depth of 12,000 ft across my study area in Bradford County, Pennsylvania. Because the time-to-depth calibration data were limited below the Onondaga Limestone, I can express the Utica Shale in time images only as "near Utica Shale".

P-wave and S-wave imaging of geologic targets used in my thesis illustrate some important differences in 3C3D seismic data. For example, the P-SV_1 (fast-S) mode provides better resolution of key geologic horizons with respect to P-P (compressional) data because P-SV wavelengths are shorter than P-P wavelengths. This fact causes S-wave imaging of geologic targets in shale-gas systems to provide dramatic information where P-wave images do not. The advantage of using converted-shear modes provide increased resolution and S-wave imaging can be applicable for most shale-gas systems in the Appalachian Basin.

In addition to resolution advantages of converted-shear wave images, S-wave images provide additional reservoir heterogeneities of key geologic targets, where P-wave images fail to identify these features. In the Utica Shale interval, a channel-like feature was identified in P-SV_1 images and was interpreted as a possible turbidite feature. This conclusion was based on the depositional environment of the Utica Shale.

Structural behavior of the Utica Shale showed dominant north-east orientation of structural lineations. This analysis was important for the possible future orientations of

horizontal wells across the study area, which should be drilled perpendicular to fracture orientation. In addition to this, S-wave anisotropy analysis of the Utica Shale was also an important indicator of fracture intensity. Seismic-based anisotropy values were around 1 percent, so I concluded the anisotropy of the Utica Shale across the study area was very small. If there were any well log information for the Utica Shale interval, it would be better to calibrate the anisotropy values of the Utica Shale from log data.

Multicomponent seismic interpretation was also used to analyze the Queenston Sandstone Formation and the Trenton Limestone Formation. Queenston Sandstone seismic analyses were important for possible hydrofracking operations to determine if this sandstone unit qualifies as an injection interval for hydrofracking flow-back fluids. The structural dip of the Queenston Sandstone was similar to the Utica Shale and there was no evidence that faults cut through the section. The Trenton Limestone also showed similar behaviors in terms of stratigraphic and structural trends. These analyses were important for understanding the Utica Shale and its associated geology.

Appendix

Table 1: Well data

Map Symbol	Source	Hole Direction	UWI	State	County Name	Basin Name	Driller Td (ft)	Elevation Gr (ft)	Latitude	Longitude	Utica Depth (ft)	Trenton Depth (ft)	Queenston Depth (ft)
1	PI	DIRECTIONAL	37015200410000	PA	BRADFORD	APPALACHIAN BASIN	12000	1280	41.9838078	-76.35209048	10947	11119	8682
2	PI	DIRECTIONAL	37015200510000	PA	BRADFORD	APPALACHIAN BASIN	12726	1770	41.9555001	-76.86115921	11438	11615	8900
3	PI	VERTICAL	37015200520000	PA	BRADFORD	APPALACHIAN BASIN	12602	1525	41.93291667	-76.58580556	11606	11842	9125
3	PI	DIRECTIONAL	37015200520100	PA	BRADFORD	APPALACHIAN BASIN	12618	1525	41.93291667	-76.58580556	11606	11845	NA
3	PI	DIRECTIONAL	37015200520200	PA	BRADFORD	APPALACHIAN BASIN	13430	1525	41.93291667	-76.58580556	11612	11851	NA
4	PI	VERTICAL	37015200530000	PA	BRADFORD	APPALACHIAN BASIN	14125	1030	41.99025828	-76.33494868	10525	10753	8383
5	PI	DIRECTIONAL	37015200550000	PA	BRADFORD	APPALACHIAN BASIN	13997	1330	41.98785582	-76.47480794	10874	11016	8730
6	PI	VERTICAL	37015201720000	PA	BRADFORD	APPALACHIAN BASIN	14300	1298	41.68443723	-76.70424758	12913	13447	10706

Table 2: Ranges of V_P/V_S (Domenico, 1984)

Rock type	Vp/Vs
Sandstone	1.59-1.76
Dolomite	1.78-1.84
Limestone	1.84-1.99
Shale	1.70-3.00

REFERENCES

Anderson, E. J., Goodwin, P. W., and Cameron, B., 1978, Punctuated aggradational cycles (PACS) in Middle Ordovician and Lower Devonian sequences, in Merriam, D.F., ed., New York State Geological Association Guidebook, 50th Annual Meeting: Syracuse, New York State Geological Association, p. 204-224.

Baird, G.C., Brett, C., Lehmann, D., 1992, The Trenton–Utica problem revisited: new observations and ideas regarding Middle-Late Ordovician stratigraphy and depositional environments in central New York. In: Goldstein, A. (Ed.), New York State Geological Association, 64th Annual Meeting, pp. 1–40.

Baird, G.C., and Brett, C.E., 1994, Revised correlation for Late Ordovician shelf-slope deposits, Mohawk Valley, New York: Implication for depositional dynamics in a foreland basin, Geological Society of America, Northeast Section, Binghamton, A4.

Calvert, A.J., 2004, A method for avoiding artifacts in the migration of deep seismic reflection data, Tectonophysics, v. 388, p. 201-212.

DeBrosse, T.A., and Vohwinkel, J.C., 1974, Oil and gas fields of Ohio: Ohio Division of Geological Survey in cooperation with Ohio Division of Oil and Gas, 1 sheet, scale 1:500,000.

Domenico, S., N., 1984, Rock lithology and porosity determination from shear and compressional wave velocity: Geophysics, 49, 1188-1195.

Ellison, M., 2014, Comparison of fracture planes in the Marcellus and Utica Shales, MicroSeismic,Inc.

Ettensohn, F.R., 1991, Flexural interpretation of relationships between Ordovician tectonism and stratigraphic sequences, central and southern Appalachians, U.S.A., in Barnes, C.R., and Williams S.H., eds., Advances in Ordovician Geology: Geological Survey of Canada Paper 90-9, p. 213-224.

Frasier, C. W., and Winterstein, D. F., 1990, Analysis of conventional and converted mode reflections at Putah Sink, California, using three-component data: Geophysics, 55, 646-659.

Goldman D., Mitchell, C.E., and Joy M.A. 1999, The stratigraphic distribution of graptolites in the classic upper Middle Ordovician Utica Shale of New York: an evolutionary succession or a response to sea-level change? Paleobiology 25(3): p. 273-294.

Hardage, B. A., M. V. DeAngelo, D. Wagner, and D. Sava, 2012, Evaluation of fracture systems and stress fields within the Marcellus Shale and Utica Shale and characterization of associated water-disposal reservoirs, Appalachian Basin: Presented at RPSEA Unconventional Gas Conference.

http://geology.com/articles/utica-shale/ Accessed June 14, 2014.

http://marcellus.psu.edu/images/UticaDepth.gif/ Accessed June 14, 2014.

http://marcellus.psu.edu/images/UticaThickness.gif/ Accessed June 14, 2014.

https://www.ihs.com/ Accessed 15 October, 2014.

Jacobi, R.D., 1981, Peripheral bulge-a casual mechanism for the Lower/Middle Ordovician disconformity along the western margin of the northern Appalachians, Earth Planet, Sci. Lett., 56, 245-251.

Kay, M., 1953, Geology of the Utica Quadrangle, New York, New York State Museum Bulletin 347, p. 126.

Keith, B. D., 1989, Regional facies of Upper Ordovician Series of Eastern North America: American Association of Petroleum Geologists, Studies in Geology, v.29, p. 1-16.

Kolata, D.R., Huff, W.D., Bergström, S.M., 2001, The Ordovician Sebree Trough: an oceanic passage to the Midcontinent United States. Geological Society of America Bulletin 113, 1067 – 1078.

Lehmann, D., Brett, C. E., Cole, R., Baird, G., 1995, Distal sedimentation in a peripheral foreland basin; Ordovician black shales and associated flysch of the western Taconic Foreland, New York State and Ontario: Geological Society of America Bulletin, v. 107, p. 708-724.

Martin, J.P., Nyahay R., Leone, J., and Smith, L.B., 2008, Developing a New Gas Resource in the Heart of the Northeastern U.S. Market: New York's Utica Shale Play, New York State: Search and Discovery Article #10160.

Nyahay, R., Leone, J., Smith, L.B., Martin, J.P., and Jarvie, D.J., 2007, Update on regional assessment of gas potential in the Devonian Marcellus and Utica Shales of New York (abs.), 2007 Eastern 26 Section, American Association of Petroleum Geologists Annual Meeting Program with Abstracts (September 16-18, 2007, Lexington, Kentucky), p. 46.

Patchen, D.G., Hickman, J.B., Harris, D.C., Drahovzal, J.A., Lake, P.D., Smith, L.B., Nyahay, Richard, Schulze, Rose, Riley, R.A., Baranoski, M.T., Wickstrom, L.H., Laughrey, C.D., Kostelnik, Jaime, Harper, J.A., Avary, K.L., Bocan, John, Hohn, M.E., and McDowell, Ronald, 2006, A geologic play book for Trenton-Black River Appalachian Basin exploration: Morgantown, W. Va., U.S. Department of Energy Report, DOE Award Number DE-FC26-03NT41856, accessed at <http://www.wvgs.wvnet.edu/www/tbr/project_reports.asp>.

Quinlan, G.M. and Beaumont, C., 1984, Appalachian thrusting, lithospheric flexure, and the Paleozoic stratigraphy of the eastern interior of North America, Canadian Journal of Earth Sciences, v. 21, p. 973-996.

Riva, J., 1969, Middle and Upper Ordovician graptolite faunas of St. Lawrence Lowlands of Quebec, and of Anticosti Island, In M. Kay, ed. North Atlantic – geology and continental drift, A symposium. American Association of Petroleum Geologists Memoir, 112: 579–595, Tulsa, Oklahoma.

Ryder, R.T., Burruss, R.C., and Hatch, J.R., 1998, Black shale source rocks and oil generation in the Cambrian and Ordovician of the Central Appalachian Basin, USA: American Association of Petroleum Geologist Bulletin, v. 82, p. 412-441.

Ryder, R.T., 2008, Assessment of Appalachian Basin oil and gas resources—Utica Lower Paleozoic Total Petroleum System: U.S. Geological Survey Open-File Report 2008–1287, accessed at <http://pubs.usgs.gov/of/2010/1287/>.

Sandanayake, C., and Bale, R.A., 2011, Application of Shear-wave Splitting Analysis to Fracture Characterization for a Shaunavon Tight Oil Reservoir, Recovery, CSPG CSEG CWLS Convention.

Scotese,C.S., 2003, Paleomap Project:Web site accessed July 29, 2011, at http://www.scotese.com Accessed September 14, 2014.

Sheriff, R. E., and Geldart, L. P., 1995, Exploration Seismology: 0521468264; Cambridge University Press.

Smith, L., 2006, Origin and reservoir characteristics of Upper Ordovician Trenton–Black River hydrothermal dolomite reservoirs in New York, U.S.A.: AAPG Bulletin, v. 90, no. 11, p. 1691–1718.

Smith, L.B., and Leone J., 2010, Integrated Characterization of Utica and Marcellus Black Shale Gas Plays, New York State: Search and Discovery Article #50289 (2010).

Thériault, R., 2012a, Caractérisation du Shale d'Utica et du Groupe de Lorraine, basses-terres du Saint-Laurent - Partie 1 : Compilation des données. Ministère des Ressources naturelles et de la Faune, Québec; DV 2012-03, 212 p.

Thériault, R., 2012b, Caractérisation du Shale d'Utica et du Groupe de Lorraine, basses-terres du Saint-Laurent - Partie 2 : Interprétation géologique. Ministère des Ressources naturelles et de la Faune, Québec; DV 2012-04, 80 p.

Tyson, R.V., and Pearson T. H., 1991, Modern and ancient continental shelf anoxia: an overview, Geological Society Special Publication No. 58, London, 1–24.

Walker K.R., Shanmugam G., and Ruppel S.C., 1983, A model for carbonate to terrigenous clastic sequences, Geological Society of America, v. 94, p. 700-712.

Wallace, L.G. and Roen, J.B., 1989, Petroleum source rock potential of the Upper Ordovician black shale sequence, northern Appalachian basin: U.S. Geological Survey Open-File Report 89 488, 66 p.

Wickstrom, L.H., Gray, J.D., and Stieglitz, R.D., 1992, Stratigraphy, structure, and production history of the Trenton Limestone (Ordovician) and adjacent strata in northwestern Ohio: Ohio Department of Natural Resources, Division of Geological Survey Report of Investigations 143, 78 p.

Zeng, H., 2006, Stratal slicing makes seismic imaging of depositional systems easier: AAPG explorer, v. 27, no. 6, p.26-27.